BIOMATERIALS FOR THE EXTRACELLULAR CONTROL OF MESENCHYMAL STEM CELL PRO-ANGIOGENIC POTENTIAL

BY

AMR ASHRAF ABDEEN

DISSERTATION

Submitted in partial fulfillment of the requirements
for the degree of Doctor of Philosophy in Materials Science and Engineering
in the Graduate College of the
University of Illinois at Urbana-Champaign, 2016

Urbana, Illinois

Doctoral Committee

Assistant Professor Kristopher A. Kilian, Chair
Professor Paul V. Braun
Professor Deborah E. Leckband
Associate Professor Hyunjoon Kong
Assistant Professor Cecilia Leal

ABSTRACT

With the prevalence of ischemic heart disease, cell based treatments have emerged as promising therapeutic options to promote angiogenesis. The use of adult mesenchymal stem cells (MSCs), particularly, is an area of active investigation. However, clinical efficacy has proved variable, likely on account of ill-defined cell delivery formulations and the inherent complexity of cellular secretion. The versatility of MSCs and their responsiveness to the environment make them very malleable to changes in the microenvironment. The use of well-defined biomaterials enables studying the influence of extracellular matrix properties on MSCs, which in turn gives criteria for the design of optimal biomaterials for therapeutic efficacy.

After a short introduction we explore using model polyacrylamide hydrogel systems in Chapter 2 to study the effects of matrix elasticity and composition on MSC pro-angiogenic potential, showing elasticity can play a large role – dependent on matrix composition. In Chapter 3 we use micropatterning to reveal how changing cell shape (modulating cellular cytoskeleton, focal adhesions and contractility) can modulate not only the pro-angiogenic potential of MSCs but their phenotype and epigenetic state. We develop a biocompatible PEG-based hydrogel system in Chapter 4 and we show that this system can be used to spatially guide angiogenesis. Finally, in Chapter 5, we demonstrate a magnetoactive hydrogel system where mechanical properties can be modulated in vitro in order to study the effects of temporal changes in matrix properties, such as those that occur during infarction.

Overall, we believe the work presented here demonstrates the importance and utility of extracellular properties in modulating stem cell behavior, especially in the context of cell-based therapies, and should aid in the development of biomaterials for the treatment of ischemic cardiovascular disease.

ACKNOWLEDGEMENTS

A great deal of thanks goes to my adviser Kris Kilian, who's supported this work all the way. His deep knowledge of the science and broad interests have made my PhD a very interesting and fun endeavor and I'm very grateful for his way of giving invaluable guidance and directing my progress while allowing me ample freedom to explore the science and shape the project. I'm further appreciative of his infectious optimism and enthusiasm for science all through my PhD, which often motivated me through several obstacles. His mentoring style is one that I would strive to model my own after.

I would also like to thank my other committee members: Professors Paul Braun, Deborah Leckband, Hyunjoon Kong and Cecilia Leal. They have helped shape the work with their insightful direction and have helped me develop as a scientist during my PhD, even from before serving on my committee.

I am further thankful to the Kilian group members. I would like to especially thank Junmin Lee from whom I've learned a lot about work ethic, resilience and humility and who contributed to several aspects of the work presented here. Further thanks to Yanfen Li, Sam Mo and Jared Weiss who directly contributed to the work presented here, often enriching it with their contributions and Doug Zhang whose helped me with figuring out several lab techniques. I would also like to thank Tiffany Huang, Phuong Le, Yi Pei and everyone else who's been through the Kilian lab over the past years as they taught me a lot and made my research journey more fruitful, enjoyable and interesting.

A lot of the work I did would also not be possible (and less interesting) without our collaborators including Ashwin Bharadwaj, Dan McDougle, Chris Liu, Xin Tang and professors Randy Ewoldt, Aditi Das, Martha Gillette, Timothy Fan and Taher Saif. I would like to thank these collaborators, especially for having to work with my (sometimes convoluted) work schedules. I would further like to thank members of prof. Jianjun Cheng's lab (Especially Ryan Baumgartner) and Andrew Smith's lab for often useful discussions and thank professors Cheng and Leal for graciously sharing their labs' equipment.

I had a great learning experience and a large part of that was due to learning from the very knowledgable staff all around UIUC. I'm very appreciative in particular of Scott Maclaren and Jenny Amos who taught me AFM; Dean Olson for teaching me all about NMR; Catalin Chiritescu for his help with AFM; Kathleen Walsh for helping me with DMA and AFM; Dianwen Zhang for his help with fluorescence microscopy; and Larry Millet for getting me started on photolithography. Further thanks goes to MatSE staff who've helped me a lot including Jay, Debbie, Sandy, Michelle, Kimberly, Cindy and Allison.

There have also been several non-academic contributors to this thesis including several friends who've supported me throughout my PhD work. I'd particularly like to thank Hazem 'Ameed' Hossam, Mohamed 'Omda' Rashad and Khaled Alshihri as well as Hatem, Sherif, Ahmed elkhouly, Moatasem, Rabie, Sobhy, Ahmed Osama, Ayman , Zafer, Mohab, Abdelaziz, Ahmed Adel, Mansour, Moustafa, Baghdady, Aziz, Abhar, Tarek, Nabawe and Amir. This is in addition to all my older friends who've kept in touch including Mostafa Hamdy, Ahmed Labib, Ahmed Hany, Ghaith,

Ibrahim Abdallauh, Ahmed Deeb, Hossam Saeed, Ahmed Adel, Ibrahim Helmy and Yousry, Shams and Karim.

Finally, I’d like to thank my family. Especially my parents, without whom none of this would be possible, and who’ve supported my passions and so often put my aspirations above all other considerations.

TABLE OF CONTENTS

CHAPTER 1

INTRODUCTION[1]

1.1 Mesenchymal Stem Cells for Angiogenesis Therapy

Cardiovascular disease is the number one cause of death in the United States accounting for about a third of all mortalities(1). Ischemic heart disease, where blood flow to the heart is restricted, is the leading cause of human mortality globally, resulting in around 7.25 million deaths each year(2). Angiogenesis therapy, aiming to stimulate blood vessel growth from pre-existing vessels, is a proposed solution for several cardiovascular conditions including myocardial infarction(3,4). Angiogenesis therapy often involves the direct delivery of cytokines to the site of injury to promote blood vessel formation. However, angiogenesis is a very complex process involving multiple mechanisms working in tandem(5) and treatments like cytokine delivery often cause unwanted effects such as aberrant vascularization(6). The use of autologous cells is a promising alternative(7) because of the low risk of rejection and the temporally regulated secretion of trophic, immunomodulatory, and pro-angiogenic molecules. In particular, mesenchymal stem cells (MSCs) are a leading candidate for implantation to promote angiogenesis, with several registered clinical trials for cardiovascular diseases(8).

---

[1] Parts of this chapter have been adapted from the following publications:
Amr A. Abdeen, Junmin Lee, and Kristopher A. Kilian, Capturing extracellular matrix properties in vitro: microengineering materials to decipher cell and tissue level processes, Experimental Biology and Medicine, 2016

MSCs are multipotent adult stem cells of mesoderm origin. They can be obtained from either bone marrow or adipose tissue and have the ability to differentiate into multiple cell types(9). The versatility and ease of access to these cells have made them prime targets for research in regenerative medicine aiming to harness these properties. Their ability to differentiate into multiple cell types has promoted their use in various applications, from cartilage repair(10) to the treatment of retinal diseases(11).

For angiogenesis therapy, the mechanism behind the therapeutic efficacy of MSCs is contentious. There have been reports of transdifferentiation of MSCs into cardiomyocytes(12) and endothelial cells(13,14); however, recent studies suggest limited long term engraftment of MSCs(15), suggesting that the dominant therapeutic role of MSCs is secretion of paracrine signals in vivo(16). Even so, trials of grafted MSCs have not lived up to the hype and clinical efficacy remains low.

The therapeutic potential of MSCs is very dependent on the context in which they are used and understanding how it is regulated is critical. Extracellular matrix (ECM) properties are some of the most potent regulators of MSC behavior, which are not usually controlled when injecting MSCs, which may explain the underwhelming performance of grafted MSCs. Hence the use of synthetic biomaterials may serve the dual purpose of elucidating MSC-ECM interactions and how they modulate MSC behavior as well as providing a controlled environment for maximizing MSCs' potential in vivo. Furthermore, it is known that MSCs are largely heterogeneous populations(17) and a unified environment presented to all cells may act to homogenize their behavior, making it more predictable.

1.2 Biomaterials for the Study/Control of Cell-ECM Interactions

In vitro cell culture has provided a convenient, cost-effective method to study specific cell lines in minimal simplified growth conditions, free of many of the outside influences seen in vivo. This allows for isolation of single cell lines to investigate their properties, testing the effects of various pharmacological agents on specific cell types and a multitude of other applications under well controlled conditions. However, these advantages come at a price; due to the differences between in vitro and in vivo cell culture conditions, cell characteristics change with long term in vitro culture. Cells adapt to the different culture conditions by changing their behavior and activities(18).

With the accumulating evidence of the role that physical and mechanical factors such as forces(19), shape(20) and architecture(21) play in regulating cell behavior, the divide between in vitro cell culture and in vivo environments presents an obstacle to studying and manipulating cells in the lab. There have been several advances in materials and fabrication techniques that have allowed for modulation of the extracellular matrix (ECM) available to cells during in vitro culture. In fact, cells reside in very complex and dynamic extracellular matrices(22–25), with very specific compositions, ligand presentations, mechanical properties and organization that vary between different tissues(26). Extracellular factors strongly influence many facets of cell behavior such as homeostasis(27,28), morphogenesis(29,30), self-renewal and differentiation of stem cells(31), development(23,32) and disease(32,33). It thus becomes clear that, in order to be able to more fully study

cell behavior in vitro, cell culture platforms in which these factors can be recapitulated and/or manipulated must be developed(34).

Although methods to confine cells to specific shapes have been demonstrated since 1967(35), the more recent spread of lithographic(36), microfluidic(37) and other patterning techniques have made micropatterning of cells much more convenient and accessible. The increasing use of both natural and synthetic soft materials(38–40) have allowed for manipulation of the form and mechanical properties of the ECM as well as ligand presentation. ECM proteins and synthetic peptides enable more precise study of specific cell-ECM interactions(22). Degradable(41) and dynamically tunable(42) platforms elucidate how cells react to changes in their microenvironments. Techniques such as 3D printing(43) and nanopatterning(44) allow for investigating processes on tissue and subcellular scales, respectively. These advances, along with others, have enabled engineered in vitro environments to be much more accurate model systems for in vivo processes, yielding considerable insights on cellular behavior(33,45).

In this section, we explore engineered environments to study and control the effects of ECM properties on cell activity. For both single cell and multiple cell systems, we consider relevant ECM properties with examples of in vitro model systems that capture these properties, highlighting some insights gleaned from such systems. Since we are considering MSCs, several instances of the study and manipulation of MSCs using tunable ECM properties will be considered.

1.3 Engineered Environments for Single Cell Culture

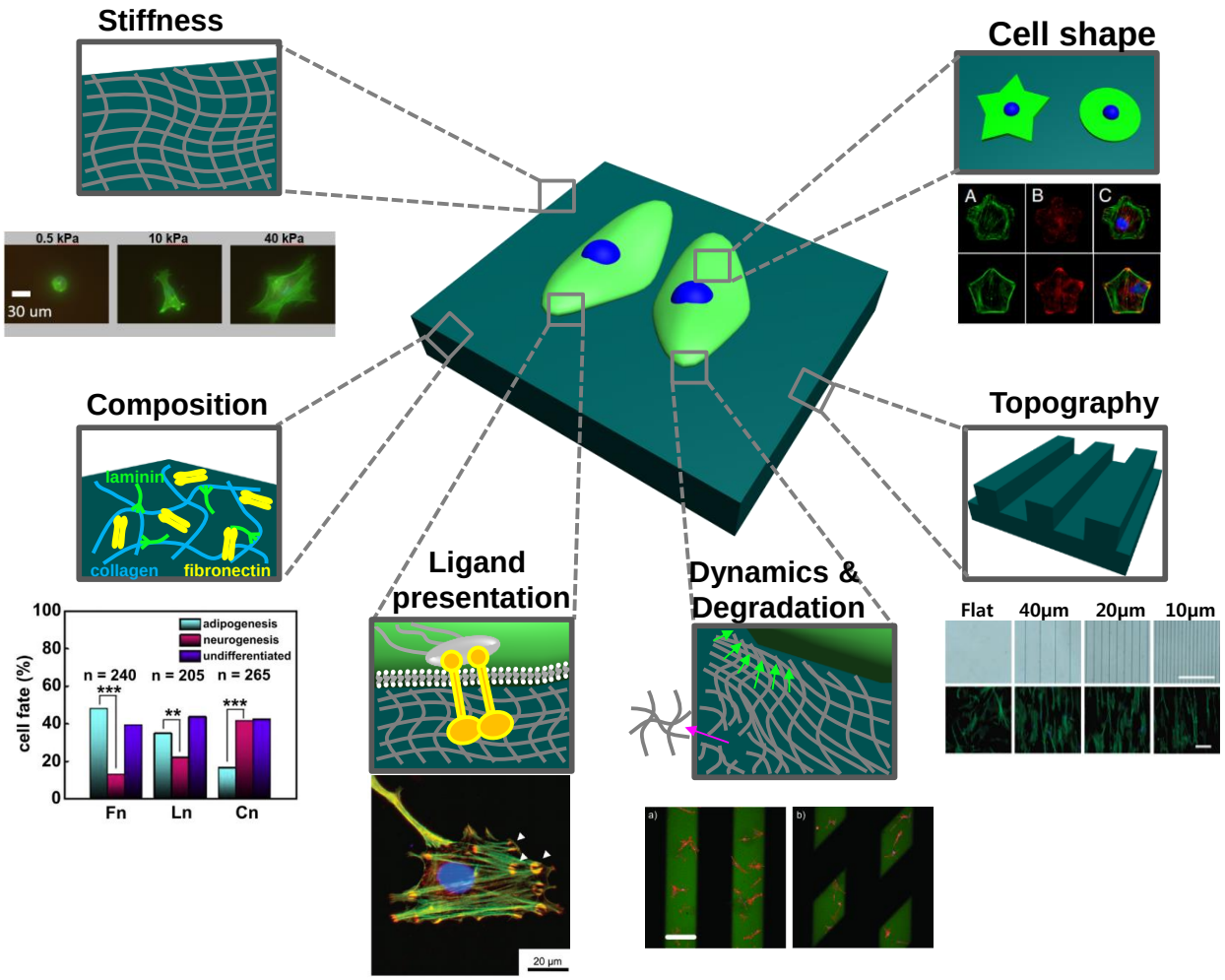

Figure 1.1 Matrix properties affect cell behavior in vitro: Elasticity – MSC morphology (and cytokine secretions) are dependent on matrix stiffness(63). Composition – MSC differentiation is highly dependent on the matrix protein conjugated to the surface [Reprinted from(66), Copyright (2013), with permission from Elsevier]. Ligand Presentation – Fibroblast focal adhesions only form on 5µm RGD functionalized gold islands with stress fibers running between adhesions [Reprinted with permission from (134), copyright (2010) American chemical society]. Dynamics and degradation – Cell adhesion can be switched on and off by switching the conjugation of ligands at the surface [Reprinted from(84), Copyright (2012), with permission from Wiley]. Topography – Substrate topography controls alignment and epigenetic reprogramming of cells [Reprinted by permission from Macmillan Publishers Ltd: Nature Materials from (124), copyright (2013)]. Cell Shape – Modifying cell shape can affect MSC cytoskeleton, focal adhesion formation and differentiation(97)

Single cells experience a myriad of different signals from their ECM (Figure 1.1).

Cells transduce and integrate these different factors into biochemical signals,

altering their behavior(46). There are a variety of cellular apparatus used to detect

extracellular signals such as growth factors and cytokine receptors, ion channels and cell-matrix and cell-cell adhesion molecules(47). Particularly, forces exerted by and on the cells through transmembrane receptors such as integrins play an important role through 'mechanotransduction' via the cellular cytoskeleton(48–51). Stem cells, with their plasticity, ability to differentiate down different lineages and importance for regenerative medicine, are particularly sensitive to extracellular cues and thus are the focus of several of these studies(52–54).

Matrix Composition

Biochemical factors present in the extracellular space are numerous and present a multitude of signals to cells, allowing for functional complexity in cell behavior(55). A wide variety of glycosaminoglycans (GAGs), proteoglycans and different glycoproteins such as collagens, fibronectins and laminins, combine together to provide a very rich signaling environment, which varies widely between different tissues. In fact, loss of function mutations in several of these proteins are embryonic lethal or post-natal lethal within 4 weeks(55), highlighting their importance. However due to the high complexity and organization, it is significantly challenging to recapitulate aspects of such an environment in vitro. A common strategy is adsorption(56) or chemical conjugation(57) of proteins onto synthetic tissue culture substrates. This method is more facile for studying the effects of single components of the ECM or simple combinations and is useful for deconstructing the roles of different ECM components and their interactions. Both adsorption and chemical conjugation however may alter protein conformation, potentially changing protein bioactivity(58). Other strategies include the use of

natural ECM components, such as GAG or collagen gels, to fabricate tissue culture environments(59) or using decellularized matrices(60). These strategies recapture several aspects of the in-vivo environment but relinquish some control over the precise environment presented to cells. Matrix composition has been found to influence diverse aspects of cell behavior such as ERK activation by mechanical strain in smooth muscle cells(61), endothelial cells network formation and their response to TGF-β(62), secretome(63) , cancer progression(64) and stem cell fate(65). We and other groups have shown previously that for mesenchymal stem cells (MSCs), matrix composition can direct cell differentiation and mediate how cells respond to other cues(66,67). Two current areas of active research are the use of cell-derived matrices to reconstitute in vitro environments(68) and synthesis of matrices that can better interact with growth factors via sequestration and other interactions(69).

Ligand Presentation

Cells will behave very differently depending on how the ligand presents to the cell. This mainly has to do with how cells interact with the proteins via focal adhesions; clusters of intracellular proteins and transmembrane integrins(70,71). These interactions physically transfer forces between the ECM and cells, facilitating mechanotransduction and cellular remodeling of the ECM(46,72). Cell-matrix interactions are sensitive to ligand density, ligand spacing, receptor clustering and ligand availability(73), in addition to composition. Furthermore, the pliability of proteins to cell generated forces tunes the availability of cryptic signaling sites(47). Several innovative methods have been developed to control these different aspects.

The use of recombinant protein fragments or peptide sequences allows for tailoring of specific cell-matrix interactions since integrin pairs react with specific peptide sequences(48) with different affinities and outcomes. For example, using different FN III9–10 fragments with variable specificities to $\alpha_5\beta_1$ integrins allows control of $\alpha_5\beta_1$-mediated MSC osteogenesis(74). Self-assembled monolayers of alkanethiolates on gold substrates can be used to present a more uniform interface to cells and control ligand density and affinity(75,76). Block copolymer micelle nanolithography(77), a technique by which very uniform arrangement of gold nanodots can be made, has been used to study effects of ligand spacing and density variations and, when combined with micropatterning, the effects of ligand clustering. The use of such methods have revealed the different binding affinities of integrins depending on peptide sequences(78) (Even depending on cyclic vs linear variants of RGD(76), a commonly used peptide sequence from fibronectin) or adhesion clustering(79). Moreover, Spatz and colleagues have demonstrated a threshold of ~60nm of ligand separation for activation of integrin function(80) and more recently have reported a more dominant role for local ligand density as opposed to global(81). Finally, density of protein tethering alters the deformations exacted on proteins by cells, altering cell signaling and MSC fate(82).

Cell shape

One of the challenges of in vitro cell culture is cell heterogeneity and poor replicability of results. Cell shape in vivo is highly variable depending on context and control many facets of cell behavior. Micropatterning of cell shape allows us to recapitulate many of these aspects in vitro, diminishes much of the heterogeneity

inherent in cell culture substrates and controls for several aspects of cellular structure such as spread area and spatial distribution of adhesions(20), allowing for better control over experiments. Furthermore, control over cell shape facilitates geometric manipulation of the structure of the cytoskeleton(20,83). There are multiple methods of micropatterning cells including lithography(36), photo-patterning(84), microfluidics(85) and microcontact printing(86). Micropatterning doesn't have to be with integrin ligands but can utilize other cellular components such as lipid bilayers(87). Cell shape can determine the structure of the cytoskeleteon(83), focal adhesions(88), intermediate filaments(89), internal cell organization(90), nuclear forces(91) and histone modifications(92,93). Consequently, cell shape and size also influence cell viability(94), stem cell multipotency(95) and fate decisions(66,96). Increasing the degree of cytoskeletal tension nudges MSCs towards an osteogenic, rather than adipogenic fate(97) and modulates integrin mediated matrix interaction(98).

Elasticity

With the elasticity of various tissues spanning orders of magnitude(99), ECM elasticity is one of the most studied physical factors influencing cell behavior. Mechanics have also been implicated in a wide array of pathologies(100,101). Cells respond to changes in ECM elasticity(102), often by changing their own properties as evidenced by fibroblasts matching stiffness to their substrates(103). Biological materials are usually heterogeneous in mechanical properties and often display nonlinear elastic behavior(104). Synthetic materials such as polymeric hydrogels and natural materials are routinely fabricated with tunable stiffness, and materials

with variable rigidities such as micropost arrays(105) have been used to probe stiffness response as well. Various cytoskeletal components and signaling pathways have been implicated in these processes including focal adhesion kinase, Rho/Rock(52) and YAP/TAZ(106) as well as nuclear elements such as lamin-A(107) and LINC complexes(108). Early studies showed that cell motion and focal adhesions are regulated by substrate elasticity(38). Engler et al. demonstrated that MSC fate depends on substrate compliance, with optimal differentiation marker expression occurring on elasticities matching in vivo elasticity(109,110). Since then, the influence of substrate elasticity on modulating several aspects of cell behavior have been well documented(111). It has further been reported that the effects on MSCs depend on how long they are exposed to a substrate and that MSC behavior is affected by their mechanical history (112,113). The mechanism, or what exactly the cells are responding to, is variable, since changing material stiffness typically entails changing material porosity, matrix tethering, and other mechanical properties. Response to mechanical properties has been attributed to matrix elasticity(114,115), density of protein tethering(82), viscoelastic creep(116), traction forces(117) and stress relaxation(118).

Topography

As opposed to flat culture substrates, basement membranes and ECM components such as collagen, which forms submicron sized fibrils, have a very hierarchical structure and are often textured, providing topographic signaling cues(119). These cues, depending on their size, can interact with integrins up to whole cells. Advances in nanofabrication have allowed the fabrications of nanoscale gratings,

posts, pits, aligned fibers and other structures that can be made isotropic, anisotropic or in gradients form(120,121). Nanotopography can affect cell morphology, adhesion, migration, proliferation and differentiation, generally through generation of anisotropic stresses in cells(121). MSC differentiation has been reported to be guided by nanotopography, for example to the neurogenic(122) or osteogenic(123) lineages. Recently, Downing et al. have shown that microgrooves can modify the epigenetics and significantly improve the reprogramming of fibroblasts(124), demonstrating the large potential of topographic cues.

Dynamic and degradable environments

The constantly changing nature of in vivo ECM is well known(64,125). As stated above, cells react to changes in ECM properties but are affected by previous environments. For example, there have been recent reports that MSCs 'remember' their previous substrates(112,113) for at least 10 days with regards to nuclear localization of RUNX2, YAP and osteogenic differentiation, although other properties such as cell area remain plastic or relatively unaffected by previous states. This is a new field of study however and more work is required to understand the mechanisms through which cells maintain this memory and its effect on cell behavior for longer terms. Dynamic materials are hence desirable to construe the effects of changing microenvironments on cells. Switchable surfaces(126), stimuli responsive materials(127) and photoresponsive materials(84) have been used to modulate matrix properties such as ligand presentation, composition, stiffness and cell shape during cell culture. Furthermore, substrate degradability may be

desirable for both probing cell behavior and for in vivo use of engineered substrates(41,128,129). A significant challenge remains engineering reversibility into these kinds of systems as opposed to one-directional changes(130).

Other factors such as dimensionality(40,131), mechanical load and shear flow are also potent regulators of cell behavior. Cell behavior is typically very different between 2D and 3D environments as evidenced by several studies(117,132,133). Although it is extremely challenging to control for multiple aspects of ECM structure in the same experiment it is important to evaluate data in context of all the appropriate properties of the system and how they relate to the relevant in vivo environments. Different components such as hydrogels and nanopatterning or micropatterning can be combined to study the effects of multiple factors concurrently(66,134). In fact, studies combining multiple cues often reveal crosstalk and interplay among different factors(72). For example, MSC response to stiffness is dependent on matrix composition in terms of adhesion(98), differentiation(66,67) and therapeutic potential(63). For this reason, it is imperative to take the whole biophysical system into consideration before making conclusions about the effects of certain parameters.

1.4 The Influence of Multicellular Interactions

In addition to all the factors influencing single cells during culture, there are multiple additional effects in play when multicellular constructs are considered together (Figure 1.2). In this situation, the position of a cell relative to other cells, cell-cell interactions, paracrine signaling and interactions with different cell types

act to instruct cellular outcomes and coordinated cell behavior. This is particularly apparent during development where the relative positions of cells can dictate their specification and differentiation(23). Although scaffolds for studying these kinds of behaviors are typically on a larger scale than those for single cells, great care must be taken to optimize the experimental parameters and define the specific interactions being studied in order to deconstruct specific cues and determine their precise influence. Here we present a brief overview of some of these factors.

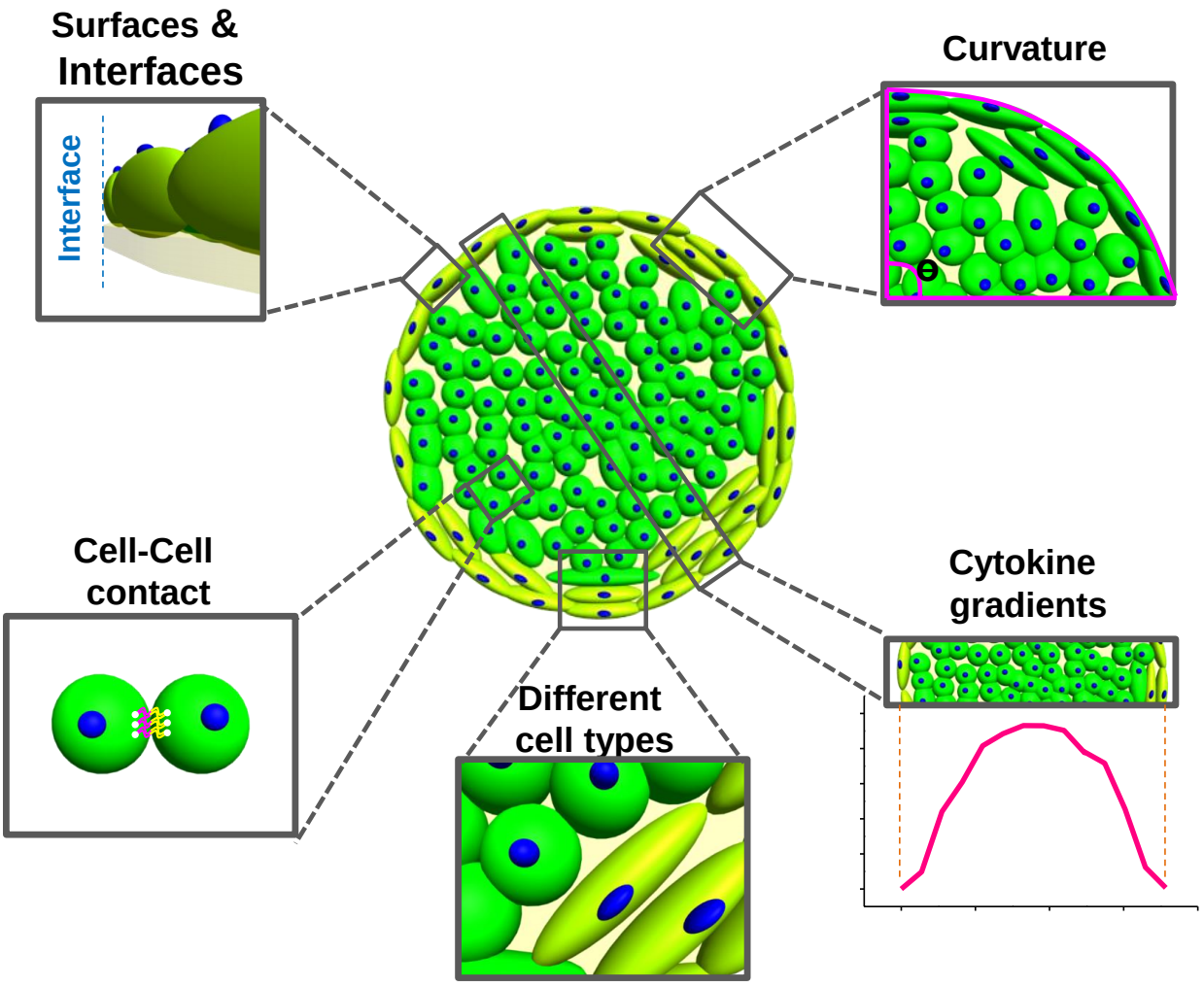

Figure 1.2 Interactions of multiple cells. Several factors are introduced when multiple cells are considered together including cell-cell contact, contact between different cell types, the introduction of interfaces and curvature and cytokine gradients across the system. These factors control effects such as collective cell behavior and cell sorting, for example.

In a typical in vivo niche there are multiple cell types in contact in different ways. Cells in contact interact through cadherins; a family of cell adhesion molecules which mediate interactions. Cadherin based cell-cell contacts are involved in a plethora of biological processes such as development, differentiation and disease(135). Multiple platforms have been developed wherein homo- and heterotypic cell-cell contacts can be controlled from a single cell-cell contact up to large scale co-cultures(136). Cells in contact have been shown to mechanically couple together(137), allowing for large scale collective cell migration(138). Tseng et al. have shown that the organization of intercellular junctions are dependent on the ECM architecture(139). Studying interactions of heterotypic cells has shown interesting phenomena such as natural cell sorting due to adhesion effects(140) and self-assembly of multicellular structures(141). Artificial boundaries between different cell types allow the investigation of interfacial interactions (in tumor-stroma for example)(142).

Cohesive forces between cells stabilize them in contact. Differences in adhesion between homophilic and heterophylic cell-cell contacts may cause cell aggregation and sorting(143), analogous to surface tension in fluids(144). The shapes of individual cells within aggregates depend on their position within the aggregate, which specifies their cortical tension and degree of cell-cell adhesion(145). However, several other factors change at the surfaces of patterned cell aggregates, thereby complicating the interpretation of behavior. Some of these factors are mechanical stresses due to traction forces(146,147), cytokine gradients caused by uneven distribution of cells(148), and differences in surface curvature. Often, these

factors feed into each other, giving an extra layer of complexity which can, however, be elucidated by usage of more controlled patterning methods such as the use of microfluidics to precisely control cytokine gradients(149).

In addition to deconstructing the influences of different factors in the microenvironment, engineered microenvironments that can simultaneously control multiple cues may be used to optimize desired outcomes. For instance, 3D printing techniques have been developed that can control matrix composition, topography, elasticity and spatial organization of different cell types which have been used to print vascularized, multiple cell-laden constructs(150).

1.5 Hypothesis and Thesis Structure

With the knowledge of the essential role the ECM plays in regulating cellular behavior and faced with the low efficacy of MSC based therapies for cardiovascular disease, we hypothesized that the physical properties of the ECM such as elasticity, composition, dimensionality and geometric presentation affect, and can be used to guide, the pro-angiogenic secretions of MSCs.

This hypothesis is tested throughout this thesis. In chapter 2, we use a polyacrylamide model system to investigate the influence of matrix elasticity and composition on the secretory profile and pro-angiogenic potential of MSCs. This is narrowed down in chapter 3 where we employ microcontact printing in order to normalize the MSC populations and study the effects of focal adhesion, cytoskeletal organization and epigenetics, modulated by geometry, on MSC phenotype and pro-angiogenic potential. Chapter 4 focuses on developing a PEG based translational

platform which can be used in vivo and in vitro to enable the spatial coordination of angiogenesis on synthetic matrices. Finally, in chapter 5, a magnetoactive hydrogel system, whereby elasticity can be modulated reversibly by attenuation of a magnetic field, is developed which allows temporal control of ECM mechanical properties. This approach enables the study of dynamic changes in mechanics, processes which are challenging to reconstruct in cell culture materials, and occur in vivo through enzymatic or chemical means.

1.6 References

1. Mozaffarian D, Benjamin EJ, Go A. S, Arnett DK, Blaha MJ, Cushman M, et al. Heart Disease and Stroke Statistics--2015 Update: A Report From the American Heart Association. Circulation. 2014. e29-e322

2. Finegold JA, Asaria P, Francis DP. Mortality from ischaemic heart disease by country, region, and age: Statistics from World Health Organisation and United Nations. Int J Cardiol. Elsevier Ireland Ltd; 2012 Dec 4.

3. Deveza L, Choi J, Yang F. Therapeutic angiogenesis for treating cardiovascular diseases. Theranostics. 2012;2(8):801–14.

4. Zachary I, Morgan RD. Therapeutic angiogenesis for cardiovascular disease: biological context, challenges, prospects. Heart. 2011 Feb 1;97(3):181–9.

5. Carmeliet P, Jain RK. Molecular mechanisms and clinical applications of angiogenesis. Nature. 2011;473(7347):298–307.

6. Epstein SE, Kornowski R, Fuchs S, Dvorak HF. Angiogenesis therapy: amidst the hype, the neglected potential for serious side effects. Circulation. 2001 Jul 3;104(1):115–9.

7. Beohar N, Rapp J, Pandya S, Losordo DW. Rebuilding the damaged heart: the potential of cytokines and growth factors in the treatment of ischemic heart disease. J Am Coll Cardiol. Elsevier Inc.; 2010 Oct 12;56(16):1287–97.

8. Ranganath SH, Levy O, Inamdar MS, Karp JM. Harnessing the mesenchymal stem cell secretome for the treatment of cardiovascular disease. Cell Stem Cell. Elsevier Inc.; 2012 Mar 2;10(3):244–58.

9. Pittenger MF, Mackay AM, Beck SC, Jaiswal RK, Douglas R, Mosca JD, et al. Multilineage Potential of Adult Human Mesenchymal Stem Cells. Science. 1999 Apr 2;284(5411):143–7.

10. Gupta PK, Das AK, Chullikana A, Majumdar AS. Mesenchymal stem cells for cartilage repair in osteoarthritis. Stem Cell Res Ther. 2012;3(4):25.

11. Mead B, Berry M, Logan A, Scott RAH, Leadbeater W, Scheven BA. Stem cell treatment of degenerative eye disease. Stem Cell Res. Elsevier B.V.; 2015;14(3):243–57.

12. Muscari C, Bonafé F, Carboni M, Govoni M, Stanic I, Gamberini C, et al. Difluoromethylornithine stimulates early cardiac commitment of mesenchymal stem cells in a model of mixed culture with cardiomyocytes. J Cell Biochem. 2008 Mar 1;103(4):1046–52.

13. Wingate K, Bonani W, Tan Y, Bryant SJ, Tan W. Compressive elasticity of three-dimensional nanofiber matrix directs mesenchymal stem cell differentiation to vascular cells with endothelial or smooth muscle cell markers. Acta Biomater. Acta Materialia Inc.; 2012 Apr;8(4):1440–9.

14. Lozito TP, Kuo CK, Taboas JM, Tuan RS. Human mesenchymal stem cells express vascular cell phenotypes upon interaction with endothelial cell matrix. J Cell Biochem. 2009 Jul 1;107(4):714–22.

15. Leiker M. Assessment of a nuclear affinity labeling method for tracking implanted mesenchymal stem cells. Cell Transplant. 2008;17(8):911–22.

16. Ankrum J, Karp JM. Mesenchymal stem cell therapy: Two steps forward, one step back. Trends Mol Med. Elsevier Ltd; 2010 May;16(5):203–9.

17. Strioga M, Viswanathan S, Darinskas A, Slaby O, Michalek J. Same or not the same? Comparison of adipose tissue-derived versus bone marrow-derived mesenchymal stem and stromal cells. Stem Cells Dev. 2012 Sep 20;21(14):2724–52.

18. Hughes P, Marshall D, Reid Y, Parkes H, Gelber C. The costs of using unauthenticated, over-passaged cell lines: How much more data do we need? Biotechniques. 2007;43(5):575–86.

19. Soediono B. Mechanical Forces: Their Effects on Cells and Tissues. Gooch KJ, Tennant CJ, editors. Journal of Chemical Information and Modeling. Berlin, Heidelberg, Heidelberg: Springer Berlin Heidelberg; 1997. 160 p.

20. Théry M. Micropatterning as a tool to decipher cell morphogenesis and functions. J Cell Sci. 2010 Dec 15;123(Pt 24):4201–13.

21. DuFort CC, Paszek MJ, Weaver VM. Balancing forces: architectural control of mechanotransduction. Nat Rev Mol Cell Biol. Nature Publishing Group; 2011 May;12(5):308–19.

22. Frantz C, Stewart KM, Weaver VM. The extracellular matrix at a glance. J Cell Sci. 2010 Dec 15;123(Pt 24):4195–200.

23. Daley WP, Peters SB, Larsen M. Extracellular matrix dynamics in development and regenerative medicine. J Cell Sci. 2008;121(Pt 3):255–64.

24. Mouw JK, Ou G, Weaver VM. Extracellular matrix assembly: a multiscale deconstruction. Nat Rev Mol Cell Biol. Nature Publishing Group; 2014;15(12):771–85.

25. Nelson CM, Bissell MJ. Of extracellular matrix, scaffolds, and signaling: tissue architecture regulates development, homeostasis, and cancer. Annu Rev Cell Dev Biol. 2006;22:287–309.

26. Adams JC, Watt FM. Regulation of development and differentiation by the extracellular matrix. Development. 1993;117(4):1183–98.

27. Humphrey JD, Dufresne ER, Schwartz MA. Mechanotransduction and extracellular matrix homeostasis. Nat Publ Gr. Nature Publishing Group; 2014;15(12):802–12.

28. Kolahi KS, Mofrad MRK. Mechanotransduction: A major regulator of homeostasis and development. Wiley Interdiscip Rev Syst Biol Med. 2010;2(6):625–39.

29. Kim HY, Nelson CM. Extracellular matrix and cytoskeletal dynamics during branching morphogenesis. Organogenesis. 2012;8(2):56–64.

30. Heisenberg C-P, Bellaïche Y. Forces in Tissue Morphogenesis and Patterning. Cell. 2013 May;153(5):948–62.

31. Wang JH-C, Thampatty BP. Mechanobiology of adult and stem cells. Int Rev Cell Mol Biol. 2008 Jan;271(08):301–46.

32. Bonnans C, Chou J, Werb Z. Remodelling the extracellular matrix in development and disease. Nat Rev Mol Cell Biol. Nature Publishing Group; 2014;15(12):786–801.

33. Lukashev ME, Werb Z. ECM signalling: Orchestrating cell behaviour and misbehaviour. Trends Cell Biol. 1998;8(11):437–41.

34. Griffith LG, Swartz MA. Capturing complex 3D tissue physiology in vitro. Nat Rev Mol Cell Biol. 2006;7(3):211–24.

35. Carter SB. Haptotactic islands: A method of confining single cells to study individual cell reactions and clone formation. Exp Cell Res. 1967 Oct;48(1):189–93.

36. Kane RS, Takayama S, Ostuni E, Ingber DE, Whitesides GM. Patterning proteins and cells using soft lithography. Biomaterials. 1999 Dec;20(23-24):2363–76.

37. Velve-Casquillas G, Le Berre M, Piel M, Tran PT. Microfluidic tools for cell biological research. Nano Today. 2010;5(1):28–47.

38. Pelham R, Wang Y. Cell locomotion and focal adhesions are regulated by substrate flexibility. Proc Natl Acad Sci. 1997;94(25):13661–5.

39. Dhandayuthapani B, Yoshida Y, Maekawa T, Kumar DS. Polymeric Scaffolds in Tissue Engineering Application: A Review. Int J Polym Sci. 2011;2011(ii):1–19.

40. Tibbitt MW, Anseth KS. Hydrogels as extracellular matrix mimics for 3D cell culture. Biotechnol Bioeng. 2009;103(4):655–63.

41. Kharkar PM, Kiick KL, Kloxin AM. Designing degradable hydrogels for orthogonal control of cell microenvironments. Chem Soc Rev. 2013;42(17):7335–72.

42. Eliyahu-Gross S, Bitton R. Environmentally responsive hydrogels with dynamically tunable properties as extracellular matrix mimetic. Rev Chem Eng. 2013 Jan 6;1–10.

43. Murphy S V, Atala A. 3D bioprinting of tissues and organs. Nat Biotechnol. Nature Publishing Group; 2014;32(8):773–85.

44. Singh AV, Patil R, Thombre DK, Gade WN. Micro-nanopatterning as tool to study the role of physicochemical properties on cell-surface interactions. J Biomed Mater Res - Part A. 2013;101(10):3019–32.

45. Rosso F, Giordano A, Barbarisi M, Barbarisi A. From Cell-ECM Interactions to Tissue Engineering. J Cell Physiol. 2004;199(2):174–80.

46. Kim SH, Turnbull J, Guimond S. Extracellular matrix and cell signalling: The dynamic cooperation of integrin, proteoglycan and growth factor receptor. J Endocrinol. 2011;209(2):139–51.

47. Vogel V, Sheetz M. Local force and geometry sensing regulate cell functions. Nat Rev Mol Cell Biol. 2006 Apr;7(4):265–75.

48. Campbell ID, Humphries MJ. Integrin structure, activation, and interactions. Cold Spring Harb Perspect Biol. 2011 Mar;3(3).

49. Schwartz MA. Integrins and extracellular matrix in mechanotransduction. Cold Spring Harb Perspect Biol. 2010 Dec;2(12):a005066.

50. Schwarz US, Gardel ML. United we stand: integrating the actin cytoskeleton and cell-matrix adhesions in cellular mechanotransduction. J Cell Sci. 2012 Jul 1;125(Pt 13):3051–60.

51. Paluch EK, Nelson CM, Biais N, Fabry B, Moeller J, Pruitt BL, et al. Mechanotransduction: use the force(s). BMC Biol. BMC Biology; 2015;13(1):47.

52. Sun Y, Chen CS, Fu J. Forcing stem cells to behave: a biophysical perspective of the cellular microenvironment. Annu Rev Biophys. 2012 Jan;41:519–42.

53. Lutolf MP, Gilbert PM, Blau HM. Designing materials to direct stem-cell fate. Nature. 2009 Nov 26;462(7272):433–41.

54. Lee DA, Knight MM, Campbell JJ, Bader DL. Stem cell mechanobiology. J Cell Biochem. 2011 Jan;112(1):1–9.

55. Rozario T, DeSimone DW. The extracellular matrix in development and morphogenesis: A dynamic view. Dev Biol. Elsevier Inc.; 2010;341(1):126–40.

56. Wilson CJ, Clegg RE, Leavesley DI, Pearcy MJ. Mediation of Biomaterial – Cell Interactions by Adsorbed Proteins : A Review. 2005;11(1).

57. Hermanson GT. Bioconjugation in the Study of Protein Interactions. Bioconjugate Tech. 2013;989–1016.

58. Thevenot P, Hu W, Tang L. Surface chemistry influences implant biocompatibility. Curr Top Med Chem. 2008;8(4):270–80.

59. Mano JF, Silva GA, Azevedo HS, Malafaya PB, Sousa RA, Silva SS, et al. Natural origin biodegradable systems in tissue engineering and regenerative medicine: present status and some moving trends. J R Soc Interface. 2007;4(17):999–1030.

60. Crapo PM, Gilbert TW, Badylak SF. An overview of tissue and whole organ decellularization processes. Biomaterials. Elsevier Ltd; 2011;32(12):3233–43.

61. Reusch HP, Chan G, Ives HE, Nemenoff RA. Activation of JNK/SAPK and ERK by mechanical strain in vascular smooth muscle cells depends on extracellular matrix composition. Biochem Biophys Res Commun. 1997;237(2):239–44.

62. Madri JA, Pratt BM, Tucker AM. Phenotypic modulation of endothelial cells by transforming growth factor-beta depends upon the composition and organization of the extracellular matrix. J Cell Biol. 1988;106(4):1375–84.

63. Abdeen AA, Weiss JB, Lee J, Kilian KA. Matrix Composition and Mechanics Direct Proangiogenic Signaling from Mesenchymal Stem Cells. Tissue Eng Part A. 2014 Oct;20(19-20):2737–45.

64. Lu P, Weaver VM, Werb Z. The extracellular matrix: A dynamic niche in cancer progression. J Cell Biol. 2012;196(4):395–406.

65. Watt FM, Huck WTS. Role of the extracellular matrix in regulating stem cell fate. Nat Rev Mol Cell Biol. Nature Publishing Group; 2013 Jul 10;14(8):467–73.

66. Lee J, Abdeen AA, Zhang D, Kilian KA. Directing stem cell fate on hydrogel substrates by controlling cell geometry, matrix mechanics and adhesion ligand composition. Biomaterials. 2013;34(33):8140–8.

67. Rowlands AS, George PA, Cooper-White JJ. Directing osteogenic and myogenic differentiation of MSCs: interplay of stiffness and adhesive ligand presentation. Am J Physiol Cell Physiol. 2008 Oct;295(4):1037–44.

68. Fitzpatrick LE, McDevitt TC. Cell-derived matrices for tissue engineering and regenerative medicine applications. Biomater Sci. Royal Society of Chemistry; 2015;3(1):12–24.

69. Hudalla GA, Murphy WL. Biomaterials that regulate growth factor activity via bioinspired interactions. Adv Funct Mater. 2011;21(10):1754–68.

70. Geiger B, Spatz JP, Bershadsky AD. Environmental sensing through focal adhesions. Nat Rev Mol Cell Biol. 2009 Jan;10(1):21–33.

71. Cavalcanti-Adam EA, Aydin D, Hirschfeld-Warneken VC, Spatz JP. Cell adhesion and response to synthetic nanopatterned environments by steering receptor clustering and spatial location. HFSP J. 2008;2(5):276–85.

72. Minton K. Cell adhesion: Integrating the integrin response. Nat Rev Mol Cell Biol. Nature Publishing Group; 2013 Jun 12;14(June):3605.

73. Satav T, Huskens J, Jonkheijm P. Effects of Variations in Ligand Density on Cell Signaling. Small. 2015;(39):n/a – n/a.

74. Martino MM, Mochizuki M, Rothenfluh DA, Rempel SA, Hubbell JA, Barker TH. Controlling integrin specificity and stem cell differentiation in 2D and 3D environments through regulation of fibronectin domain stability. Biomaterials. 2009 Feb;30(6):1089–97.

75. Mrksich M. Using self-assembled monolayers to model the extracellular matrix. Acta Biomater. 2010;5(3):832–41.

76. Kilian KA, Mrksich M. Directing stem cell fate by controlling the affinity and density of ligand-receptor interactions at the biomaterials interface. Angew Chem Int Ed Engl. 2012 May 14;51(20):4891–5.

77. Lohmüller T, Aydin D, Schwieder M, Morhard C, Louban I, Pacholski C, et al. Nanopatterning by block copolymer micelle nanolithography and bioinspired applications. Biointerphases. 2011;6(1):MR1–R12.

78. Roca-Cusachs P, Iskratsch T, Sheetz MP. Finding the weakest link: exploring integrin-mediated mechanical molecular pathways. J Cell Sci. 2012 Jul 1;125(Pt 13):3025–38.

79. Roca-Cusachs P, del Rio A, Puklin-Faucher E, Gauthier NC, Biais N, Sheetz MP. Integrin-dependent force transmission to the extracellular matrix by alpha-actinin triggers adhesion maturation. Proc Natl Acad Sci. 2013 Mar 20;

80. Arnold M, Cavalcanti-Adam EA, Glass R, Blümmel J, Eck W, Kantlehner M, et al. Activation of Integrin Function by Nanopatterned Adhesive Interfaces. ChemPhysChem. 2004;5(3):383–8.

81. Deeg JA, Louban I, Aydin D, Selhuber-Unkel C, Kessler H, Spatz JP. Impact of Local versus Global Ligand Density on Cellular Adhesion. Nano Lett. 2011;11(4):1469–76.

82. Trappmann B, Gautrot JE, Connelly JT, Strange DGT, Li Y, Oyen ML, et al. Extracellular-matrix tethering regulates stem-cell fate. Nat Mater. Nature Publishing Group; 2012 Jan;11(7):642–9.

83. Théry M, Pépin A, Dressaire E, Chen Y, Bornens M. Cell distribution of stress fibres in response to the geometry of the adhesive environment. Cell Motil Cytoskeleton. 2006 Jun;63(6):341–55.

84. DeForest CA, Anseth KS. Photoreversible patterning of biomolecules within click-based hydrogels. Angew Chem Int Ed Engl. 2012 Feb 20;51(8):1816–9.

85. Tumarkin E, Tzadu L, Csaszar E, Seo M, Zhang H, Lee A, et al. High-throughput combinatorial cell co-culture using microfluidics. Integr Biol (Camb). 2011 Jun;3(6):653–62.

86. Alom Ruiz S, Chen CS. Microcontact printing: A tool to pattern. Soft Matter. 2007;3(2):168.

87. Hughes LD, Boxer SG. DNA-based patterning of tethered membrane patches. Langmuir. 2013;29(39):12220–7.

88. Chien F-C, Kuo CW, Yang Z-H, Chueh D-Y, Chen P. Exploring the Formation of Focal Adhesions on Patterned Surfaces Using Super-Resolution Imaging. Small. 2011;7(20):2906–13.

89. Shabbir SH, Cleland MM, Goldman RD, Mrksich M. Geometric control of vimentin intermediate filaments. Biomaterials. 2014;35(5):1359–66.

90. Théry M, Racine V, Piel M, Pépin A, Dimitrov A, Chen Y, et al. Anisotropy of cell adhesive microenvironment governs cell internal organization and orientation of polarity. Proc Natl Acad Sci. 2006;103(52):19771–6.

91. Versaevel M, Grevesse T, Gabriele S. Spatial coordination between cell and nuclear shape within micropatterned endothelial cells. Nat Commun. Nature Publishing Group; 2012;3:671.

92. Jain N, Iyer KV, Kumar A, Shivashankar G V. Cell geometric constraints induce modular gene-expression patterns via redistribution of HDAC3 regulated by actomyosin contractility. Proc Natl Acad Sci. 2013 Jun 24;110(28):3–8.

93. Le Beyec J, Xu R, Lee S-Y, Nelson CM, Rizki A, Alcaraz J, et al. Cell shape regulates global histone acetylation in human mammary epithelial cells. Exp Cell Res. 2007;313(14):3066–75.

94. Chen CS. Geometric Control of Cell Life and Death. Science. 1997 May 30;276(5317):1425–8.

95. Zhang D, Kilian KA. The effect of mesenchymal stem cell shape on the maintenance of multipotency. Biomaterials. 2013 May;34(16):3962–9.

96. McBeath R, Pirone DM, Nelson CM, Bhadriraju K, Chen CS. Cell shape, cytoskeletal tension, and RhoA regulate stem cell lineage commitment. Dev Cell. 2004 Apr;6(4):483–95.

97. Kilian KA, Bugarija B, Lahn BT, Mrksich M. Geometric cues for directing the differentiation of mesenchymal stem cells. Proc Natl Acad Sci. 2010 Mar 16;107(11):4872–7.

98. Lee J, Abdeen AA, Tang X, Saif TA, Kilian KA. Geometric guidance of integrin mediated traction stress during stem cell differentiation. Biomaterials. Elsevier Ltd; 2015 Nov;69:174–83.

99. Akhtar R, Sherratt MJ, Cruickshank JK, Derby B. Characterizing the elastic properties of tissues. Mater Today. Elsevier Ltd; 2011;14(3):96–105.

100. Jaalouk DE, Lammerding J. Mechanotransduction gone awry. Nat Rev Mol Cell Biol. 2009 Jan;10(1):63–73.

101. Takahashi K, Kakimoto Y, Toda K, Naruse K. Mechanobiology in cardiac physiology and diseases. J Cell Mol Med. 2013 Feb;17(2):225–32.

102. Discher DE, Janmey P, Wang Y-L. Tissue cells feel and respond to the stiffness of their substrate. Science. 2005 Nov 18;310(5751):1139–43.

103. Solon J, Levental I, Sengupta K, Georges PC, Janmey PA. Fibroblast Adaptation and Stiffness Matching to Soft Elastic Substrates. Biophys J. 2007;93(12):4453–61.

104. Storm C, Pastore JJ, MacKintosh FC, Lubensky TC, Janmey PA. Nonlinear elasticity in biological gels. Nature. 2005 May 12;435(7039):191–4.

105. Han SJ, Bielawski KS, Ting LH, Rodriguez ML, Sniadecki NJ. Decoupling substrate stiffness, spread area, and micropost density: a close spatial relationship between traction forces and focal adhesions. Biophys J. 2012 Aug 22;103(4):640–8.

106. Dupont S, Morsut L, Aragona M, Enzo E, Giulitti S, Cordenonsi M, et al. Role of YAP/TAZ in mechanotransduction. Nature. Nature Publishing Group; 2011 Jun 9;474(7350):179–83.

107. Swift J, Ivanovska IL, Buxboim A, Harada T, Dingal PCDP, Pinter J, et al. Nuclear lamin-A scales with tissue stiffness and enhances matrix-directed differentiation. Science. 2013 Aug 30;341(6149):1240104.

108. Wang N, Tytell JD, Ingber DE. Mechanotransduction at a distance: mechanically coupling the extracellular matrix with the nucleus. Nat Rev Mol Cell Biol. 2009 Jan;10(1):75–82.

109. Engler AJ, Sen S, Sweeney HL, Discher DE. Matrix elasticity directs stem cell lineage specification. Cell. 2006 Aug 25;126(4):677–89.

110. Engler AJ, Griffin MA, Sen S, Bönnemann CG, Sweeney HL, Discher DE. Myotubes differentiate optimally on substrates with tissue-like stiffness: pathological implications for soft or stiff microenvironments. J Cell Biol. 2004 Sep 13;166(6):877–87.

111. Han F, Zhu C, Guo Q, Yang H, Li B. Cellular modulation by the elasticity of biomaterials. J Mater Chem B. Royal Society of Chemistry; 2016;

112. Yang C, Tibbitt MW, Basta L, Anseth KS. Mechanical memory and dosing influence stem cell fate. Nat Mater. 2014;13(6):645–52.

113. Lee J, Abdeen AA, Kilian KA. Rewiring mesenchymal stem cell lineage specification by switching the biophysical microenvironment. Sci Rep. 2014;4:5188.

114. Wen JH, Vincent LG, Fuhrmann A, Choi YS, Hribar KC, Taylor-Weiner H, et al. Interplay of matrix stiffness and protein tethering in stem cell differentiation. Nat Mater. 2014;13(10):979–87.

115. Huebsch N, Lippens E, Lee K, Mehta M, Koshy ST, Darnell MC, et al. Matrix Elasticity of Void-Forming Hydrogels Controls Matrix elasticity of void-forming

hydrogels controls Transplanted Stem Cell-Mediated bone. 2015;14(September):1–19.

116. Cameron AR, Frith JE, Cooper-White JJ. The influence of substrate creep on mesenchymal stem cell behaviour and phenotype. Biomaterials. Elsevier Ltd; 2011 Sep;32(26):5979–93.

117. Khetan S, Guvendiren M, Legant WR, Cohen DM, Chen CS, Burdick J a. Degradation-mediated cellular traction directs stem cell fate in covalently crosslinked three-dimensional hydrogels. Nat Mater. Nature Publishing Group; 2013 May;12(5):458–65.

118. Chaudhuri O, Gu L, Klumpers D, Darnell M, Bencherif SA, Weaver JC, et al. Hydrogels with tunable stress relaxation regulate stem cell fate and activity. Nat Mater. 2015;(November).

119. Kim D-H, Provenzano PP, Smith CL, Levchenko A. Matrix nanotopography as a regulator of cell function. J Cell Biol. 2012;197(3):351–60.

120. Norman JJ, Desai TA. Methods for Fabrication of Nanoscale Topography for Tissue Engineering Scaffolds. Ann Biomed Eng. 2006;34(1):89–101.

121. Bettinger CJ, Langer R, Borenstein JT. Engineering substrate topography at the Micro- and nanoscale to control cell function. Angew Chemie - Int Ed. 2009;48(30):5406–15.

122. Yim EKF, Pang SW, Leong KW. Synthetic nanostructures inducing differentiation of human mesenchymal stem cells into neuronal lineage. Exp Cell Res. 2007;313(9):1820–9.

123. Dalby MJ, Gadegaard N, Tare R, Andar A, Riehle MO, Herzyk P, et al. The control of human mesenchymal cell differentiation using nanoscale symmetry and disorder. Nat Mater. Nature Publishing Group; 2007 Dec;6(12):997–1003.

124. Downing TL, Soto J, Morez C, Houssin T, Fritz A, Yuan F, et al. Biophysical regulation of epigenetic state and cell reprogramming. Nat Mater. Nature Publishing Group; 2013;12(12):1154–62.

125. Cox TR, Erler JT. Remodeling and homeostasis of the extracellular matrix: implications for fibrotic diseases and cancer. Dis Model Mech. 2011;4(2):165–78.

126. Banik BL, Brown JL. 8 - Interaction of responsive/switchable surfaces with cells. In: Zhang Z, editor. Switchable and Responsive Surfaces and Materials for Biomedical Applications. Oxford: Woodhead Publishing; 2015. p. 45–64.

127. Kim J, Hayward RC. Mimicking dynamic in vivo environments with stimuli-responsive materials for cell culture. Trends Biotechnol. Elsevier Ltd; 2012 Aug;30(8):426–39.

128. Raeber GP, Lutolf MP, Hubbell JA. Molecularly engineered PEG hydrogels: a novel model system for proteolytically mediated cell migration. Biophys J. 2005 Aug;89(2):1374–88.

129. Kloxin AM, Kloxin CJ, Bowman CN, Anseth KS. Mechanical properties of cellularly responsive hydrogels and their experimental determination. Adv Mater. 2010 Aug 17;22(31):3484–94.

130. Burdick JA, Murphy WL. Moving from static to dynamic complexity in hydrogel design. Nat Commun. Nature Publishing Group; 2012 Jan;3:1269.

131. Baker BM, Chen CS. Deconstructing the third dimension: how 3D culture microenvironments alter cellular cues. J Cell Sci. 2012 Jul 1;125(13):3015–24.

132. Fischbach C, Kong HJ, Hsiong SX, Evangelista MB, Yuen W, Mooney DJ. Cancer cell angiogenic capability is regulated by 3D culture and integrin engagement. Proc Natl Acad Sci. 2009 Jan 13;106(2):399–404.

133. DeVolder R, Kong H-J. Hydrogels for in vivo-like three-dimensional cellular studies. Wiley Interdiscip Rev Syst Biol Med. 2012;4(4):351–65.

134. Aydin D, Louban I, Perschmann N, Blümmel J, Lohmüller T, Cavalcanti-Adam EA, et al. Polymeric substrates with tunable elasticity and nanoscopically controlled biomolecule presentation. Langmuir. 2010 Oct 5;26(19):15472–80.

135. Leckband D, Prakasam A. Mechanism and Dynamics of Cadherin Adhesion. Annu Rev Biomed Eng. 2006;8(1):259–87.

136. Goubko CA, Cao X. Patterning multiple cell types in co-cultures: A review. Mater Sci Eng C. Elsevier B.V.; 2009;29(6):1855–68.

137. Huang S, Brangwynne CP, Parker KK, Ingber DE. Symmetry-breaking in mammalian cell cohort migration during tissue pattern formation: Role of random-walk persistence. Cell Motil Cytoskeleton. 2005;61(4):201–13.

138. Petitjean L, Reffay M, Grasland-Mongrain E, Poujade M, Ladoux B, Buguin A, et al. Velocity Fields in a Collectively Migrating Epithelium. Biophys J. Biophysical Society; 2010;98(9):1790–800.

139. Tseng Q, Duchemin-Pelletier E, Deshiere A, Balland M, Guillou H, Filhol O, et al. Spatial organization of the extracellular matrix regulates cell-cell junction positioning. Proc Natl Acad Sci. 2012;109(5):1506–11.

140. Lecuit T, Lenne P-F. Cell surface mechanics and the control of cell shape, tissue patterns and morphogenesis. Nat Rev Mol Cell Biol. 2007 Aug;8(8):633–44.

141. Jakab K, Norotte C, Marga F, Murphy K, Vunjak-Novakovic G, Forgacs G. Tissue engineering by self-assembly and bio-printing of living cells. Biofabrication. 2010;2(2):022001.

142. Shen K, Luk S, Hicks DF, Elman JS, Bohr S, Iwamoto Y, et al. Resolving cancer–stroma interfacial signalling and interventions with micropatterned tumour–stromal assays. Nat Commun. Nature Publishing Group; 2014;5:5662.

143. Foty RA, Steinberg MS. Differential adhesion in model systems. Wiley Interdiscip Rev Dev Biol. 2013;2(5):631–45.

144. Beysens DA, Forgacs G, Glazier JA. Cell sorting is analogous to phase ordering in fluids. Proc Natl Acad Sci. 2000;97(17):9467–71.

145. Manning ML, Foty RA, Steinberg MS, Schoetz E-M. Coaction of intercellular adhesion and cortical tension specifies tissue surface tension. Proc Natl Acad Sci. 2010 Jul 13;107(28):12517–22.

146. Nelson CM, Jean RP, Tan JL, Liu WF, Sniadecki NJ, Spector A a, et al. Emergent patterns of growth controlled by multicellular form and mechanics. Proc Natl Acad Sci. 2005 Aug 16;102(33):11594–9.

147. Gomez EW, Chen QK, Gjorevski N, Nelson CM. Tissue geometry patterns epithelial-mesenchymal transition via intercellular mechanotransduction. J Cell Biochem. 2010;110(March):44–51.

148. Nelson CM, Vanduijn MM, Inman JL, Fletcher DA, Bissell MJ. Tissue geometry determines sites of mammary branching morphogenesis in organotypic cultures. Science. 2006;314(5797):298–300.

149. Keenan TM, Folch A. Biomolecular gradients in cell culture systems. Lab Chip. 2008;8(1):34–57.

150. Kolesky DB, Truby RL, Gladman AS, Busbee TA, Homan KA, Lewis JA. 3D bioprinting of vascularized, heterogeneous cell-laden tissue constructs. Adv Mater. 2014;26(19):3124–30.

CHAPTER 2

MATRIX COMPOSITION AND MECHANICS DIRECTS PRO-ANGIOGENIC SIGNALING FROM MESENCHYMAL STEM CELLS[1]

2.1 Introduction

Research efforts aimed at controlling the MSC secretome for clinical applications have explored multiple strategies including hypoxic(1,2), pharmacological(3), cytokine(4), or growth factor(5) preconditioning, and/or genetic manipulations(6,7). An important aspect of the MSC microenvironment that has been shown to influence growth and differentiation—but has been relatively unexplored in guiding the MSC secretome—is the physical characteristics of the extracellular matrix(8–12). It has been shown that treating matrigel cultures of HUVECs with conditioned media from MSCs cultured under tension leads to enhanced tubulogenesis and signaling through the FGFR1 pathway(13). In addition, MSCs cultured on compliant substrates show dramatic differences in Il-8 expression as substrate stiffness increases(14). These reports suggest that the mechanical microenvironment surrounding MSCs can play a significant role in regulating pro-angiogenic signaling. In addition to mechanical properties, the composition of the matrix might have a role as well as it has been shown to influence cell spreading

[1] This chapter is adapted from the following publication:
Amr A. Abdeen, Jared B. Weiss, Junmin Lee, and Kristopher A. Kilian, Matrix composition and mechanics directs pro-angiogenic signaling from mesenchymal stem cells, Tissue Engineering, Part A, 2014, 20 (19-20), 2737-2745.

and MSC differentiation(10,12). In a recent study, the effect of matrix composition was investigated in a fibrin-based MSC-HUVEC co-culture system(15). This work demonstrates that the collagen/fibrin ratio can affect network formation and an inverse relation between matrix stiffness and network formation exists. While this study provides some insight into the complex interplay of ligand composition and matrix mechanics, the precise role these factors play in directing pro-angiogenic signaling remains to be revealed.

In this chapter we use a model polyacrylamide hydrogel system, where we can independently tune matrix composition and stiffness, to investigate pro-angiogenic signaling from adherent MSCs. Cells cultured on fibronectin hydrogels show stiffness dependence in secretion of pro-angiogenic molecules as determined by monitoring tubulogenesis from endothelial cells in matrigel. Using soft-lithography to restrict cell spreading, we find partial abrogation of the stiffness trend. Quantitative RT-PCR reveals a complex regulation of secretory molecules from MSCs in response to substrate stiffness and matrix protein composition. The approach presented here may prove a facile method to screen for optimum conditions that promote secretion of pro-angiogenic factors towards the development of injectable biomaterials for cell-based regenerative therapies.

2.2 Materials and Methods

General materials and methods are given in Appendix A.

Fluorescent protein labelling

Fibronectin, collagen and laminin were labelled with fluorescein isothiocyanate (FITC) using a procedure adapted from literature(16). The protein to be labelled is prepared as 1 mg/ml in carbonate buffer (pH=9). A 1 mg/ml FITC solution is prepared and 10 µl are added per ml of protein solution. The reaction is left to proceed at room temperature for 2 hours in the dark and excess FITC is removed by running the reaction mixture through centrifuge filter units with a 10,000 MWCO (Millipore). Standard curves were generated using a Nanodrop nd-1000 spectrophotometer (Thermo Fisher Scientific).

Vascularization assays

Conditioned media was collected from the cultured MSCs (p2-p8) and the cells were fixed and stained by day 4. 25 µL of matrigel was pipetted into each well of a 48 well plate. The plate was then placed in the incubator for 30 minutes to form the gel structure. hMVECs of low passage (p2-p6) were seeded at ~15,000 cells/well. 500 µL of conditioned media obtained from the gels at 4 days were added at each condition. The assay was incubated and Images of the wells were taken at different time-points using a Cannon Rebel DSLR camera on an inverted microscope at 40x zoom.

For blocking experiments, VEGF blocking antibody (R&D Systems) was added to the conditioned media right after adding the hMVECs according to the manufacturer's instructors.

Polymerase Chain Reaction (RT-PCR) analysis:

For PCR analysis, cells were lysed at 2 days using TRIZOL reagent (Life Technologies). RNA was isolated by chloroform extraction (Fischer) and ethanol precipitation. The amounts of RNA were normalized and then cDNA first strand synthesis was performed with a superscript III kit (Invitrogen) as per the vendor's instructions. For the PCR reactions, the following primers were used (Table 2.1) along with a SYBR green master mix (Invitrogen) in 20μL reactions in a realtime PCR machine (Eppendorf). The PCR results for each factor were normalized to GAPDH and then between different biological replicates the samples were normalized to the glass condition.

Marker	Forward	Reverse
GAPDH	CTC TGC TCC TCC TGT TCG AC	GTT TCT CTC CGC CCG TCT TC
VEGF	CTG CTG TCT TGG GTG CAT TG	GGC ACG ACC GCT TAC CTT
Angiogenin	GCA GCG AAT AAG TAC GTG GC	CAG AGA CTA CCC CTG GCT GA
Il-8	ACC GGA AGG AAC CAT CTC AC	CGC TGT AGG TCA GAA AGA TGT G
IL-6	GTCAGGGGTGGTTATTGCAT	AGTGAGGAACAAGCCAGAGC
HGF	CCCTGTAGCCTTCTCCTTGA	CGCTGGGAGTACTGTGCAAT
IGF	TCATCCACGATGCCTGTCT	TGGATGCTCTTCAGTTCGTG
EGF	TGGTTCCTTCTGTGTCAATCC	GTACTCTCGCAGGAAATGGG
TIMP-1	GCC TGT CTA CTC AGC TTG GC	TTG GGA AAG CAG TTC CAG CC
TIMP-2	ATG TCC AGA ACC CGG CAA TG	TTC CCT GCA GGT TAG ACC CC

Table 2.1 PCR primers used

Protein Expression Analysis:

Conditioned media from the hMSC cultures was separated in SDS polyacrylamide gels and transferred to a nitrocellulose membrane (General Electric Healthcare) in 25 mM Tris, 192 mM glycine, 0.1% SDS, and 20% methanol using a semi-dry electroblotting system (Amersham Biosciences). Membranes were blocked with 5% bovine serum albumin in Tris-buffered saline (TBS; 50 mM Tris pH 8.0, 150 mM

NaCl) for 1 h at room temperature, primary antibodies (Santa Cruz Biotechnology) were added in TBS buffer plus 0.1% Tween-20 (TBS-T), incubated overnight at 4°C with shaking, followed by washing with TBS-T. Horseradish peroxidase-conjugated antirabbit secondary antibodies (Invitrogen) were used to detect labelling of the transferred material using a substrate kit (Amresco).

Data analysis:

Tube formation was quantitated using the ImageJ software (NIH). Images were converted to black and white, background subtracted and were thresholded to identify cells. The 'analyze particles' function was then used to identify tubes from isolated cells to quantitate tube area as a fraction of total area (Figure 2.1). Statistical significance was determined using ANOVA for comparing multiple groups and using two-tailed p-values from unpaired t-test for comparing two groups.

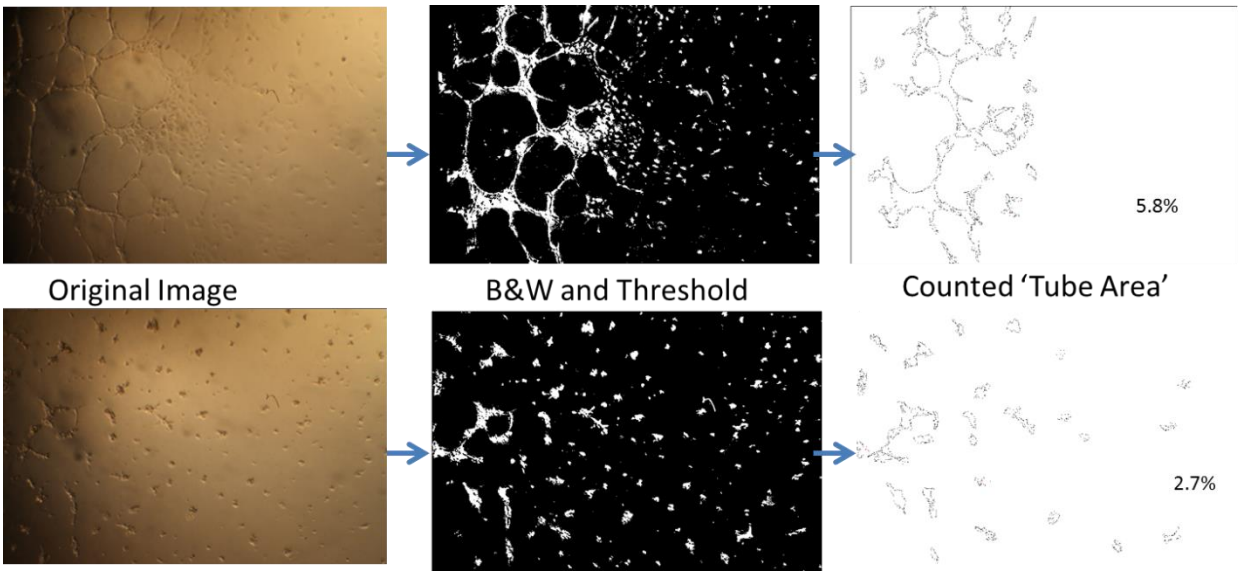

Figure 2.1 Analysis method for quantifying tube area. Images are analyzed using ImageJ. Images are turned into black and white and then thresholded. Images are then analyzed to quantify tube area excluding 'particles' below a certain threshold size.

2.3 Results

Polyacrylamide gel fabrication and chemical modification

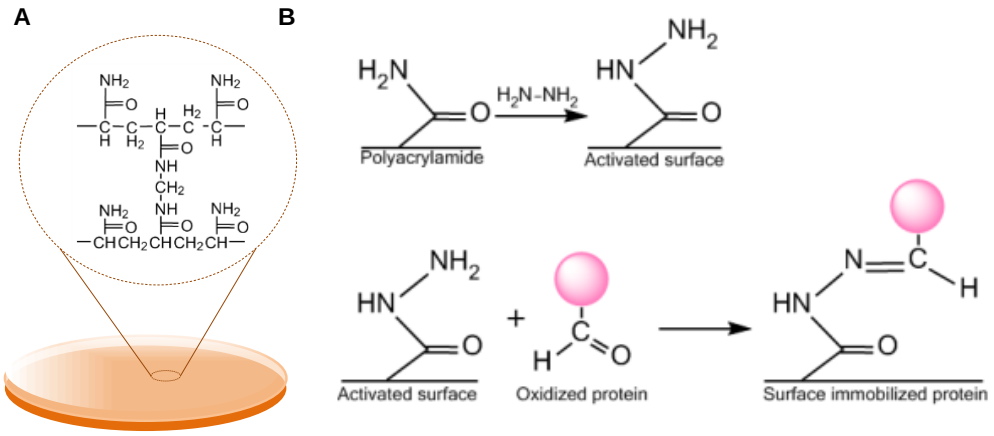

Figure 2.2 Polyacrylamide gel fabrication and conjugation (A) Polyacrylamide gel structure. (B) Hydrazine treatment of the gel surface yields hydrazide groups which react with the activated proteins to covalently attach the protein to the gel surface.

In order to study how the combination of matrix protein and hydrogel stiffness influence MSC adhesion and secretion, we utilized a polyacrylamide hydrogel fabrication procedure (17,18) (Figure 2.2A). Three gels of different Young's modulus were prepared to cover a physiologically relevant range: 0.5, 10 and 40 kPa. Young's moduli were confirmed using AFM contact force measurements (Figure 2.3). The gels were optically transparent which is important to enable confocal immunofluorescence analysis of adherent cells. Next, we optimized a chemical modification procedure in order to covalently couple common extracellular matrix proteins to the hydrogel surfaces(18). Hydrazine hydrate was applied to the hydrogels to modify the acrylamide moieties at the surface of the gel to yield distal reactive hydrazide groups (Figure 2.2B). We chose matrix proteins that are

common constituents in the perivascular microenvironment—fibronectin, collagen and laminin—and oxidized the proteins using sodium periodate. Addition of the oxidized protein to the hydrogel surface leads to rapid conjugation within 1 hour.

A

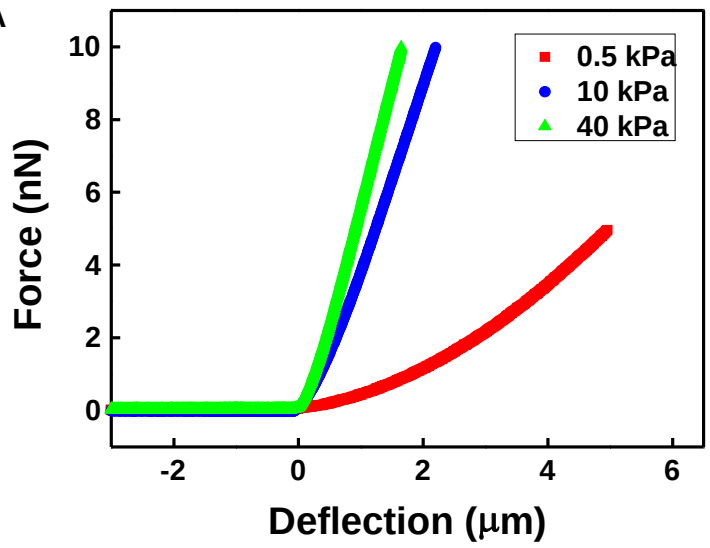

B

Desired Young's Modulus (kPa)	Acrylamide (wt%)	Bis-Acrylamide (wt%)	Measured Young's Modulus (kPa)
0.5	3	0.06	0.6
10	10	0.1	11.2
40	8	0.48	33.18

Figure 2.3 AFM contact force measurements of hydrogel elasticity (A) Force-deflection curves of in different formulations of polyacrylamide. (B) Measured Young's moduli for these formulations.

To verify bioconjugation, we first mixed an Alexa-647 conjugated fibrinogen with the selected matrix protein to confirm protein conjugation and pattern fidelity as demonstrated in a previous report(19). Immunofluorescence analysis of the conjugated gels indicates higher fluorescence intensity on the gels that were treated with hydrazine, thus confirming conjugation (Figure 2.4). To ascertain the conjugation efficiency between protein and across gels of different stiffness, we

labelled our three matrix proteins with fluorescein isothiocyanate (FITC) prior to oxidation. After conjugation to the surface, the raw surface fluorescence was normalized to standard curves for each fluorescence protein solution (Figure 2.5). This analysis reveals comparable protein conjugation for fibronectin, laminin and collagen immobilized to gels of the same stiffness. However, there are significant increases in all protein conjugations as the stiffness is increased. Since stiffness is increased by changing cross-link density, it is unsurprising that the quantity of conjugated protein increases as available attachment points on the surface increase.

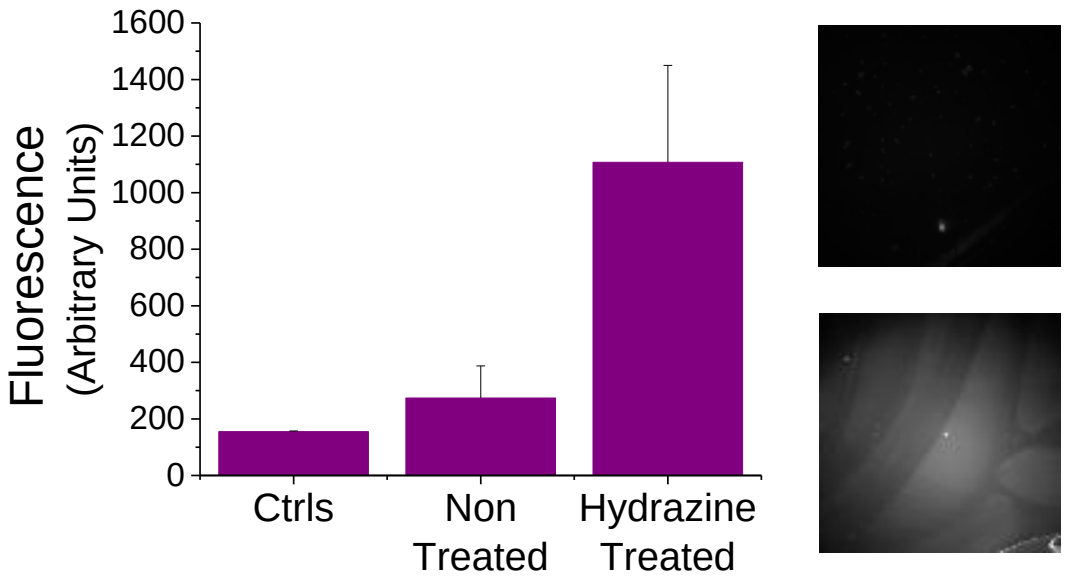

Figure 2.4 (left) fluorescence measurements made with Alexa-546 fibrinogen to confirm protein immobilization. (right) fluorescence image of non hydrazine treated(top) vs hydrazine treated (bottom). Error bars represent standard deviation from at least 3 replicates

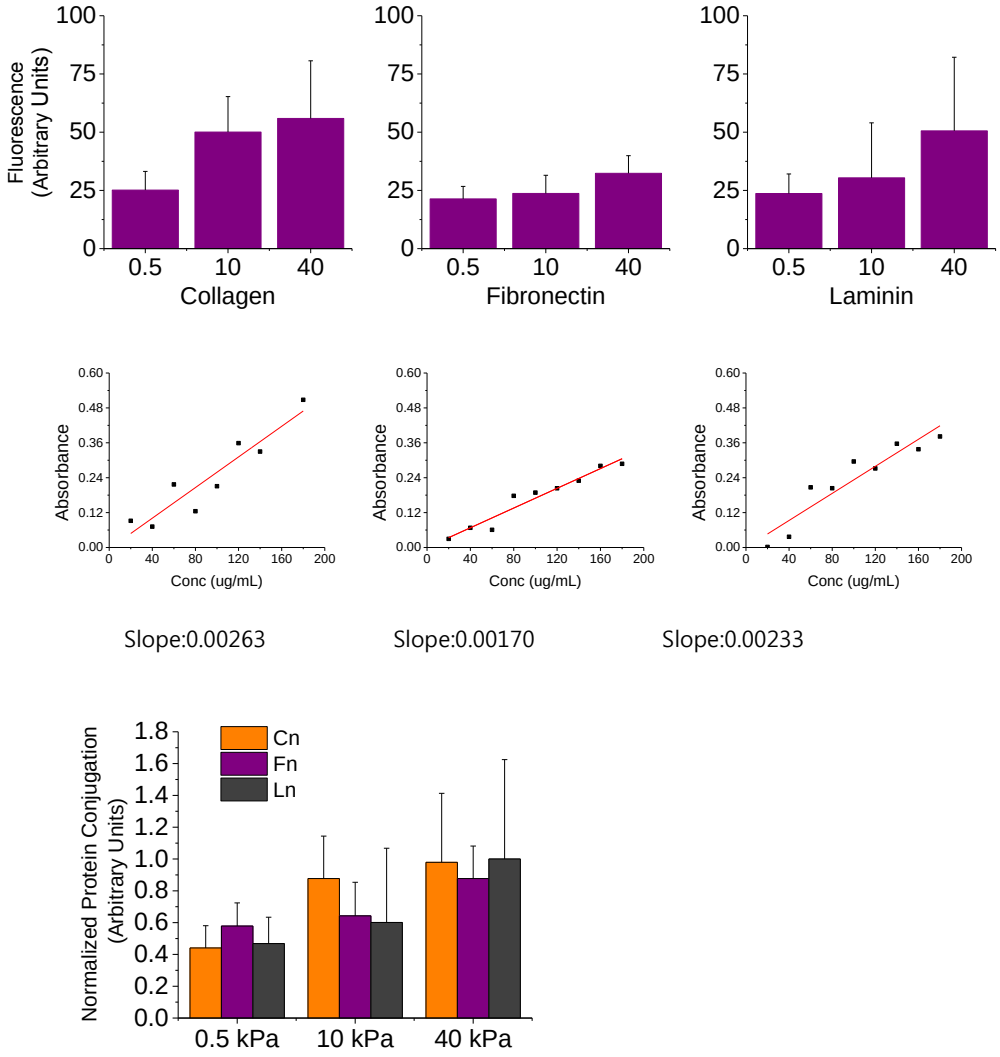

Figure 2.5 Surface fluorescence intensity of FITC conjugated proteins to hydrogels of different stiffness (top), the corresponding standard curves of these proteins in solution (middle) after subtracting baseline values and surface intensities normalized to standard curve slopes (bottom).

Mesenchymal stem cell culture on protein functionalized gels

We next tested MSC adhesion to our protein functionalized hydrogels. The ECM-protein conjugated gels showed a significantly higher degree of MSC adhesion compared to the unmodified gels confirming the validity of our conjugation strategy. MSCs showed very different morphologies across substrates of different

mechanical properties (Figure 2.6A). The cells were mostly small and round on the soft, compliant substrates with many instances of two or more cells grouped together, suggesting a preference for intercellular adhesion. There were similar numbers of cells across the tested gel surfaces (Figure 2.6B). The cell projected area increased with increasing stiffness (Figure 2.6C) which is consistent with literature that has demonstrated increased cell spreading with substrates of increased stiffness(10,20). On the intermediate 10 kPa gels, the cells were more elongated, and stress fibers appeared more coherent. On the stiffest gels, the cells show the highest spreading with the presence of a robust cytoskeleton. In our system, we noted no appreciable differences in MSC morphology across the different matrix proteins.

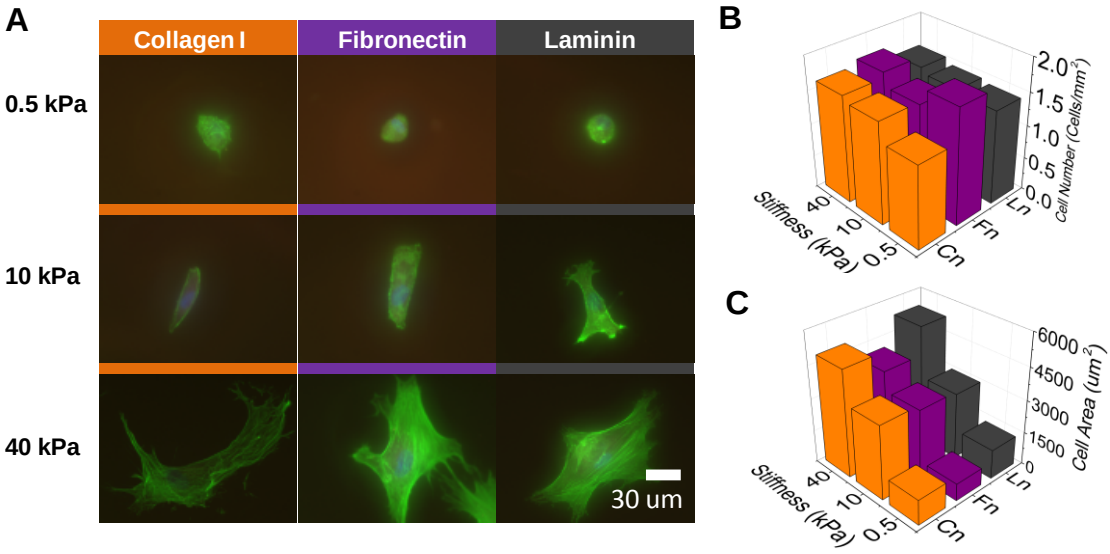

Figure 2.6 MSCs on polyacrylamide hydrogels of different stiffness and ligand composition (A) Phalloidin (green) and DAPI (blue) staining of MSCs on different combinations of stiffness and protein. (B) Cell numbers across the different conditions. (C) Average cell area across the different conditions.

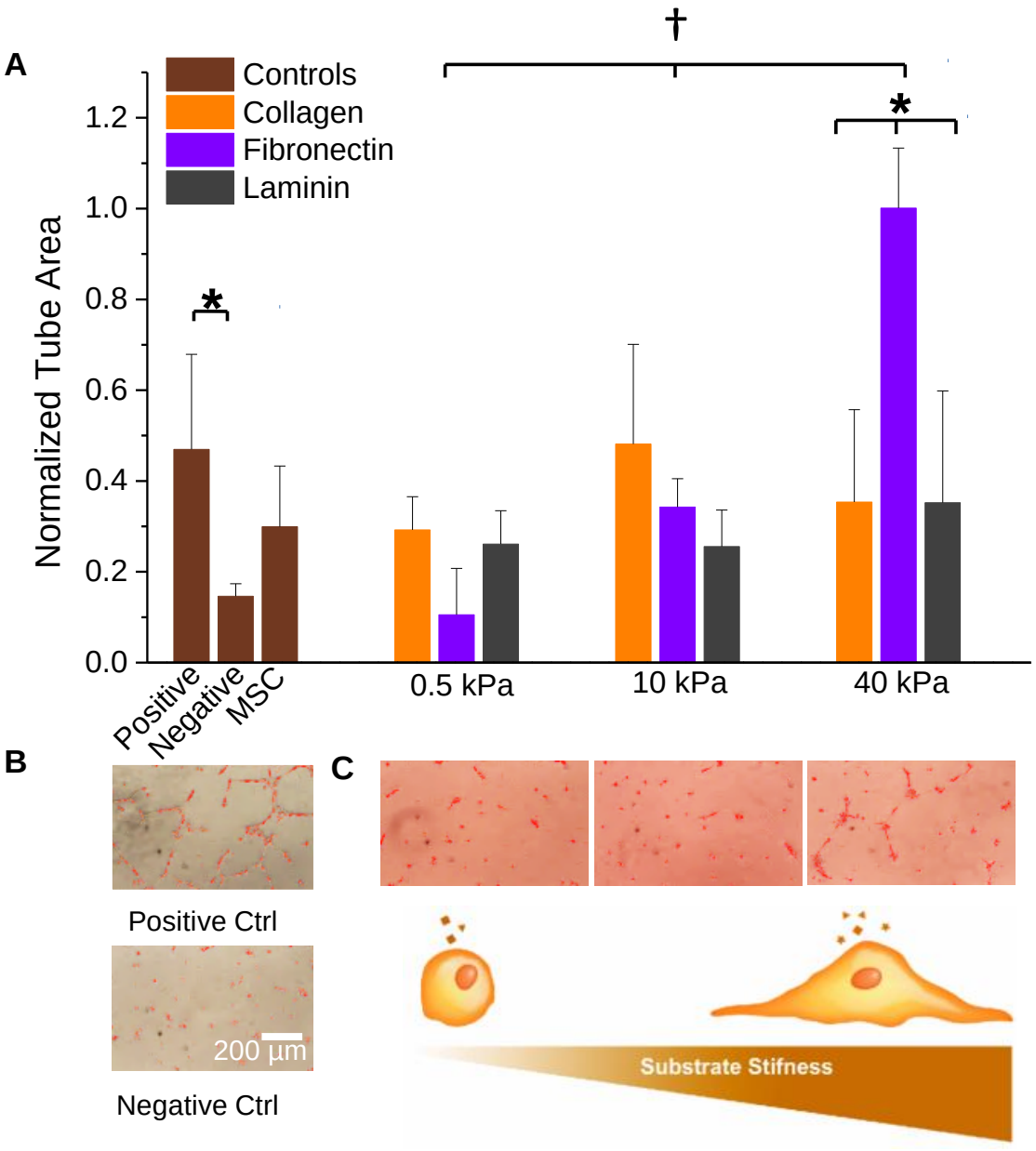

*Figure 2.7 Effects of MSC conditioned media on HMVEC tubulogenesis (A) Average HMVEC tube area after treatment with conditioned media from MSCs cultured across varying stiffness hydrogels and ligand composition. (B) HMVECs under positive (EGM supplemented with growth factor cocktail used for HMVEC culture) and negative controls (unsupplemented media). (C) (top) HMVECs cultured under media from the Fibronectin 0.5, 10 and 40 kPa conditions respectively, (bottom) substrate stiffness changes MSC cell spreading characteristics and affects their secretory profiles. Error bars represent standard deviation from 3 replicates (N=3). * indicates p value <0.05 and † indicates p<0.001 using one way ANOVA .*

To study the effect of conditioned media from MSCs on vessel formation we explored a matrigel assay using hMVECs (Figure 2.7A). Cells cultured in regular endothelial growth media (EGM; negative control) had very little tube formation while cells cultured in the same media with supplemented growth factors containing a variety of pro-angiogenic molecules had approximately 3-fold more tube formation (Figure 2.7B). Although MSC media (supplemented with FBS) showed considerably less tube formation than the pro-angiogenic media containing growth factors, there was approximately 2-fold higher tubulogenesis than the negative control. It should be noted that MSC media had a higher amount of supplemented FBS (10%) than positive controls (2%) while negative controls had no FBS. This may explain the increase see in MSC media compared to the negative controls due to protein content of the FBS which may include growth factors.

When comparing the MSC conditioned media collected from the hydrogel substrates to the positive and negative controls, there were subtle trends observed in the degree of tubulogenesis although not statistically significant. However, for the fibronectin condition, we observed a stiffness dependent effect where the tube formation increases with increasing stiffness. This was not observed with the other proteins. Strikingly, the Fibronectin-40 kPa condition is approximately 6-fold higher than the Fibronectin-0.5 kPa condition and 2-fold higher than the positive control containing an empirically derived cocktail of growth factors. These differences are readily apparent in the images of the hMVECs (Figure 2.7C, top). The differences in tubulogenesis coincide with changes observed in MSC spreading across gels of different stiffness. This suggests that cell spreading—in conjunction with the

composition of matrix protein—may affect the secretory profile of MSCs (Figure 2.7C, bottom). To test whether cell spreading on fibronectin matrices is responsible for regulating pro-angiogenic signaling, we compared fibronectin coated glass coverslips to the fibronectin-40 kPa hydrogel substrates. Interestingly, even when the number of cells is ~7-fold higher and the degree of spreading is higher, we see less tubulogenesis compared to the fibronectin-40 kPa (Figure 2.8).

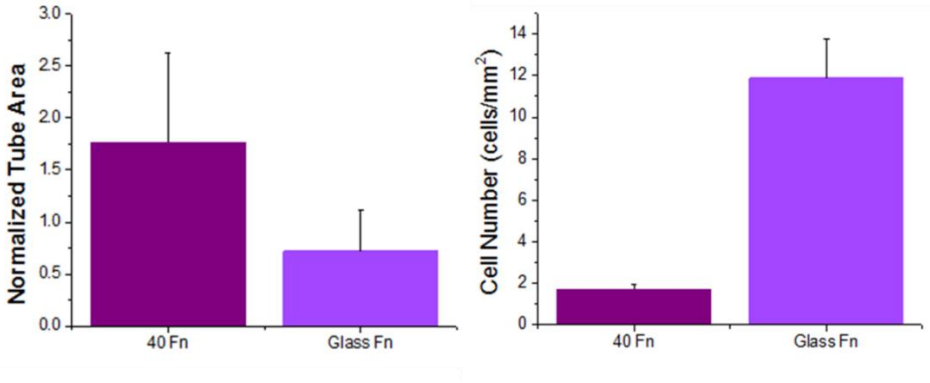

Figure 2.8 Comparing 40kPA gels to the glass condition showing differences in tubulogenesis and cell numbers.

Restricting cell spreading using micropatterned surfaces

To further explore the role of cell spreading on the fibronectin modified hydrogel substrates, we investigated the use of soft-lithography to confine cells to prescribed areas across our surfaces. MSCs were captured in small fibronectin coated islands (3000 μm^2) across the different stiffness gels (Figure 2.9A,B) and the conditioned media from these cultures was added to the hMVEC tube formation assay (Figure 2.9C). Using a high feature density PDMS stamp for the patterned culture yields a higher number of MSCs on the patterned substrate compared to the un-patterned condition (Figure 2.10). Restricting the cells' adhesion area reduced tube formation

at the Fn-40 kPa condition while not significantly affecting the 0.5 or 10 kPa conditions. Interestingly, the conditions with fewer cells—but with optimal spreading on 40 kPa Fibronectin—leads to conditioned media that promotes enhanced tubulogenesis. Therefore, normalizing cell number across patterned and un-patterned conditions may foster an even higher functional outcome when MSCs are allowed to spread. These observations suggest that cell spread area is a factor in controlling the pro-angiogenic secretory properties of MSCs cultured under the Fn-40 kPa condition.

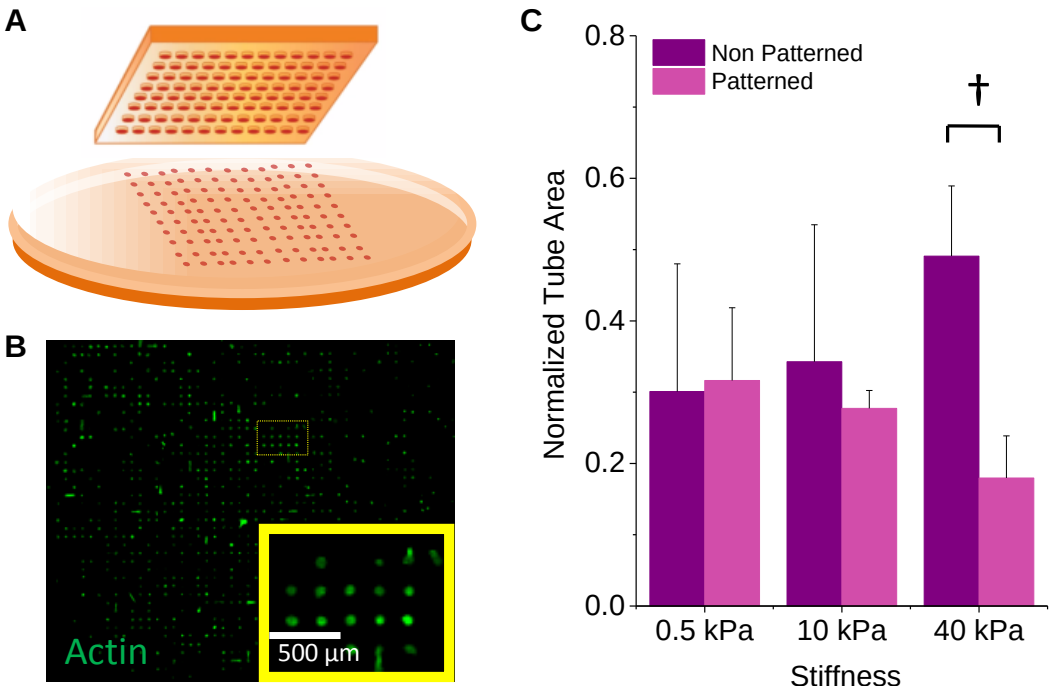

Figure 2.9 MSC Patterning to restrict cell area under the fibronectin condition (A) Fibronectin was patterned on the surface of the gels via soft lithography with a PDMS stamp into 3000um^2 islands. (B) Immunofluorescence image of cells patterned on the surface of a 10 kPa gel (magnified view in inset; green - actin). (C) Effect of restricting cell area on HMVEC tubulogensis. Error bars represent standard deviation from 3 replicates (N=3). † indicates p value <0.01.

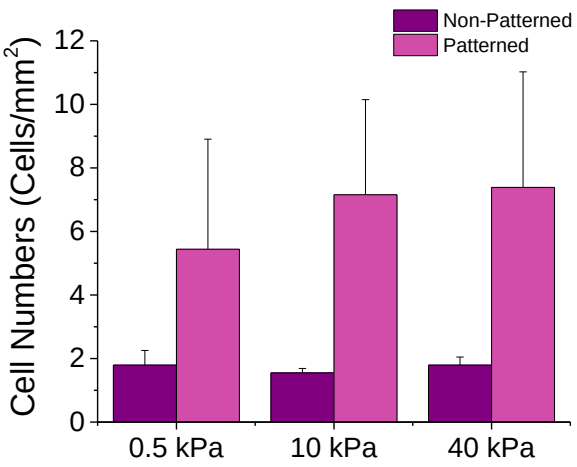

Figure 2.10 Cell numbers across patterned and non-patterned Fn conjugated gels.

Increased cell spreading has been shown to increase cytoskeletal tension and influence aspects of cell fate decisions(8,21,22). To test whether cytoskeletal tension on account of increased spreading is responsible for enhanced secretion from cells cultured on these matrices, we added the small molecules blebbistatin and Y27632 (inhibitors of non-muscle myosin and Rho associated protein kinase (ROCK) respectively) to the adherent MSCs at concentrations that do not significantly alter cell morphology or viability. With the addition of these pharmacological modulators of actomyosin contractility to the MSCs we do not see a statistically significant difference in the functional tubulogenesis assay (Figure 2.11).

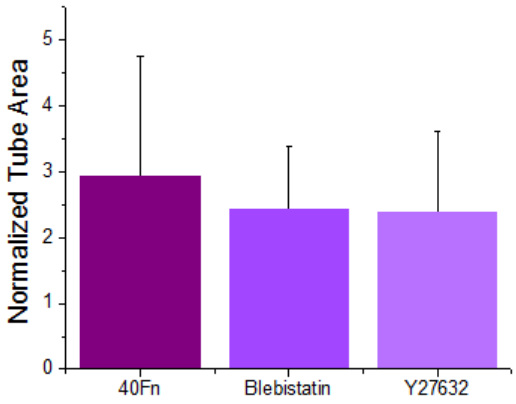

Figure 2.11 Effect of adding drugs inhibiting actomyosin contractility to MSCs on HMVEC tubulogenesis

Quantitative RT-PCR analysis of pro-angiogenic transcripts in MSCs on fibronectin coated surfaces

To investigate whether the differences we observed for the fibronectin condition were due to a change in the secretory profiles of MSCs when cultured on these surfaces we performed real-time polymerase chain reaction (RT-PCR) for a number of cytokines which are known to influence angiogenesis and are secreted by MSCs(23). For angiogenesis promoters we selected vascular endothelial growth factor (VEGF), angiogenin, insulin-like growth factor (IGF), hepatocyte growth factor (HGF), epidermal growth factor (EGF), Interleukin 6 (Il-6) and Interleukin 8 (Il-8) while we selected the tissue inhibitors of metalloproteases, Timp1 and Timp2, as negative regulators of angiogenesis. The PCR results show that all of these factors are modulated by substrate stiffness (Figure 2.12). VEGF expression increased significantly with increasing stiffness with expression in MSCs cultured on 40 kPa gels approximately 3-fold higher than cells cultured on 0.5 kPa gels. Interestingly, all three gel conditions show higher VEGF expression than cells

cultured on glass, which suggests that physiological stiffness will elevate secretion from MSCs. Angiogenin and IGF also show a stiffness dependent trend in expression which increases with gel stiffness. There was no detectable angiogenin expression for the 0.5kPa condition. The expression of Il-6, Il-8 and EGF did not show stiffness dependence. For the angiogenesis inhibitors, Timp1 was expressed 2-fold higher when cells are cultured on gels than on glass with no significant differences between the different gel conditions. Timp2 was similar between all conditions except the 10kPa where it was approximately 4-fold higher.

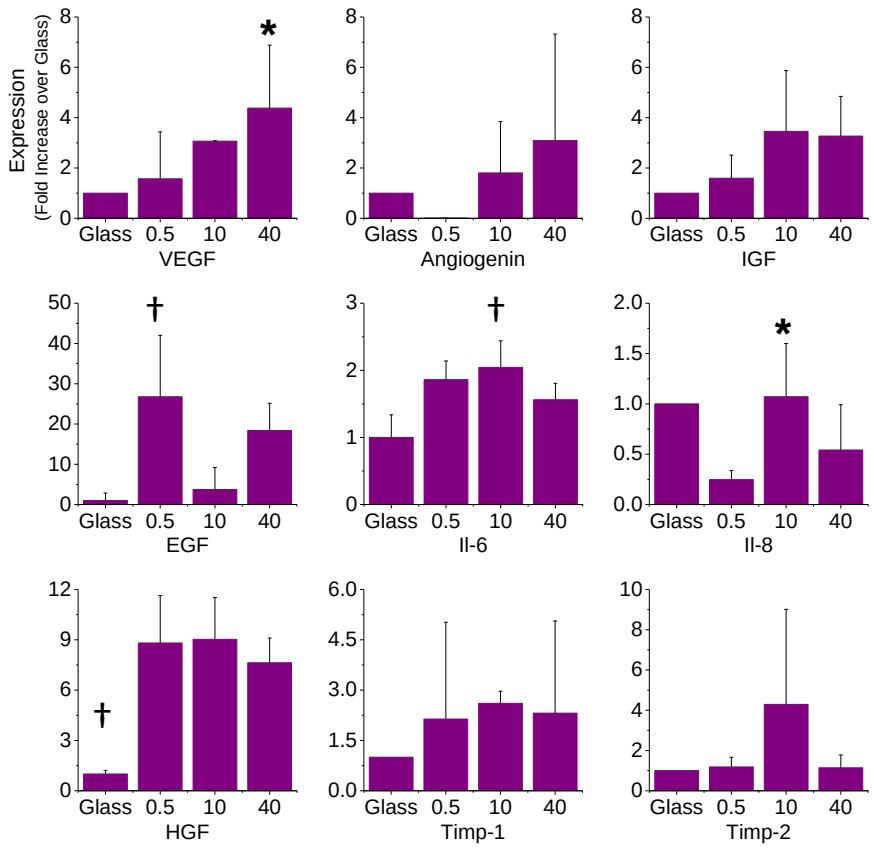

*Figure 2.12 RT-PCR analysis of cytokines involved in angiogenesis. PCR shows differences in expression across different stiffnesses in VEGF, angiogenin, IGF, EGF, Il-6, Il-8, HGF (promoters of angiogenesis) & Timp1 and Timp2 (inhibitors of angiogenesis). The results are shown as fold change relative to the glass condition. Error bars represent standard deviation from at least 5 replicates (N=5). * indicates p value <0.05 and † indicates p<0.01 using one way ANOVA .*

From the gene expression analysis of our panel of putative angiogenesis modulators, we see differential expression depending on both stiffness and specific molecules. While regulation of angiogenesis is a complex interplay between multiple factors, we selected to inhibit VEGF as it was shown to be significantly influenced by substrate stiffness. Protein expression analysis of VEGF was checked using western blotting of conditioned media for VEGF proteins (Figure 2.13A) with a trend of increasing VEGF with increasing stiffness, again with the exception of glass substrates, being noted. To isolate the effects of VEGF, blocking antibodies for VEGF were added to conditioned media prior to seeding of the hMVECs on matrigel. After quantitation, we observe no significant difference in tubulogenesis. To better discern differences between our media conditions, we performed the blocking assay with a supplement of 20% growth media which increased the degree of tubulogenesis across all MSC media conditions. Blocking VEGF in the supplemented conditioned media led to partial abrogation of the stiffness dependent trend; however this data is not statistically significant and merely suggests that VEGF may be one of several factors that regulate tubulogenesis in our assays (Figure 2.13).

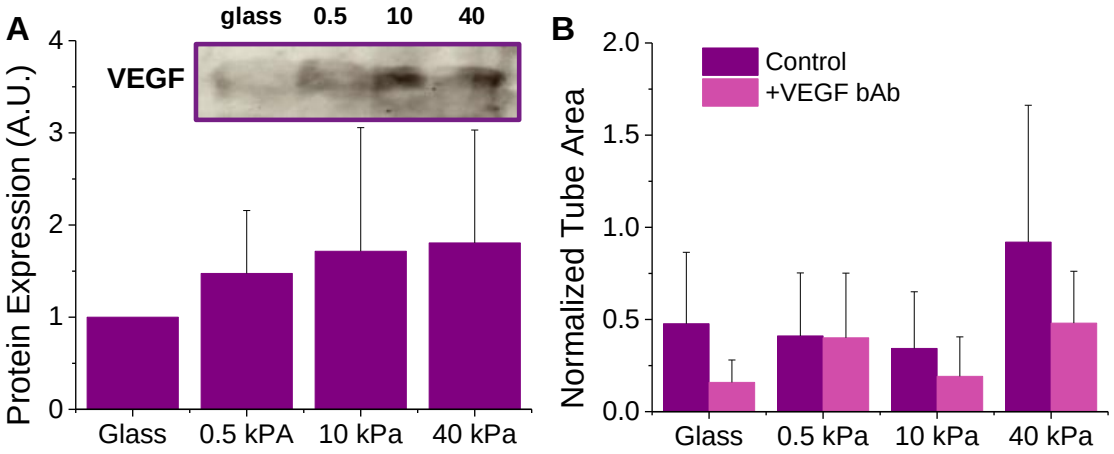

Figure 2.13 (A)Western blotting analysis of VEGF protein expression in the conditioned media after 4 days relative to the glass condition. Inset shows representative blot. (B) The effect of blocking VEGF in conditioned media. Adding VEGF blocking antibody decreases the observed HMVEC tubulogenesis differentially across the conditions. Error bars represent standard deviation from 3 replicates (N=3).

2.4 Discussion

MSCs are an exciting cell-based therapeutic candidate for the treatment of cardiovascular disease with demonstrated clinical efficacy(24). The precise role of MSCs in the healing response remains controversial but is believed to be associated with spatiotemporal secretion of molecules that reduce scarring and increase angiogenesis. Since the clinical efficacy of MSC therapy has proved variable, successful implementation of these cells will require homogenous delivery conditions that are well understood. In this paper we demonstrate an approach to study the biochemical and physical properties of the extracellular matrix surrounding MSCs that guide angiogenic secretory profiles. MSCs were cultured on polyacrylamide hydrogels that are covalently conjugated with matrix proteins collagen I, laminin and fibronectin. The choice of these proteins was guided by the in vivo composition of the native MSC microenvironment that is postulated to be

located in the perivascular space. The adhesion and morphological characteristics of MSCs on these materials shows a stiffness dependence which is in line with previous work(8,10,20). The cell numbers between the different conditions are comparable which enables our empirical observations to be related to secretory effects alone. We note that while conjugation efficiency was similar across ligands, protein incorporation was higher for stiffer gels, likely due to the increased number of reactive groups as cross-link density is increased.

To study the combined role of stiffness and matrix protein on the secretory profile of MSCs, we collected conditioned media from all conditions and applied it to a model angiogenesis assay using hMVECs within matrigel. MSC conditioned media led to enhanced tubulogenesis across all of the conditions; however, only in the case of hydrogels modified with fibronectin did we see a clear trend relating to the influence of substrate mechanical properties. Specifically, we observe an increase in tubulogenesis for hMVECs exposed to MSC-fibronectin conditioned media where 40 kPa is always higher than the lower stiffness conditions. Interestingly, conditioned media from the fibronectin coated glass condition—which will have a modulus on the order of GPa—shows less of a pro-angiogenic effect in the tubulogenesis assay. This result suggests that secretion is not only related to mechanics and there exists an optimal combination of stiffness and adhesion protein for directing pro-angiogenic signaling. Analogous to this finding are earlier reports that demonstrate optimal, physiologically-relevant stiffness regimes for guiding MSC differentiation(8,10).

Previous reports have indicated that the cytoskeletal tension of MSCs can enhance secretion of paracrine factors (9,13). To determine if differences in MSC spreading and actomyosin contractility across the surfaces is responsible for secretion of pro-angiogenic molecules, we restricted cell area using micropatterned hydrogels. Patterning MSCs in small circular islands abrogated the trend in stiffness related secretion, giving support to the idea that cell area is implicated in controlling the angiogenic potential of these cells. However, adding drugs to inhibit actomyosin contractility (Blebbistatin; Y27632) did not cause a significant change in angiogenic potential. This suggests that although spreading plays a role in modulating angiogenic potential, actomyosin contractility is not a major factor.

To further understand MSC secretion on our protein coated hydrogels, we performed gene expression analysis using RT-PCR of key angiogenic molecules. The pro-angiogenic factors VEGF, IGF and Angiogenin show a stiffness-dependent increase in expression that correlates with the functional tubulogenesis assay results. IL8 expression is lowest for MSCs cultured on the 0.5 kPa gel and comparable across glass, 10 kPa and 40 kPa conditions, which suggests this cytokine is not involved in the observed enhancement in tubulogenesis. The expression of Il-6, HGF, EGF and anti-angiogenesis molecules Timp1 and Timp2 does not show a consistent trend across these conditions; however, Timp 2 expression is low in MSCs cultured on the 40 kPa which will assist angiogenic signaling. Importantly, the expression of VEGF, IGF and Angiogenin in MSCs adherent to fibronectin-coated glass is negligible, further validating the result of the tubulogenesis assay. Taken together, these results show that matrix stiffness

influences cytokine expression in a complex way and that the interplay of these factors leads to the final macroscopic result we see in our functional tubulogenesis assays. Since VEGF in particular shows a statistically significant increase in expression on the 40 kPa condition, we chose to inhibit VEGF signaling using function blocking antibodies. VEGF blocking leads to a modest decrease in the stiffness dependent trend in tubulogenesis which suggests that VEGF may play a role in modulating the observed matrix effects. While the differential cytokine expression and blocking experiment provide some clues as to the role of the ECM in promoting differences in the MSC secretome, this system remains very complex, comprising many signaling molecules and intercellular signaling pathways. Future work will benefit from large scale temporal cytokine profiling towards understanding the complex interplay between soluble factors during angiogenesis.

A caveat associated with 2-D assays is that they do not fully replicate the complex signaling associated with 3-D environments(25,26). For instance, Mooney and colleagues demonstrated 35-fold enhancement in IL-8 secretion for oral squamous cell carcinoma cells (OSCC-3) when they were cultured in 3-D alginate compared to the 2-D alginate surfaces(27). MSC encapsulation within hydrogels has been shown to improve their viability during transplantation(28). Ultimately, materials selection for MSC-based therapies will require 3-D materials and we believe that the design parameters obtained from 2-D systems such as the one described here will assist the development of more clinically efficacious 3-D formulations for MSC-based therapies. This is further explored in Chapter 4.

In this chapter, we demonstrate a platform to study the effect of MSC culture conditions—including matrix stiffness and adhesion protein composition—on their angiogenic potential. These physical and biochemical cues have a prominent effect on secretion, demonstrating that MSCs are sensitive to their extracellular environments. This system may prove useful as a platform for dissecting the role of materials properties on the secretion of molecules from cells, and as a top-down screening method to optimize culture conditions and materials in order to attain maximum efficacy from cell-based therapies.

In Chapter 3 we use micropatterning in order to further characterize the system and separate the effects of spreading and contractility.

2.5 References

1. Kinnaird T, Stabile E, Burnett MS, Lee CW, Barr S, Fuchs S, et al. Marrow-derived stromal cells express genes encoding a broad spectrum of arteriogenic cytokines and promote in vitro and in vivo arteriogenesis through paracrine mechanisms. Circ Res. 2004 Mar 19;94(5):678–85.

2. Ohnishi S, Yasuda T, Kitamura S, Nagaya N. Effect of hypoxia on gene expression of bone marrow-derived mesenchymal stem cells and mononuclear cells. Stem Cells. 2007 May;25(5):1166–77.

3. Afzal MR, Haider HK, Idris NM, Jiang S, Ahmed RPH, Ashraf M. Preconditioning promotes survival and angiomyogenic potential of mesenchymal stem cells in the infarcted heart via NF-kappaB signaling. Antioxid Redox Signal. 2010 Mar 15;12(6):693–702.

4. Pasha Z, Wang Y, Sheikh R, Zhang D, Zhao T, Ashraf M. Preconditioning enhances cell survival and differentiation of stem cells during transplantation in infarcted myocardium. Cardiovasc Res. 2008 Jan;77(1):134–42.

5. Herrmann JL, Wang Y, Abarbanell AM, Weil BR, Tan J, Meldrum DR. Preconditioning mesenchymal stem cells with transforming growth factor-alpha improves mesenchymal stem cell-mediated cardioprotection. Shock. 2010 Jan;33(1):24–30.

6. Ranganath SH, Levy O, Inamdar MS, Karp JM. Harnessing the mesenchymal stem cell secretome for the treatment of cardiovascular disease. Cell Stem Cell. Elsevier Inc.; 2012 Mar 2;10(3):244–58.

7. Yang F, Cho S-W, Son SM, Bogatyrev SR, Singh D, Green JJ, et al. Genetic engineering of human stem cells for enhanced angiogenesis using biodegradable polymeric nanoparticles. Proc Natl Acad Sci. 2010 Feb 23;107(8):3317–22.

8. Engler AJ, Sen S, Sweeney HL, Discher DE. Matrix elasticity directs stem cell lineage specification. Cell. 2006 Aug 25;126(4):677–89.

9. Kilian KA, Bugarija B, Lahn BT, Mrksich M. Geometric cues for directing the differentiation of mesenchymal stem cells. Proc Natl Acad Sci. 2010 Mar 16;107(11):4872–7.

10. Rowlands AS, George PA, Cooper-White JJ. Directing osteogenic and myogenic differentiation of MSCs: interplay of stiffness and adhesive ligand presentation. Am J Physiol Cell Physiol. 2008 Oct;295(4):1037–44.

11. Zhang D, Kilian KA. The effect of mesenchymal stem cell shape on the maintenance of multipotency. Biomaterials. 2013 May;34(16):3962–9.

12. Lee J, Abdeen AA, Zhang D, Kilian KA. Directing stem cell fate on hydrogel substrates by controlling cell geometry, matrix mechanics and adhesion ligand composition. Biomaterials. 2013;34(33):8140–8.

13. Kasper G, Dankert N, Tuischer J, Hoeft M, Gaber T, Glaeser JD, et al. Mesenchymal stem cells regulate angiogenesis according to their mechanical environment. Stem Cells. 2007 Apr;25(4):903–10.

14. Seib FP, Prewitz M, Werner C, Bornhäuser M. Matrix elasticity regulates the secretory profile of human bone marrow-derived multipotent mesenchymal stromal cells (MSCs). Biochem Biophys Res Commun. Elsevier Inc.; 2009 Nov 27;389(4):663–7.

15. Rao RR, Peterson AW, Ceccarelli J, Putnam AJ, Stegemann JP. Matrix composition regulates three-dimensional network formation by endothelial cells and mesenchymal stem cells in collagen/fibrin materials. Angiogenesis. 2012 Jun;15(2):253–64.

16. Hoffmann C, Leroy-Dudal J, Patel S, Gallet O, Pauthe E. Fluorescein isothiocyanate-labeled human plasma fibronectin in extracellular matrix remodeling. Anal Biochem. 2008 Jan 1;372(1):62–71.

17. Tse JR, Engler AJ. Preparation of hydrogel substrates with tunable mechanical properties. Curr Protoc Cell Biol. 2010 Jun;Chapter 10:Unit 10.16.

18. Damljanovic V, Christoffer Lagerholm B, Jacobson K. Bulk and micropatterned conjugation of extracellular matrix proteins to characterized polyacrylamide substrates for cell mechanotransduction assays. Biotechniques. 2005 Dec;39(6):847–51.

19. Tseng Q, Wang I, Duchemin-Pelletier E, Azioune A, Carpi N, Gao J, et al. A new micropatterning method of soft substrates reveals that different tumorigenic signals can promote or reduce cell contraction levels. Lab Chip. 2011 Jul 7;11(13):2231–40.

20. Pelham R, Wang Y. Cell locomotion and focal adhesions are regulated by substrate flexibility. Proc Natl Acad Sci. 1997;94(25):13661–5.

21. McBeath R, Pirone DM, Nelson CM, Bhadriraju K, Chen CS. Cell shape, cytoskeletal tension, and RhoA regulate stem cell lineage commitment. Dev Cell. 2004 Apr;6(4):483–95.

22. Gilbert PM, Havenstrite KL, Magnusson KEG, Sacco A, Leonardi N a, Kraft P, et al. Substrate elasticity regulates skeletal muscle stem cell self-renewal in culture. Science. 2010 Aug 27;329(5995):1078–81.

23. Skalnikova H, Motlik J, Gadher SJ, Kovarova H. Mapping of the secretome of primary isolates of mammalian cells, stem cells and derived cell lines.

Proteomics. 2011 Feb;11(4):691–708.

24. Samper E, Diez-Juan A, Montero JA, Sepúlveda P. Cardiac cell therapy: boosting mesenchymal stem cells effects. Stem Cell Rev. 2013 Jun;9(3):266–80.

25. Huebsch N, Arany PR, Mao AS, Shvartsman D, Ali OA, Bencherif SA, et al. Harnessing traction-mediated manipulation of the cell/matrix interface to control stem-cell fate. Nat Mater. Nature Publishing Group; 2010 Jun;9(6):518–26.

26. Baker BM, Chen CS. Deconstructing the third dimension: how 3D culture microenvironments alter cellular cues. J Cell Sci. 2012 Jul 1;125(13):3015–24.

27. Fischbach C, Kong HJ, Hsiong SX, Evangelista MB, Yuen W, Mooney DJ. Cancer cell angiogenic capability is regulated by 3D culture and integrin engagement. Proc Natl Acad Sci. 2009 Jan 13;106(2):399–404.

28. Aguado BA, Mulyasasmita W, Su J, Lampe KJ, Heilshorn SC. Improving viability of stem cells during syringe needle flow through the design of hydrogel cell carriers. Tissue Eng Part A. 2012 May;18(7-8):806–15.

CHAPTER 3

CYTOSKELETAL PRIMING OF MESENCHYMAL STEM CELLS TO A MEDICINAL PHENOTYPE[1]

3.1 Introduction

We have previously shown in chapter 2 that ECM changes can affect the pro-angiogenic potential of MSCs in vitro(1), with a maximum response occurring when MSCs are fully spread on relatively stiff fibronectin conjugated matrices. Deciphering the role of extracellular signals that guide MSC state and pro-angiogenic potential is imperative to ensuring reproducible efficacy during cell-based therapies.

Accompanying changes in the ECM, cells in the perivascular space are also transformed during injury. These transformations are difficult to study as cell identity in vivo is dynamic with significant overlap between different populations in the perivascular space. This complicates finding and targeting specific populations for therapy. An alternative would be identifying master regulators which may act to promote pro-angiogenic states in multiple cell populations to work in concert in healing. Two well-known such regulators of angiogenesis are hypoxia(2) and vascular endothelial growth factor (VEGF)(3). Cytoskeletal state is also enhanced in

[1]This chapter is adapted from the following publication:
Amr A. Abdeen, Junmin Lee, Yanfen Li, and Kristopher A. Kilian, Cytoskeletal priming of mesenchymal stem cells to a medicinal phenotype (Submitted)

multiple cell types during angiogenesis. Endothelial cell organization and angioenesis(4) is Rho-activity dependent; fibroblasts form stress fibers and express contractile proteins such as alpha smooth muscle actin (α-SMA) during wound healing(5,6); and pericytes' contractility influences sprouting and proliferation of endothelial cells(7,8). We hypothesized that MSC pro-angiogenic behavior would similarly be enhanced through cytoskeletal manipulation.

In this chapter, we show that engineering the contractility state of single MSCs will modulate the epigenetic state and prime a pro-angiogenic 'medicinal' phenotype. Primed MSCs demonstrate enhanced secretion of angiogenic cytokines and association with endothelial cells in coculture. Analysis of molecular markers suggests a switch from multipotent stem cell to a pericytic state that promotes angiogenic remodeling. We propose that this approach will serve as a physical preconditioning step to 'activate' MSCs prior to autologous therapy.

3.2 Methods

General materials and methods are given in Appendix A.

In vitro tubulogenesis assay

The in vitro vascularization assay was performed as described previously(1). Briefly, 25μL of thawed reduced growth factor matrigel (Trevigen) was used to coat the bottoms of 48 well plates and then allowed to gel for 30 minutes at 37^{o}C. Then, 15,000 hMVECs were seeded per well in 100μL of unsupplemented EBM-2 media (Lonza) and 400μL of MSC conditioned media was added to each well.

Unsupplemented EBM-2 media was used as a negative control while fully supplemented EGM-2 was used as a positive control. After 8 hours tube formation was imaged using a Rebel T3 Camera (Canon) at 25x and tube area quantified using imageJ. For co-culture experiments, primed MSCs were additionally seeded at 5,000 cells/well.

Co-culture

For co-culture experiments, red and green cell tracker (Invitrogen) were used on hMVECs and MSCs, respectively as per manufacturer instructions. Cells were fixed as above (without permeabilization) and imaged.

Angiogenic cytokines array

For cytokine analysis in the conditioned media we used human antibody angiogenesis array membrane (Abcam – ab134000) as per manufacturer instructions. Membranes were blocked and then conditioned media samples were incubated overnight with the membranes at 4^{o}C. Prepared membranes were exposed to x-ray film for detection and, after development, films were scanned and analyzed using the ImageJ plugin 'Protein array analyzer' (written by Gilles Carpentier, 2010, available at http://rsb.info.nih.gov/ij/macros/toolsets/Protein%20Array%20Analyzer.txt)

Chick chorioallantoic assay

Embryonated chicken eggs at Day 10 were obtained from the University of Illinois poultry farm (Urbana, IL). A hole with approximate width of 15mm was drilled and

polyacrylamide hydrogels with MSCs seeded on it in patterned or non-patterned conditions were placed on the chorioallantoic membrane (CAM), face down. The hole was covered with scotch tape and the eggs were incubated for 5 days at 37^{o}C and ~50% humidity. On the fifth day after incubation, embryos were fixed with 4% PFA and the hydrogels and surrounding CAMS were excised. The explants were imaged and the area covered with blood vessels over the gels was quantified using ImageJ as for the vascularization assays.

Data analysis and statistics

Cell area, nuclear area and marker expression levels were analyzed using ImageJ. MSC/hMVEC overlap area was performed by thresholding fluorescent images of cell tracked MSCs and hMVECs and using the imageJ image calculator's 'AND' operation to get the overlapping area. Error bars represent standard error and N value the number of experimental replicates. Unpaired T-tests were used to compare two groups while ANOVA was used to compare multiple groups with post hoc analysis. P values lower than 0.05 were considered significant.

3.3 Results

Tuning the pro-angiogenic potential of mesenchymal stem cells through single cell contractility engineering

Previously, we demonstrated optimal matrix properties to guide the pro-angiogenic potential of MSCs, where cell spread area on rigid matrices conjugated with fibronectin played a key role in augmenting secretion of pro- angiogenic

molecules(1). However, in vivo cells are surrounded by the extracellular matrix, and the spreading characteristics of MSCs observed on planar substrates are not observed. Therefore, we asked whether patterning single cells within the same footprint, in geometries presenting different degrees of subcellular adhesive space, could be used to modulate cytoskeletal tension in the absence of spreading. We employed microcontact printing of fibronectin islands onto hydrazine hydrate treated polyacrylamide (PA) hydrogels to facilitate covalent conjugation. After MSCs are cultured for 2 days in the desired geometries, MSC conditioned medium is collected and added to hMVECs on matrigel for 8 hours, after which the amount of tube formation by hMVECs is quantified as a measure of the pro-angiogenic potential of the MSC culture conditions (Figure 3.1A).

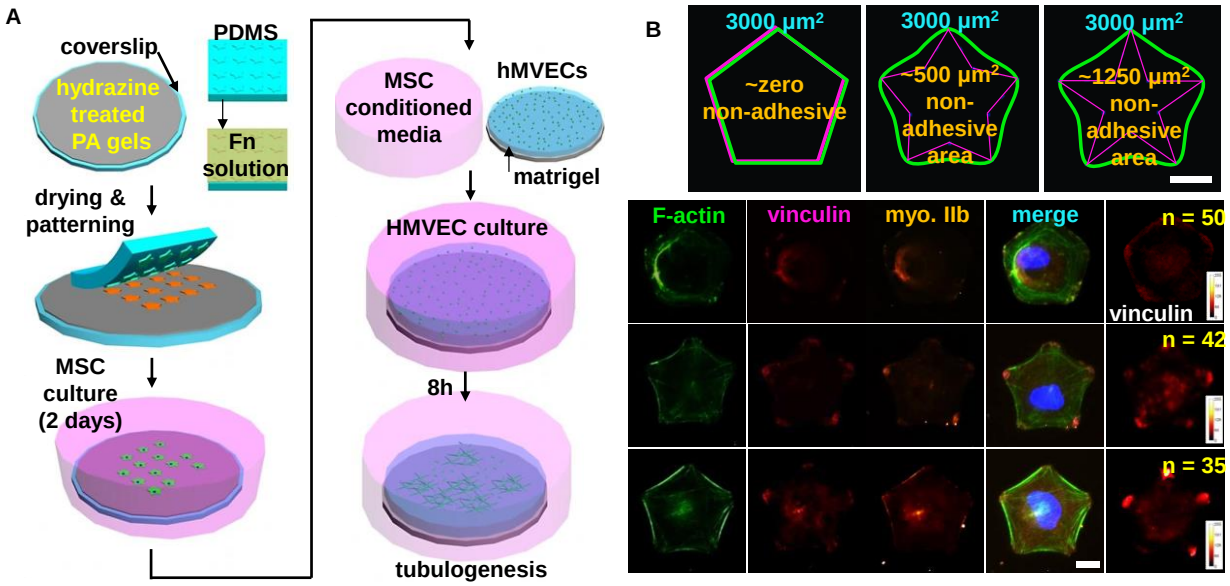

Figure 3.1 Patterning modulates MSC contractility to influence pro-angiogenic potential (A) Experimental procedure for micropatterning MSCs and in vitro tubulogenesis assay. (B) Focal adhesion and cytoskeletal staining of MSCs cultured on patterns with different non-adhesive areas. Scale bar: 25μm.

We utilized three different shapes of relatively small area (3,000 μm^2) to ensure the cells are not fully spread, a pentagon and two 5-pointed stars presenting variable subcellular adhesive area. The points of the star span non-adhesive space (~500 and 1250 μm^2), causing reinforcement of peripheral actin and formation of stress fibers(9), and increased stability of focal adhesion at apexes. Vinculin heat maps demonstrate increased focal adhesion area at the points of the shapes as the non-adhesive space increases (Figure 3.1B). Similar trends were observed for focal adhesion protein paxillin, $\alpha_5\beta_1$ and $\alpha_v\beta_3$ integrins, and myosin IIb (Figure 3.2) Cells attached to the patterns at approximately the same fraction and exhibited similar projected cell areas (Figure 3.3).

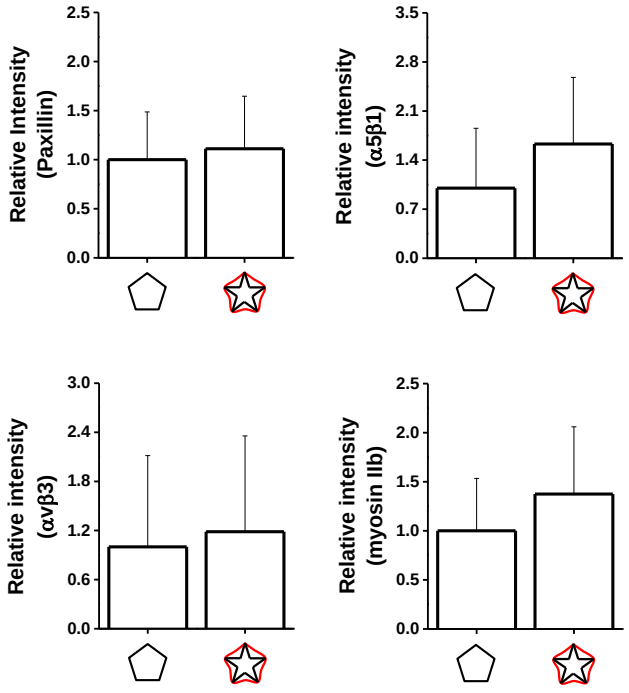

Figure 3.2 Relative intensity of Paxillin, Integrins α5β1 and αvβ3 and myosin II-b.

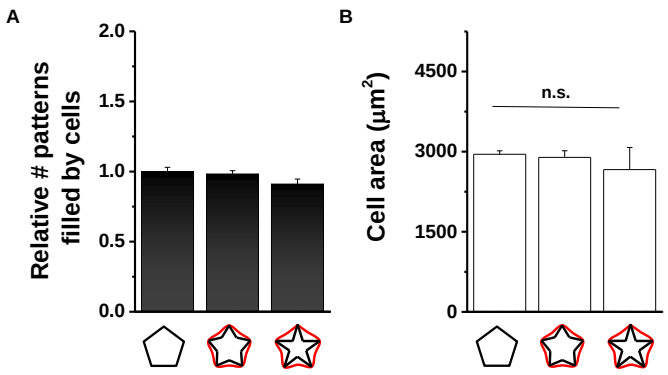

Figure 3.3 (A) Number of patterns occupied and (B) Average cell area of cells patterned with different non adhesive space.

Conditioned media collected from MSCs cultured in these shapes was used to promote tubulogenesis in hMVECs cultured in matrigel. Tube formation shows a dependence on the non-adhesive area upon which cells are patterned (Figure 3.4), with conditioned media from star-shaped MSCs showing the highest degree of tubulogenesis as compared to our positive controls (hMVEC growth media). hMVEC cultures supplemented with conditioned media from star-shaped MSCs show ~2-fold higher tube formation compared to cells cultured on pentagon patterns. We also evaluated the influence of cellular elongation on secretion since changes in aspect ratio have previously been demonstrated to increase cytoskeletal tension(10). Tube formation assays demonstrate increasing pro-angiogenic potential as MSCs are cultured within shapes of increasing aspect ratio (Figure 3.5), peaking at 1:8 and decreasing at 1:12, presumably as elongation beyond 1:8 destabilizes the cytoskeleton(11).

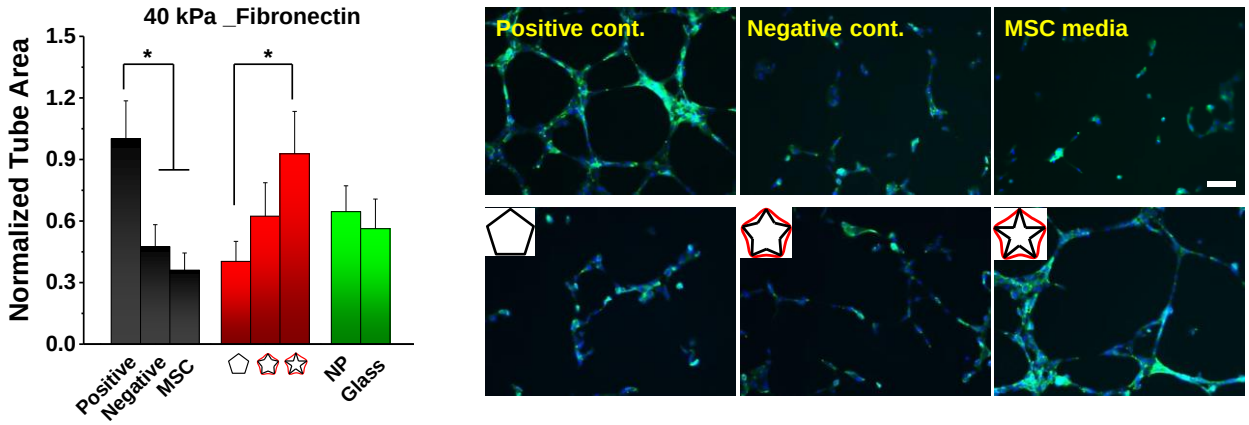

*Figure 3.4 (left) Tube area of hMVECs after being treated with conditioned media from MCs cultured at different conditions (N=6). (right) Representative images of hMVEC tube formation at different conditions. Scale bar: 100μm. * P<0.05.*

Overall, this data indicates a strong correlation between cytoskeletal tension of MSCs and their secretion of pro-angiogenic cytokines. This is not the case, however, when comparing to MSCs on glass substrates which, while having the largest spread areas and most robust stress fibers, show little enhancement to MSC pro-angiogenic potential. This demonstrates the importance of studying cells at more physiologically relevant conditions. In order to further understand the process, we looked at how the angiogenic secretome of MSCs was modulated by engineering contractility.

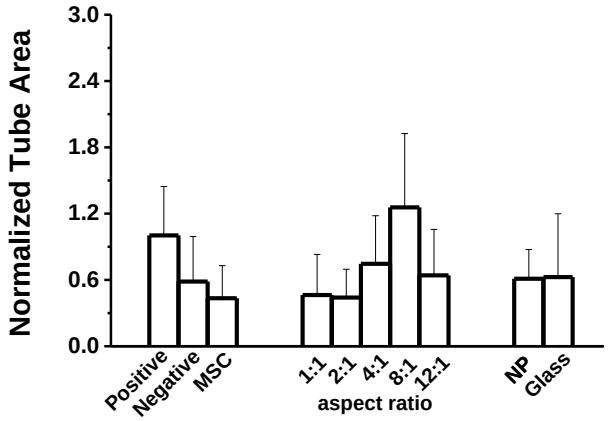

Figure 3.5 Normalized tube area of hMVECs with conditioned medium from MSCs patterned in 5000 μm2 circles of varying aspect ratios.

The influence of single cell contractility on the secretome

Protein arrays were used to investigate the influence of cell contractility state on the pro-angiogenic secretory profile of MSCs. The relative concentrations of a panel of 20 different angiogenic cytokines in MSC conditioned media were compared using a cytokine array for conditioned media. To simplify the analysis, we compared cytokines secreted by MSCs patterned on pentagonal shapes to those patterned in star shapes which had the largest cytoskeletal tension. Figure 3.6A shows a heat map of protein expression normalized to cell number. We see an increase in expression of pro-angiogenic proteins secreted from star-patterned MSCs across the broad spectrum of cytokines compared to molecules secreted from pentagon-patterned MSCs. For further study, we selected three of the most potent angiogenic regulators with the highest differential expression between pentagon and star MSCs, namely IGF-1, RANTES and VEGF (Figure 3.6B) to investigate their effects on hMVEC tube formation. The addition of function blocking antibodies to MSC conditioned medium targeting any of these factors lowered hMVEC tube

formation from star-patterned MSCs; only a modest decrease was observed from pentagon-patterned MSCs (Figure 3.6C). Suppression of a single factor decreases angiogenesis considerably, even in the presence of other factors, suggesting the importance of synergy during promotion of angiogenesis.

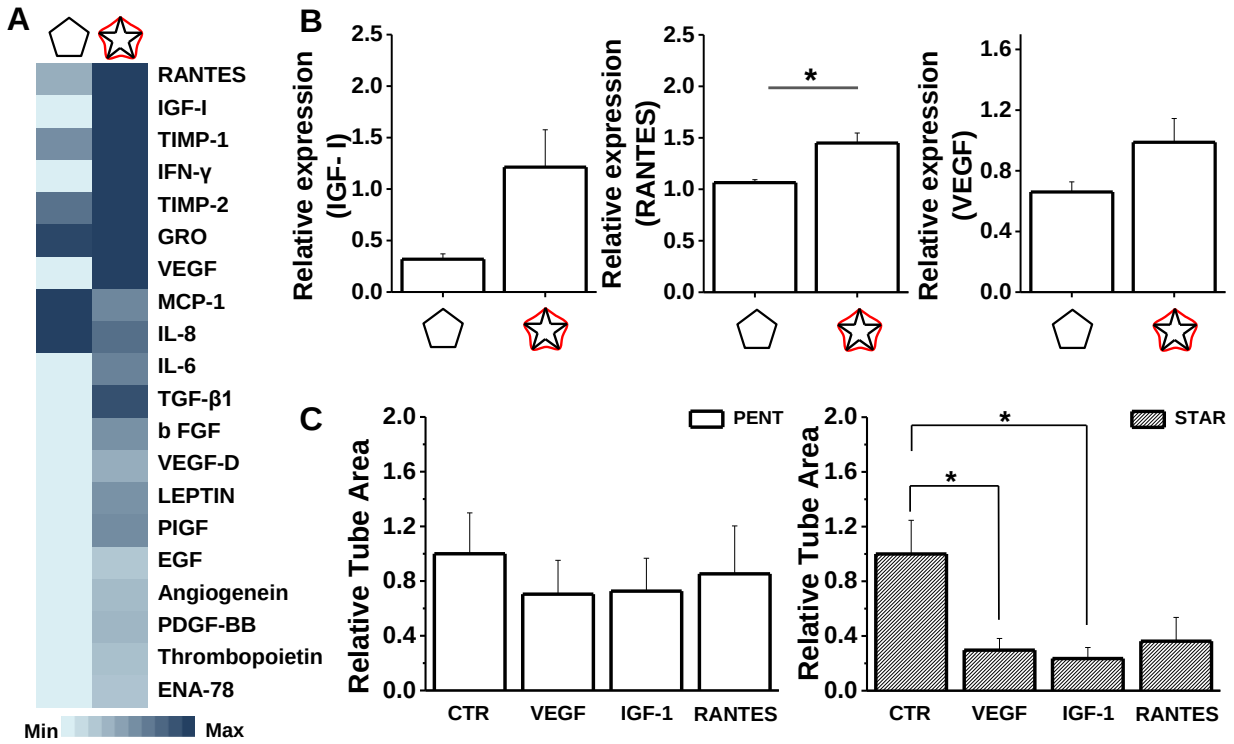

*Figure 3.6 MSC contractility modulates the secretome (A) Heat map of cytokine expression in conditioned media of MSCs cultured in pentagon or star patterns, shown as fold change over the non-patterned condition. (B) Relative expression (fold change over NP) of IGF-1, RANTES & VEGF. (C) Effect of adding blocking antibodies to IGF-1, RANTES & VEGF to MSC conditioned media on tube formation of hMVECs. * P<0.05.*

Activated mesenchymal stem cells associate with vascular endothelial cells in co-culture

To explore how activation may influence heterotypic interactions in culture, we passaged pentagon-patterned and star-patterned MSCs for 2 days then trypsinized and co-cultured them with hMVECs. An in vitro angiogenesis assay was performed and tube formation and MSC localization on tubes were analyzed after 8 hours via cell tracker. Representative images of the formed tube networks with pentagon-patterned and star-patterned MSCs show higher tube formation with higher association of MSCs (with MSCs spreading along the tubes) for star patterned MSCs (Figure 3.7A). Quantitation of tube area shows a 1.5 fold increase in tube formation when MSCs are cultured on star rather than pentagon geometries prior to co-culture (Figure 3.7B). Both conditions show higher tube formation than lone hMVECs. Furthermore, MSC coverage of the tubes was ~1.8 times higher in star than pentagon (Figures. 3.7C).

Although there have been several reports of MSC-endothelial cell co-cultures, only a subset explore the effect of preconditioning MSCs on their behavior in co-culture(12). Here we observe a pronounced effect of preconditioning on MSC-hMVECs interactions, highlighting the importance of considering MSC culture conditions prior to therapeutic use. Since broad changes in the secretome and association with endothelial cells indicated a more directed switch in MSC behavior, we then looked into changes in MSC state.

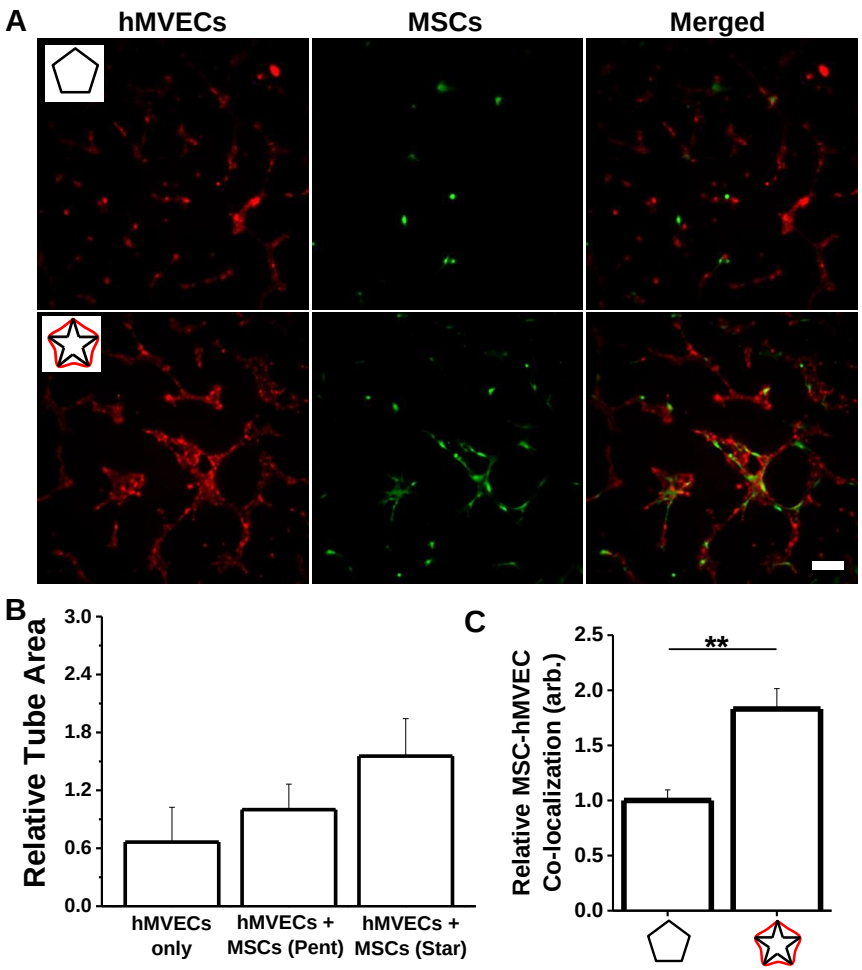

*Figure 3.7 Activated MSCs exhibit pericytic behavior in co-culture with endothelial cells (A) Representative immunofluorescence images of hMVEC tube formation (red) and MSCs (green) when co-cultured on matrigel for 8 hours. Scale bar: 100μm. (B) Quantitation of relative tube area of hMVECs or hMVECs co-cultured with MSCs primed via patterning into pentagon or star shapes (N=3). (C) Quantitation of area of MSCs overlapping hMVECs, indicative of MSC attachment to formed vasculature (N=5). ** P<0.01.*

Activation of mesenchymal stem cells to a pericyte state

Since the contractility state of MSCs influences the secretome, we sought to investigate the putative phenotypic switch through changes in expression of a panel of markers: MSC multipotency marker endoglin/CD105; the pericyte and activated fibroblast marker α-SMA(13); CD146(14) as a pericyte marker that is used to

separate MSCs from pericytes, and RGS-5(15). RGS-5 is also upregulated during activation of pericytes through neovascularization and wound healing(16). Immunofluorescence imaging and quantitation of average marker intensity (Figure 3.8) shows a ~1.5 fold increase in α-SMA & CD-146 expression and a ~1.25 fold increase in RGS-5 expression from pentagon to star, along with a slight decrease in endoglin expression (~20%). Taken together, this suggests that MSCs initiate secretion of angiogenic molecules through adoption of an activated pericyte-like state via a process mediated by actomyosin contractility. Notably, MSCs cultured on non-patterned (NP) surfaces and glass demonstrate low expression of these markers compared to patterned MSCs.

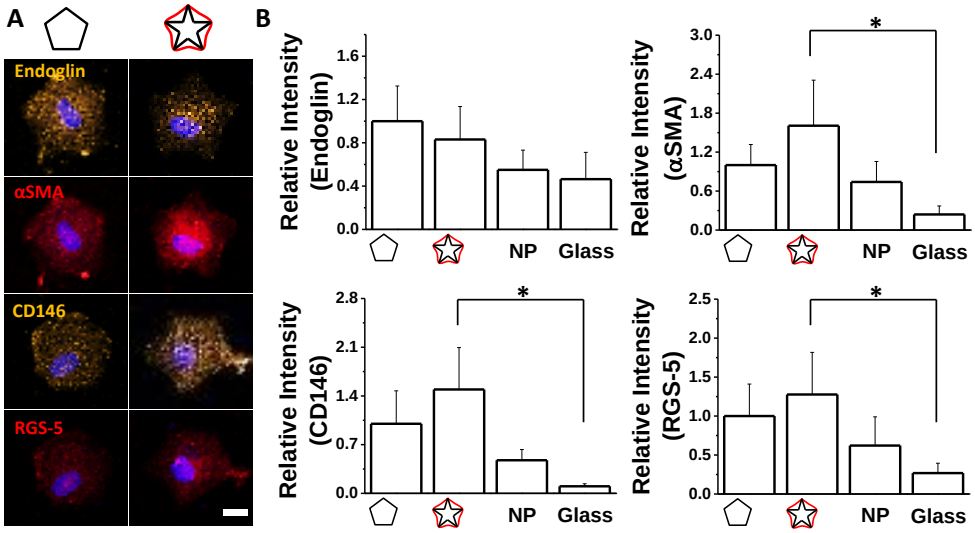

*Figure 3.8. MSC activation into a pericytic state (A) Representative immunofluorescent images of patterned MSCs showing Endoglin/CD105, αSMA, CD146 and RGS-5 expression in pentagon and star geometries. (B) Average marker intensities relative to the pentagon condition. * P<0.05. Scale bar: 25μm.*

Previously it was shown that isolated pericytes adopt MSC characteristics during culture on rigid substrates in vitro(14,17). The converse appears to be true here,

where MSCs cultured on patterned hydrogels express elevated pericyte markers. Elevated endoglin expression in pentagon-patterned MSCs may be consistent with increased quiescence(18), although the degree of change in expression is low. Higher CD146 expression in star-patterned MSCs is especially telling since CD146 is a particularly robust pericytic marker. In fact, Raghunath et al(19) have shown pro-angiogenic and pericytic activity of sorted CD146+ MSCs but not CD146- MSCs. Furthermore, increased RGS-5 expression is consistent with both a more pericytic state and increased angiogenic activity.

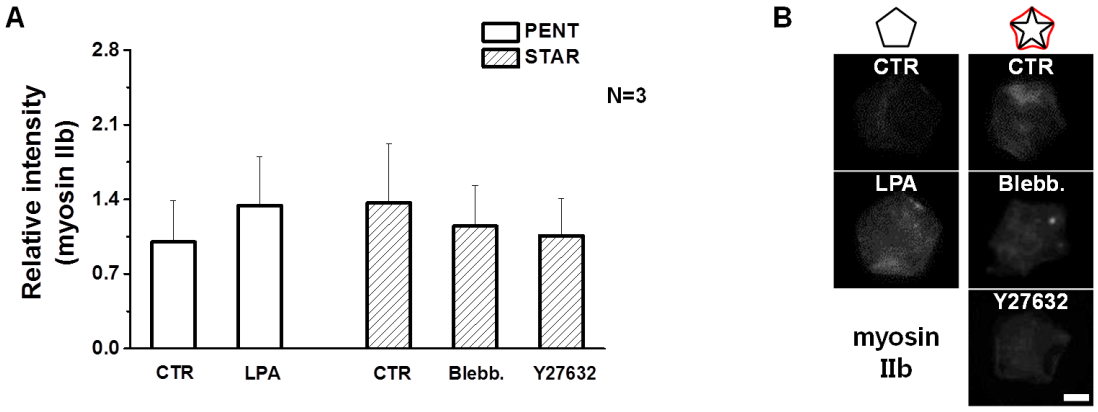

Figure 3.9 (A) Average myosin II intensity of patterned MSCs untreated or treated with LPA, Blebbistatin and Y27632 (N=3). (B) Representative immunofluorescent images of patterned MSCs showing myosin II expression.

In order to confirm the role of actomyosin contractility in pericyte activation, we added the RhoA activator lysophosphatidic acid (LPA)(20) to MSCs cultured in pentagon patterns, and Blebbistatin (inhibitor of Myosin II) and an inhibitor of Rho associated protein kinase (ROCK; Y27632) to MSCs cultured in star patterns. Immunofluorescent staining of myosin IIb shows ~35% increases in myosin IIb intensity in LPA treated MSCs in pentagon shapes giving comparable intensity to

MSCs in star patterns. Blebbistatin and Y27632, on the other hand, showed a modest decrease in myosin IIb intensity compared to controls: ~15% and 23% lower respectively (Figure 3.9). Treatment of pentagon-patterned MSCs with LPA leads to a more than 3 fold increase in tube formation from MSC conditioned media while Blebbistatin and Y27632 treatment of MSCs in star shapes caused a modest decrease of ~35% in tube formation (Figure 3.10). Blocking of $\alpha_5\beta_1$ and $\alpha_v\beta_3$ integrins using function blocking antibodies did not play a significant role on the angiogenic potential of either pentagon-patterned or star-patterned MSCs. With MSCs adopting an activated pericytes-like state by confinement, we asked whether cytoskeletal engineering through patterning was affecting the epigenetic state of MSCs.

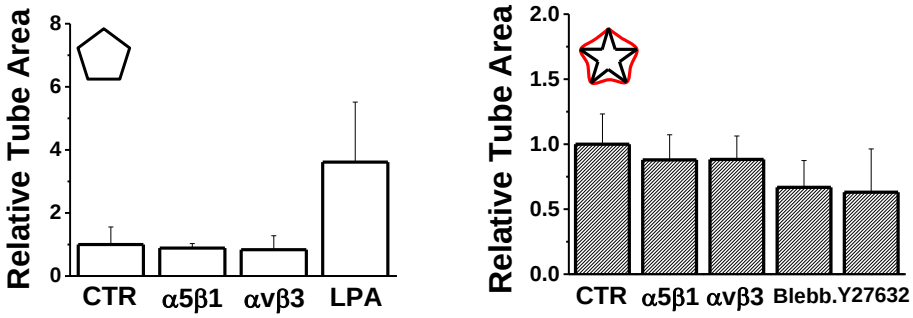

Figure 3.10 (left)Effect of treatment of pentagon-patterned MSCs with blocking antibodies to integrins α5β1 and αvβ3 or LPA to enhance contractility (N=5). (right) Effect of treatment of star-patterned MSCs with blocking antibodies to integrins α5β1 and αvβ3 or Blebbistatin and Y27632 to reduce contractility (N=3).

Mesenchymal stem cell activation is regulated through histone state.

Cell activity is regulated through modifications of specific histone marks, with cytoskeletal tension playing a role in guiding nuclear organization(21,22), chromatin structure and gene expression(23,24). Analysis of nuclear area for patterned and non-patterned MSCs demonstrate a significant decrease in nuclear area of both pentagon-patterned and star-patterned MSCs (Figure 3.11A); hence, we suspected changes in chromatin architecture. Acetylation of histones at lysine residues effectively neutralizes positive charge and leads to chromatin de-condensation(25). We examined the magnitude of lysine acetylation in patterned and non-patterned cells and see a significant decrease in global lysine acetylation in both star-patterned and pentagon-patterned MSCs when compared to non-patterned MSCs. We also examined several specific marks including H3K9me3, a hallmark of heterochromatin(26), H3K9ac, an indicator of active promoters(27), and H3K36me2, an indicator of gene transcription(28). Immunofluorescence staining of patterned versus non-patterned MSCs show demonstrate decreased acetylation and methylation marks in micropatterned cells indicating a chromatin state which is less actively transcribed than non-patterned cells.

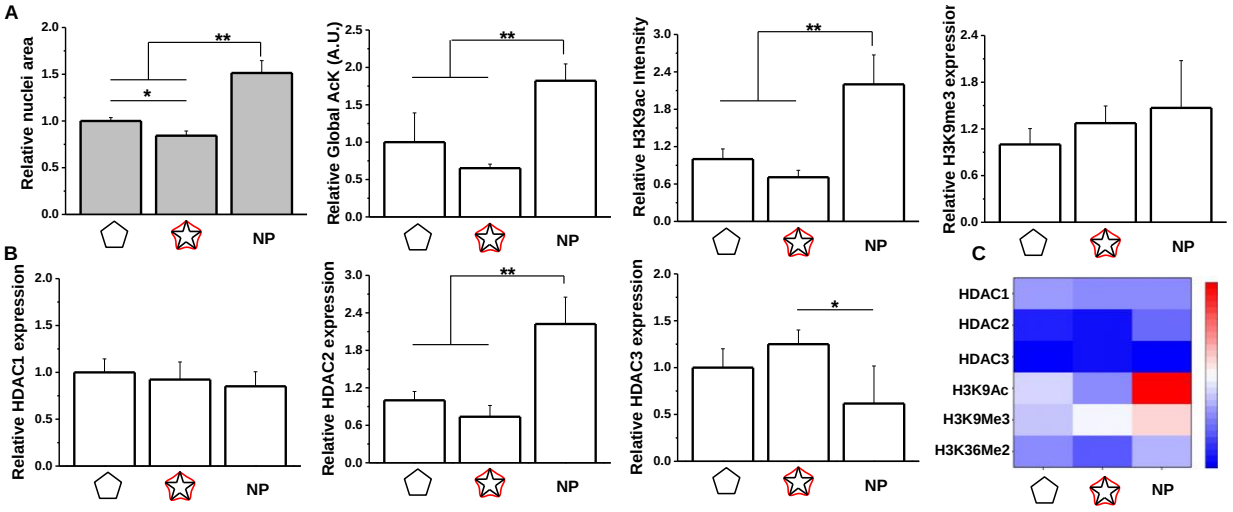

*Figure 3.11 Histone state regulate mesenchymal stem cell activation (A) Relative nuclear area between non-patterned, pentagon shaped or star shaped MSCs and relative intensity of H3K9 acetylation, trimethylation or dimethylation of H3K36. (B) Relative expression of HDACs 1, 2 &3. (C) Heat map comparing the chromatin modifications markers across non-patterned, pentagon shaped or star shaped MSCs. * P<0.05, **P<0.01.*

To further investigate regulation of chromatin state, we examined the expression level of class 1 histone deacetylases (Figure 3.11B). There is no change in HDAC1 expression across conditions, while HDAC2 shows significantly higher expression in non-patterned MSCs. HDAC3 shows slightly higher expression for cells cultured in the star geometry. Taken together, these results suggest that single cell confinement regulates chromatin structure and transcription sites, with evidence for HDAC2 mediated deacetylation at H3K9. This results in a less "active" chromatin as MSCs are primed for a specific role, consistent with previous work demonstrating decreased H3K9 acetylation during differentiation(29).

In-ovo pro-angiogenic potential of MSCs enhanced by patterning

Having seen that patterning of MSCs affects their epigenetic state, their phenotype and their pro-angiogenic potential we next tested whether enhanced pro-angiogenic potential persists in the more complicated in-ovo environment of chick chorioallantoic membranes (CAMs)(30), with existing vascular networks. We placed hydrogels with unpatterned, star-patterned or pentagon-patterned MSCs on the CAMs of 10-day old chick embryos and looked at vascular formation after 5 days (Figure 3.12). We see enhanced vessel formation in CAMs where hydrogels with star patterned MSCs were added compared to pentagon patterned and non-patterned MSCs, with vessels that are much bigger and more mature being formed on CAMs supplemented with star-patterned MSCs. This shows that the enhanced pro-angiogenic effect of patterning MSCs does persist when applied to the in-ovo CAM system, showing an important intermediate step towards translation.

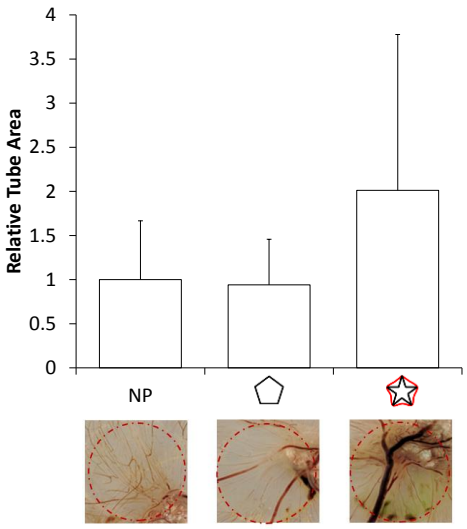

Figure 3.12 Relative tube area (normalized to cell number) on CAMs with implanted polyacrylamide hydrogels with MSCs patterned in pentagon or star shapes or unpatterned. (bottom) representative images of CAMs from the different conditions. The implanted hydrogels (outline in red dashes) were 8mm in diameter.

3.4 Discussion

Autologous MSC therapy is considered one of the most promising treatments for cardiovascular disease; however, the majority of cells die during implantation and clinical efficacy has proved variable. Preconditioning MSCs to augment pro-angiogenic potential has been demonstrated through engineering hypoxia or cytokine signaling(12) to program MSCs into a angiogenic mode. In this work we have demonstrated a biophysical approach to activate MSCs through single cell contractility engineering, to reveal a medicinal state which exhibits broad pro-angiogenic potential, and enhanced association with model vasculature in vitro.

The observed overall increase in cytokine secretion is consistent with previous reports of enhanced angiogenic secretory profiles of MSCs on stiffer substrates and our previous observation of the abrogation of these effects by restricting MSC spreading on stiff substrates(1,31). This overall increase, however, stands in contrast to previous observations of differential modulation of cytokines in responses to changes in substrate mechanics and is more in line with large scale changes in MSC secretory profile seen through more potent chemical preconditioning or hypoxia treatments(12). This suggests a 'switch' in phenotype which activates a pro-angiogenic secretory profile. During wound repair MSCs home towards sites of injury and take on a more active migratory state. This is in contrast to the more quiescent state observed during homeostasis(32,33).

A proposed trophic response to injury is the 'activation' of MSCs into a medicinal state which organizes a regenerative microenvironment, with subsequent

stabilization spurred by MSCs reacquiring a more quiescent pericytic phenotype(34,35). Activated pro-angiogenic pericytes acquire a more amoeboid morphology, are more migratory, and support endothelial cell proliferation and migration(36). In all cases, MSCs exhibit remarkably robust and versatile plasticity between different phenotypes to regulate angiogenesis both in vitro and in vivo(13).

Furthermore, perturbation of pericytes' contractility through Rho-GTPase has been shown to affect regulation of endothelial cell proliferation, with Rho-GTPase activated cells losing the capability of growth arresting endothelial cells(7). In support of a contractility mechanism guiding pericyte activity, Herman and colleagues showed how increasing spreading and actin cytoskeletal organization through MRIP silencing in pericytes promotes endothelial cell tubulogenesis in-vitro(8). Our observation of higher association of MSCs from star patterns with hMVECs, and higher tube formation coupled with increased CD146 expression, is consistent with the proangiogenic behavior observed for CD146 positive MSCs (19). This evidence, combined with the proposed perivascular source of MSCs(17) and MSC-pericyte plasticity(13), has led us to hypothesize that a cytoskeletal switch induced by microengineering contractility will activate MSCs into a pericytic, pro-angiogenic phenotype.

Overall, in this chapter we show evidence that engineering the adhesion and cytoskeletal machinery modulates MSC pro-angiogenic activity through actomyosin contractility, lysine acetylation and chromatin remodeling, with subsequent specification of a medicinal, pericytic phenotype. Microengineered substrates are a

useful platform to normalize cell state across a heterogeneous population, and may prove a versatile route to "priming" a patients cells for medicinal activity. Preliminary results from CAM assays show that these enhancements in pro-angiogic potential persist in chick embryos.

The results from chapters 2 and 3 show that ECM properties have a powerful role in modulating MSC pro-angiogenic potential. However, translation requires biocompatible materials that can be used in vivo. This is the subject of the next chapter.

3.5 References

1. Abdeen AA, Weiss JB, Lee J, Kilian KA. Matrix Composition and Mechanics Direct Proangiogenic Signaling from Mesenchymal Stem Cells. Tissue Eng Part A. 2014 Oct;20(19-20):2737–45.

2. Krock BL, Skuli N, Simon MC. Hypoxia-Induced Angiogenesis: Good and Evil. Genes Cancer. 2011;2(12):1117–33.

3. Johnson KE, Wilgus TA. Vascular Endothelial Growth Factor and Angiogenesis in the Regulation of Cutaneous Wound Repair. Adv wound care. 2014;3(10):647–61.

4. Mammoto A, Connor KM, Mammoto T, Yung CW, Huh D, Aderman CM, et al. A mechanosensitive transcriptional mechanism that controls angiogenesis. Nature. Nature Publishing Group; 2009;457(7233):1103–8.

5. Chen W, Frangogiannis NG. Fibroblasts in post-infarction inflammation and cardiac repair. Biochim Biophys Acta - Mol Cell Res. Elsevier B.V.; 2013;1833(4):945–53.

6. Darby I, Skalli O, Gabbiani G. α-smooth muscle actin is transiently expressed by myofibroblasts during experimental wound healing. Lab Investig. Nature Publishing Group; 63(1):21–9.

7. Kutcher ME, Kolyada AY, Surks HK, Herman IM. Pericyte Rho GTPase mediates both pericyte contractile phenotype and capillary endothelial growth state. Am J Pathol. American Society for Investigative Pathology; 2007;171(2):693–701.

8. Durham JT, Surks HK, Dulmovits BM, Herman IM. Pericyte contractility controls endothelial cell cycle progression and sprouting: insights into angiogenic switch mechanics. AJP Cell Physiol. 2014;307(9):C878–92.

9. Théry M. Micropatterning as a tool to decipher cell morphogenesis and functions. J Cell Sci. 2010 Dec 15;123(Pt 24):4201–13.

10. Kilian KA, Bugarija B, Lahn BT, Mrksich M. Geometric cues for directing the differentiation of mesenchymal stem cells. Proc Natl Acad Sci. 2010 Mar 16;107(11):4872–7.

11. Lee J, Abdeen AA, Tang X, Saif TA, Kilian KA. Geometric guidance of integrin mediated traction stress during stem cell differentiation. Biomaterials. Elsevier Ltd; 2015 Nov;69:174–83.

12. Ranganath SH, Levy O, Inamdar MS, Karp JM. Harnessing the mesenchymal stem cell secretome for the treatment of cardiovascular disease. Cell Stem Cell. Elsevier Inc.; 2012 Mar 2;10(3):244–58.

13. Kelly-goss MR, Sweat RS, Stapor PC, Peirce SM, Murfee WL. Targeting pericytes for angiogenic therapies. Microcirculation. 2014;21(4):345–57.

14. Crisan M, Yap S, Casteilla L, Chen C-W, Corselli M, Park TS, et al. A perivascular origin for mesenchymal stem cells in multiple human organs. Cell Stem Cell. 2008 Sep 11;3(3):301–13.

15. Mitchell TS, Bradley J, Robinson GS, Shima DT, Ng YS. RGS5 expression is a quantitative measure of pericyte coverage of blood vessels. Angiogenesis. 2008;11(2):141–51.

16. Berger M, Bergers G, Arnold B, H??mmerling GJ, Ganss R. Regulator of G-protein signaling-5 induction in pericytes coincides with active vessel remodeling during neovascularization. Blood. 2005;105(3):1094–101.

17. Caplan AI. All MSCs Are Pericytes? Cell Stem Cell. 2008;3(3):229–30.

18. Zhang D, Kilian KA. The effect of mesenchymal stem cell shape on the maintenance of multipotency. Biomaterials. 2013 May;34(16):3962–9.

19. Blocki A, Wang Y, Koch M, Peh P, Beyer S, Law P, et al. Not All MSCs Can Act as Pericytes: Functional In Vitro Assays to Distinguish Pericytes from Other Mesenchymal Stem Cells in Angiogenesis. Stem Cells Dev. 2013;22(17):2347–55.

20. Shi YU, Li H, Zhang X, Fu Y, Huang YAN, Lui PPY, et al. Continuous cyclic mechanical tension inhibited Runx2 expression in mesenchymal stem cells through RhoA-ERK1/2 pathway. J Cell Physiol. 2011;226(8):2159–69.

21. Wang N, Tytell JD, Ingber DE. Mechanotransduction at a distance: mechanically coupling the extracellular matrix with the nucleus. Nat Rev Mol Cell Biol. 2009 Jan;10(1):75–82.

22. Versaevel M, Grevesse T, Gabriele S. Spatial coordination between cell and nuclear shape within micropatterned endothelial cells. Nat Commun. Nature Publishing Group; 2012;3:671.

23. Jain N, Iyer KV, Kumar A, Shivashankar G V. Cell geometric constraints induce modular gene-expression patterns via redistribution of HDAC3 regulated by actomyosin contractility. Proc Natl Acad Sci. 2013 Jun 24;110(28):3–8.

24. Le Beyec J, Xu R, Lee S-Y, Nelson CM, Rizki A, Alcaraz J, et al. Cell shape regulates global histone acetylation in human mammary epithelial cells. Exp Cell Res. 2007;313(14):3066–75.

25. Struhl K. Histone acetylation and transcriptional regulatory mechanisms. Genes and Development. 1998. p. 599–606.

26. Peters AHFM, O'Carroll D, Scherthan H, Mechtler K, Sauer S, Schöfer C, et al. Loss of the Suv39h histone methyltransferases impairs mammalian heterochromatin and genome stability. Cell. 2001;107(3):323–37.

27. Karmodiya K, Krebs AR, Oulad-Abdelghani M, Kimura H, Tora L. H3K9 and H3K14 acetylation co-occur at many gene regulatory elements, while H3K14ac marks a subset of inactive inducible promoters in mouse embryonic stem cells. BMC Genomics. BioMed Central; 2012 Jan;13(1):424.

28. Rao B, Shibata Y, Strahl BD, Lieb JD. Dimethylation of histone H3 at lysine 36 demarcates regulatory and nonregulatory chromatin genome-wide. Mol Cell Biol. 2005 Nov;25(21):9447–59.

29. Krejcí J, Uhlírová R, Galiová G, Kozubek S, Smigová J, Bártová E. Genome-wide reduction in H3K9 acetylation during human embryonic stem cell differentiation. J Cell Physiol. 2009 Jun;219(3):677–87.

30. Ponce ML, Kleinmann HK. The chick chorioallantoic membrane as an in vivo angiogenesis model. Curr Protoc Cell Biol. 2003;Chapter 19:Unit 19.5.

31. Seib FP, Prewitz M, Werner C, Bornhäuser M. Matrix elasticity regulates the secretory profile of human bone marrow-derived multipotent mesenchymal stromal cells (MSCs). Biochem Biophys Res Commun. Elsevier Inc.; 2009 Nov 27;389(4):663–7.

32. Rustad KC, Gurtner GC. Mesenchymal Stem Cells Home to Sites of Injury and Inflammation. Adv wound care. 2012;1(4):147–52.

33. Murphy MB, Moncivais K, Caplan AI. Mesenchymal stem cells: environmentally responsive therapeutics for regenerative medicine. Exp Mol Med. Nature Publishing Group; 2013 Jan;45(11):e54.

34. Caplan AI, Correa D. The MSC: An injury drugstore. Cell Stem Cell. Elsevier Inc.; 2011;9(1):11–5.

35. Stratman AN, Malotte KM, Mahan RD, Davis MJ, Davis GE. Pericyte recruitment during vasculogenic tube assembly stimulates endothelial basement membrane matrix formation. Blood. 2009 Dec 3;114(24):5091–101.

36. Díaz-Flores L, Gutiérrez R, Madrid JF, Varela H, Valladares F, Acosta E, et al. Pericytes. Morphofunction, interactions and pathology in a quiescent and activated mesenchymal cell niche. Histol Histopathol. 2009;24(7):909–69.

CHAPTER 4

SPATIALLY DEFINED STEM CELL-LADEN HYDROGEL ISLANDS FOR DIRECTING ENDOTHELIAL TUBULOGENESIS[1]

4.1 Introduction

We have shown previously that stiffer matrix, protein composition, and cell contractility act together to significantly alter the secretome and angiogenic potential of MSCs. For cell-based therapies, MSC delivery involves a more complex 3-D environment that would benefit from a design that recapitulates aspects of in vivo tissue(1). It is well-established that signaling in 3-D matrices will influence cell behavior and secretory profiles differently than in 2-D assays(2,3). Furthermore, MSC encapsulation within hydrogels has been shown to improve their viability during transplantation(4). As cell death is a major roadblock in using cell-based therapies, the protective potential of hydrogels in-vivo is an important factor. Taken together, this suggests that 3-D environments may play an important role in MSC angiogenic potential.

Feedback between different cell types can also direct angiogenesis. In vivo, MSCs often secrete trophic factors in response to heterotypic cell-cell signaling(5). Endothelial cells have been reported to alter gene expression profiles of MSCs(6,7). Matrix properties also control network formation in 3-D co-culture systems(8).

---

[1] This chapter is adapted from the following publication:
Amr A. Abdeen, Junmin Lee, Samuel H Mo, and Kristopher A. Kilian, Spatially defined stem cell-laden hydrogel islands for directing endothelial tubulogenesis, Journal of Materials Chemistry B, 2015, 3, 7896-7898

In this chapter, we demonstrate a chemical strategy to conjugate matrix proteins to poly(ethylene glycol) (PEG) hydrogels. We use these hydrogels as a platform to investigate the differences between 2-D and 3-D culture of MSCs on their angiogenic potential using a secondary in-vitro angiogenesis assay. Using the same material we can compare the influence of dimensionality when cells are either cultured on the surface or within the gel. Finally, we show how, using UV photopolymerization, we can 'pattern' vascularization in an MSC-endothelial cell co-culture system towards biomimetic architectures to study heterotypic signaling. The approach presented here may prove valuable for the design of 3-D biomaterials that are clinically viable for regenerative medicine.

4.2 Methods

General materials and methods are given in Appendix A.

PEGDA gel fabrication

Polyethylene glycol (PEG-10000 Molecular weight) was modified as described previously(9) to form PEG diacrylates(PEGDA). Briefly, PEG (1 mmol) was dried by co-distillation with toluene 3 times. The dried PEG was then redissolved in dichloromethane (DCM) and toluene (DCM:toluene 5:3). Triethylamine and acryloyl chloride (3 mmol each) were then added under stirring overnight at room temperature. The reaction was filtered and K_2CO_3 (3g) was added under stirring for 1.5 hours. The PEGDA was then filtered, concentrated under vacuum and extracted with diethylether. Lyophilized PEGDA power was stored at -20°C.

Amine groups on proteins were acrylated by the addition of NHS-acrylate (at a molar ratio of 10:1) for 4 hours in carbonate buffer (pH 9, 1M NaCl)(10).

To make 2D surfaces, 18mm glass coverslips (Fischer Scientific) were cleaned with ethanol then DI water. The slides were then dried and activated by treatment with 3-(trimethoxysilyl)propyl methacrylate 20% solution in ethanol with 0.3% glacial acetic acid. The slides were then baked at 95 °C for 1 hour. A 30wt% solution of PEGDA and 50μg/ml acrylated fibronectin and 0.05% 2-Hydroxy-4'-(2-hydroxyethoxy)-2-methylpropiophenone (UV Initiator) was made and 20 μL was pooled between the activated coverslip and a hydrophobically treated glass microscope slide. This setup was placed in a UV crosslinker (Spectronics) and subjected to UV light at an intensity of ~5mW/cm2 for 10 minutes. For 3D gel fabrication, MSCs were trypsinized and pelleted and then resuspended in the gel solution. The gel was formed from solution as described above.

To confirm increased protein incorporation after acrylation, Alexa 546-conjugated fibrinogen (Invitrogen) was acrylated and PEGDA gels were formed with either acrylated or unacrylated fluorescent fibrinogen. After extensive washing, fluorescence was measured across several gels using an Incell analyzer microscope (General Electric) to compare remaining amounts of fibrinogen conjugated to gels.

Immunofluorescence

For immunofluorescence, gels were rinsed with PBS, fixed with 4% paraformaldehyde for 20 minutes and permeabilized with 0.1% Triton-X for 30 minutes. 1% bovine serum albumin was used for blocking. Nuclei and actin were

stained with DAPI (1:5000) and Alexa-Fluor 488-phalloidin (1:200), respectively. Paxillin was stained with a primary rabbit-anti-vinculin (ABCAM) and secondary 555-Alexa fluor goat anti-rabbit antibody (Invitrogen). Imaging was performed using a Zeiss Axiovert 200M inverted fluorescence microscope.

Vascularization assay

Conditioned media from MSCs was used for a vascularization assay as described in Appendix A.

Patterning MSC Islands

Patterned islands of MSCs encapsulated in PEGDA were formed by sandwiching MSCs suspended in PEGDA gel solution (with initiatior and acrylated fibronectin) between 2 slides, one hydrophobic and one treated for gel attachment using 20% (3-(trimethoxysilyl)propyl methacrylate solution in ethanol. This sandwich was then placed in contact with a photomask that is transparent where encapsulated MSCs are desired. UV light is shined through the mask using a mask aligner onto the PEGDA so that the initiator is activated only at the transparent areas in the mask. After 10 minutes of UV exposure, the excess PEGDA solution is washed away.

To assess the shapes of the islands, we encapsulated 5%(v/v) FITC-labeled 1μm beads(Invitrogen - F-8823) inside the PEGDA islands and these were imaged with a Carl Zeiss LSM 700 confocal scope. Z-stack images were used to make profiles of the islands

In order to confirm MSC patterning, MSCs were incubated for 30 minutes with cell tracker green CMFDA dye (Invitrogen) as per manufacturer's instructions prior to encapsulation. The labeled cells were pelleted and excess cell tracker disposed of before encapsulation. MSCs in islands were visualized by fluorescently imaging the PEGDA islands.

MSC-hMVEC co-culture

For MSC and hMVEC co-culture, MSC encapsulating PEG islands are formed as described above and then ~50ul of matrigel is placed on top of encapsulated MSC islands and sandwiched with another hydrophobic slide. After 30 minutes in the incubator, the matrigel solidifies and the gel is detached and hMVECs are seeded on top of the matrigel. The co-cultures are kept with a 50:50 mixture of MSC and hMVEC media. Images of the surface were taken after 8-24 hours of co-culture.

4.3 Results

In order to compare MSCs cultured on the surface of 2-D gels to cells encapsulated inside a more clinically relevant 3-D hydrogel architecture, we used a poly(ethylene glycol) diacrylate (PEGDA) system. We modified the end groups of PEG as previously reported(9) (Figure 4.1A) and confirmed modification using NMR (Figure 4.2). In order to incorporate protein into the 3-dimensional matrix, proteins were acrylated by reacting pendant amines with NHS-acrylate. We used a UV sensitive initiator to incorporate the matrix protein into the gels and confirmed higher protein incorporation in the NHS-acrylate condition using fluorescently labeled fibrinogen (Figure 4.1B). Based on our previous work(11), we used fibronectin as the matrix

protein and PEGDA hydrogels with an elasticity of around 40 kPa, as this condition had previously shown the highest angiogenic potential. (Chapter 2)

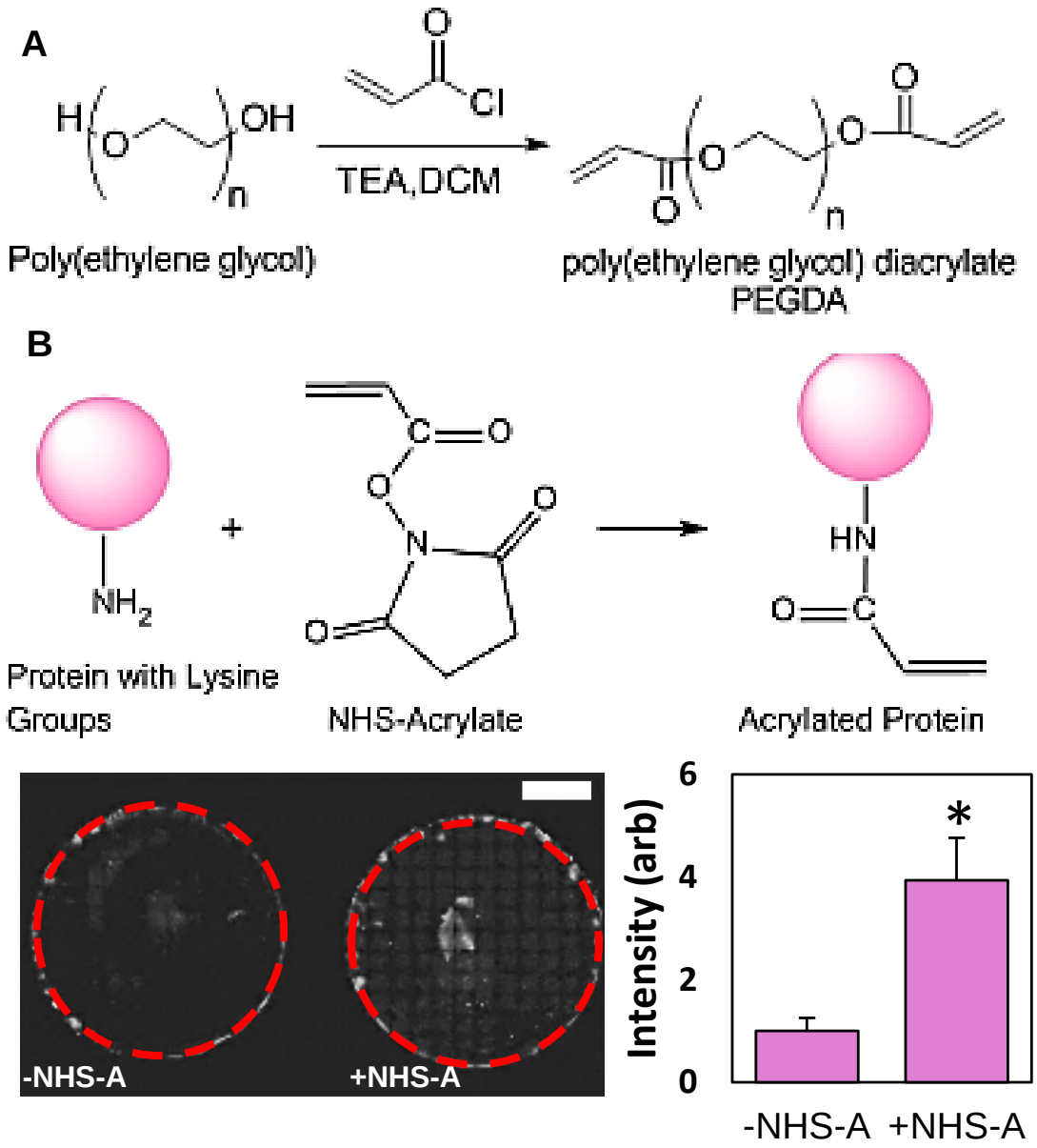

*Figure 4.1 Protein conjugated PEG gels for MSC culture (A) Acryloyl chloride was used for end group modification of PEG into PEGDA (B) (top) NHS-acrylate (NHS-A) was used for the acrylation of proteins via pendant amine groups.(bottom) Higher incorporation of protein was confirmed using fluorescent protein. Scale bar is 5mm. * P<0.05.*

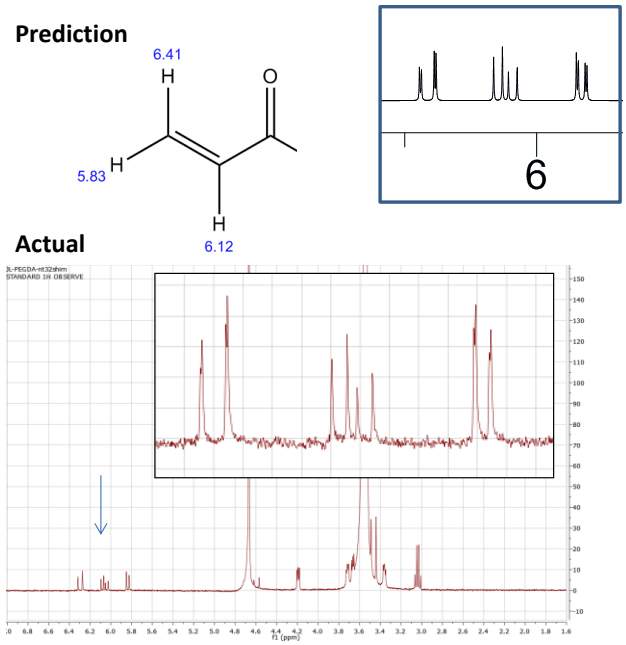

Figure 4.2 NMR confirmation of PEG modification into PEGDA shows an acrylation of ~85%-95%.

PEGDA gels were made that were either flat with MSCs seeded on top (2-D) or they were mixed with MSCs before gelation so that the MSCs were encapsulated inside the gel (3-D). MSCs were cultured in both the 2-D and 3-D conditions for 2 days. Morphologically, MSCs look very different when cultured in 2-D vs 3-D. On the flat 2-D surfaces, MSCs were spread out with a robust actin cytoskeleton, while inside the 3-D gels, the cells were more rounded up with a significantly smaller projected area (Figure 4.3). Paxillin staining shows focal adhesion formation on the surface of 2-D gels.

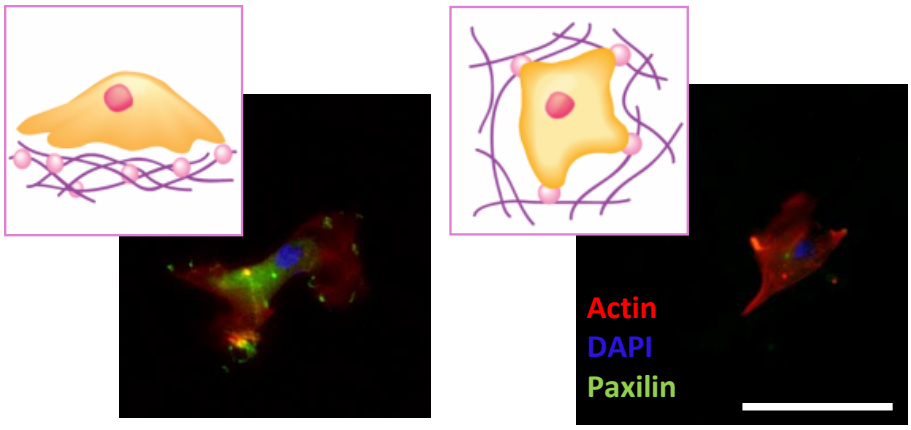

Figure 4.3 MSC morphology when cultured on the surface of PEG gels (2-D) or encapsulated inside (3-D). Scale bar is 100μm

After MSC culture, the conditioned media was used for an in-vitro tubulogenesis assay to investigate the differences in angiogenic potential(11). After 2 days of culture, conditioned media containing cytokines secreted by MSCs was collected and then added to hMVECs seeded on a 3D matrigel matrix. After 8 hours, hMVECs angiogenic tube formation was quantitated and normalized to hMVEC tubulogenesis in complete growth factor supplemented media (EGM-2). Conditioned media collected from MSCs cultured in the 3-D environment showed approximately 2-fold increase in tubulogenesis compared to MSCs cultured in the 2-D system (Figure 4.4A). These differences can be discerned in the morphology of the hMVEC tubes (Figure 4.4B).Both conditions showed less than half the tube formation of hMVECs in complete medium, possibly due to the large number of growth factors included in that medium. It should be noted that hMVECs show very low tubulogenesis when cultured in serum free medium.

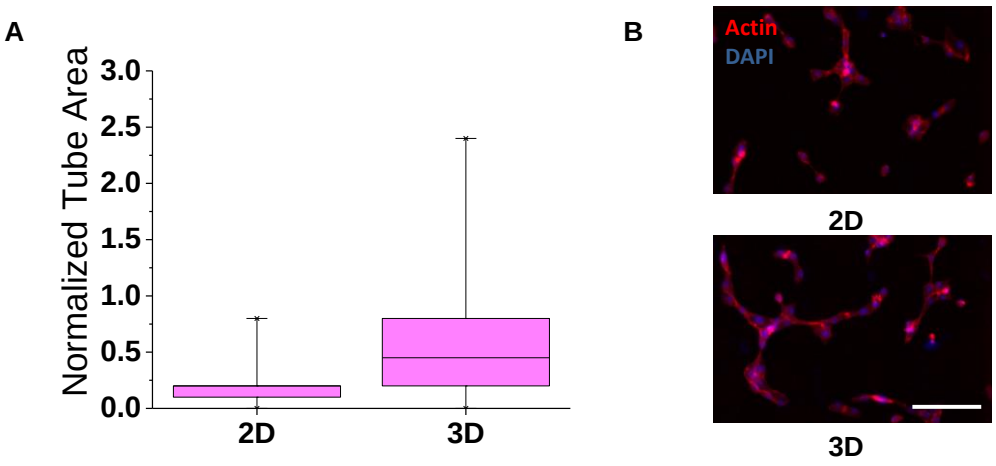

Figure 4.4 In-vitro angiogenesis assay of MSC-conditioned media (A) Box and whisker plot of quantitation of angiogenesis from conditioned media from MSCs cultured in 2-D or 3-D (B) Representative images of tube formation with conditioned media from 2-D and 3-D cultured MSCs. Scale bar is 200μm.

In 3-D environments cells are in contact with the extracellular matrix on all sides, which will significantly influence the propagation of signals from the outside-in to regulate cell behavior. Cytokine secretions have been reported to increase up to 35-fold in 3-D vs 2-D environments(3), so it is not surprising that the encapsulation of MSCs leads to higher pro-angiogenic activity. Although composition and mechanics are important factors, this result indicates that dimensionality, ligand presentation and other factors present in the switch from 2-D to 3-D culture(1) have a major role in directing pro-angiogenic signaling from MSCs.

A direct readout of angiogenesis in one platform would be useful in the study of materials properties that direct pro-angiogenic signaling from MSCs. Towards this end, we designed and developed a co-culture system where both encapsulated MSCs and hMVECs can be cultured together (Figure 4.5). By photopolymerizing gels

under UV light through a photomask, we made 'islands' of MSCs encapsulated in PEGDA.

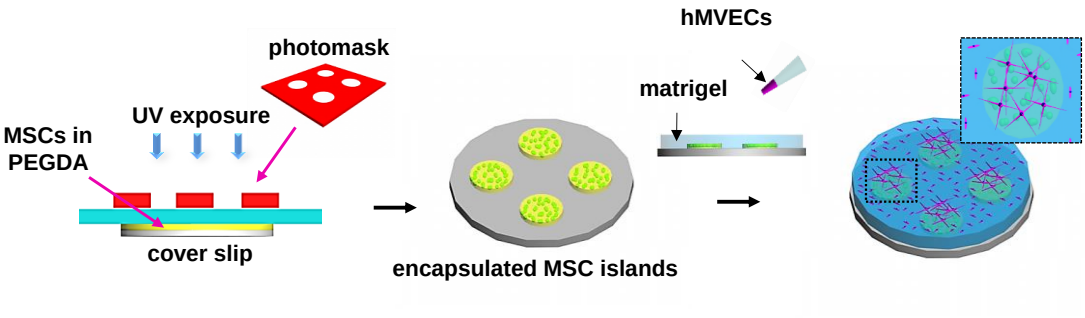

Figure 4.5 Schematic showing the procedure for co-culturing PEG encapsulated MSCs and hMVECs on matrigel.

To check the fidelity of these patterns we incorporated fluorescent beads in the PEGDA islands and imaged the islands using confocal microscopy (Figure 4.6A). Islands were of good dimensional accuracy and show good cross-sectional profiles and their shapes are not limited to circular but can be varied to adopt a range of geometries. After MSCs are encapsulated in these islands, cell patterning in the islands was verified using cell tracker (Figure 4.6B).

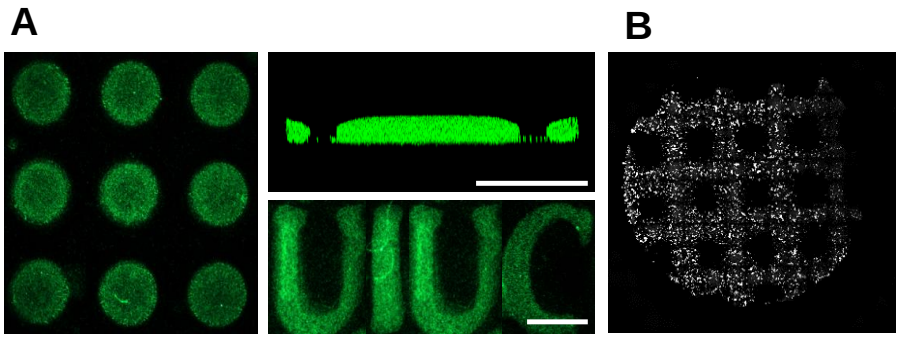

Figure 4.6 (A) Confocal images of fluorescent beads embedded into PEGDA islands showing top view (left) and profile. PEGDA islands can also be formed into irregular letters. Scale bars are 500μm (B) Fluorescence image of MSCs captured in a PEG grid. Scale bar is 5mm.

After encapsulating MSCs, matrigel was added on top of the islands and then placed in the incubator to gel. hMVECs are then seeded on top of the matrigel and tube formation was monitored. After 8 hours, there is tube formation on the areas of the matrigel above the MSC islands with very little tubulogenesis elsewhere (Figure 4.7). Due to the gelling of the matrigel, small bubbles are trapped at the base of the islands and can be seen around the edges. Tube formation may be enhanced on top of the islands due to closer proximity of these areas to MSCs or higher concentration of MSC-secreted cytokines.

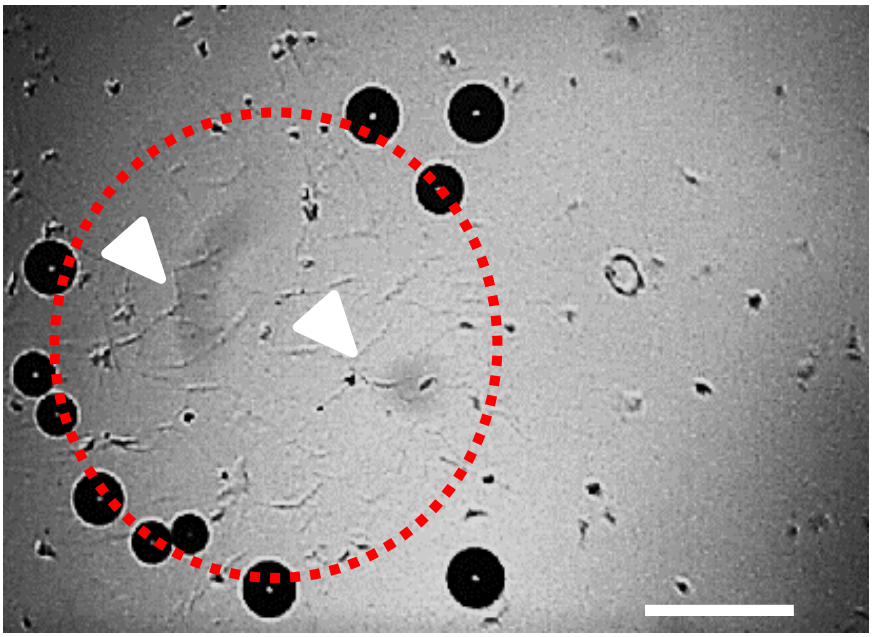

Figure 4.7 Brightfield images of hMVECs at the surface of matrigel after 8 hours of co-culture. Dotted outline indicates PEG island; pink arrows indicate tube formation; white arrow indicates rounded cells. Scale bar is 1mm.

4.4 Discussion

We developed a chemical strategy to conjugate proteins within a 3-D poly(ethylene) glycol hydrogel towards tissue-mimetic architectures for exploration of heterotypic cell-cell signaling. We show the importance of dimensionality and ligand presentation on MSC angiogenic efficacy. We extend this to a heterotypic co-culture system where presence of MSCs greatly increases tube formation from surrounding hMVECs. Spatial control of angiogenesis signaling in vitro, with supporting MSC co-culture, may be a good model for studying vasculature-pericyte interactions. Furthermore, this system is modular allowing assessment of virtually any hydrogel and cell type of interest to aid the design of cell-based therapeutic biomaterials.

Finally, the in-vivo applicability of this system can allow making hydrogel patches with encapsulated cells that can be transplanted in vivo. The amenability to in-vivo use coupled with the enhancement of pro-angiogenic potential of MSCs in hydrogels with optimized properties make a compelling case for this system for in-vivo translation.

4.5 References

1. Baker BM, Chen CS. Deconstructing the third dimension: how 3D culture microenvironments alter cellular cues. J Cell Sci. 2012 Jul 1;125(13):3015–24.

2. Huebsch N, Arany PR, Mao AS, Shvartsman D, Ali OA, Bencherif SA, et al. Harnessing traction-mediated manipulation of the cell/matrix interface to control stem-cell fate. Nat Mater. Nature Publishing Group; 2010 Jun;9(6):518–26.

3. Fischbach C, Kong HJ, Hsiong SX, Evangelista MB, Yuen W, Mooney DJ. Cancer cell angiogenic capability is regulated by 3D culture and integrin engagement. Proc Natl Acad Sci. 2009 Jan 13;106(2):399–404.

4. Aguado BA, Mulyasasmita W, Su J, Lampe KJ, Heilshorn SC. Improving viability of stem cells during syringe needle flow through the design of hydrogel cell carriers. Tissue Eng Part A. 2012 May;18(7-8):806–15.

5. Murphy MB, Moncivais K, Caplan AI. Mesenchymal stem cells: environmentally responsive therapeutics for regenerative medicine. Exp Mol Med. Nature Publishing Group; 2013 Jan;45(11):e54.

6. Pedersen TO, Blois AL, Xing Z, Xue Y, Sun Y, Finne-Wistrand A, et al. Endothelial microvascular networks affect gene-expression profiles and osteogenic potential of tissue-engineered constructs. Stem Cell Res Ther. Stem Cell Research & Therapy; 2013;4(3):52.

7. Saleh FA, Whyte M, Ashton P, Genever PG. Regulation of mesenchymal stem cell activity by endothelial cells. 2011;20(3).

8. Rao RR, Peterson AW, Ceccarelli J, Putnam AJ, Stegemann JP. Matrix composition regulates three-dimensional network formation by endothelial cells and mesenchymal stem cells in collagen/fibrin materials. Angiogenesis. 2012 Jun;15(2):253–64.

9. Aydin D, Louban I, Perschmann N, Blümmel J, Lohmüller T, Cavalcanti-Adam EA, et al. Polymeric substrates with tunable elasticity and nanoscopically controlled biomolecule presentation. Langmuir. 2010 Oct 5;26(19):15472–80.

10. Shoemaker SG, Hoffman AS, Priest JH. Synthesis and properties of vinyl monomer/enzyme conjugates - Conjugation of L-asparaginase with N-succinimidyl acrylate. Appl Biochem Biotechnol. 1987;15:11–24.

11. Abdeen AA, Weiss JB, Lee J, Kilian KA. Matrix Composition and Mechanics Direct Proangiogenic Signaling from Mesenchymal Stem Cells. Tissue Eng Part A. 2014 Oct;20(19-20):2737–45.

CHAPTER 5

TEMPORAL MODULATION OF STEM CELL ACTIVITY USING MAGNETOACTIVE HYDROGELS[1]

5.1 Introduction

Cells adapt to and respond to their local microenvironment in a context dependent fashion, that depends on spatiotemporal control of biophysical and biochemical properties(1). This sensitivity to the environment enables cells to maintain ECM homeostasis by responding to external changes(2) and allows highly versatile stem cells to take on multiple roles in different niches(3). However, contrary to the polymeric cell culture substrates used in most cellular studies, cellular environments are not static. In fact, the ECM is constantly changing in normal(4) and diseased(5,6) tissue. Several reports have shown that, in addition to sensing their current environment, stem cells are affected by or 'remember' their mechanical history(7–9). In addition, although great care is usually given to the temporal regulation of chemical factors used in several protocols (during somatic cell reprogramming(10) for instance), there is no reason to assume that mechanical regulation is not just as important. In fact, a recent study utilizing tunable polymeric materials to study the effects of parameters such as anisotropic

[1]This chapter is based on the following publication:
Amr A. Abdeen, Junmin Lee, N. Ashwin Bharadwaj, Randy H. Ewoldt, and Kristopher A. Kilian, Magnetoactive hydrogels for temporal modulation of stem cell activity, Advanced Healthcare Materials, 2016, DOI: 10.1002/adhm.201600349.

topgraphic cues(11) or stress relaxation(12) reveal highly dynamic cellular responses. Therefore, there is a need for in-vitro cell culture platforms with externally tunable mechanical properties in order to study the temporal effect of these parameters(13).

There have been several innovative strategies for making tunable stiffness systems. For example, pH(14), DNA strands(15) and calcium ion concentration(16) have been used to reversibly change substrate stiffness. However, these factors may affect cellular signaling and stiffness changes occur over different time scales. Another strategy is to alter the structure of the hydrogel using multi-step crosslinking(17) (for stiffening) or controlled degradation(18) (for softening) using various methods. For example, Kloxin et al. used photodegradable hydrogels to tune the gel microenvironment through visible light irradiation(19). Although these methods work well for one-directional changes in elasticity, they can cause irreversible changes in gel structure and do not offer reversibility. Rosales et al.(20) used an azobenzene based reversibly photo-switchable PEG hydrogel. However these gels can thermally relax and only show a modest change in modulus. Reversibility and the ability to modulate stiffness in a controlled manner are important to study continuous, temporally modulated changes that occur in vivo such as during development, homeostasis or disease (For example, fibrosis or wound healing)(21) or in vitro to ascertain how long it takes for changes in cell behavior to become permanent (mechanical dosing). MSCs, for instance, show irreversible changes in localization of transcriptional co-activator Yes-associated

protein (YAP) in the nucleus by 10 days of culture in stiff conditions but these changes could be reversed by switching the environment before 10 days(8).

In this chapter we adapt magnetorheological gels(22) and elastomers(23,24) into a magnetically tunable hydrogel platform for cell culture. We modify carbonyl iron (CI) particles for incorporation into polyacrylamide hydrogels and we demonstrate over two orders of magnitude shift in hydrogel compliance in response to magnetic fields. The gel stiffness can be easily and reversibly changed using permanent magnets, obviating the need for complex instrumentation, and thus making this technique amenable to virtually any research laboratory. Using mesenchymal stem cells as a model adult stem cell with therapeutic potential we show how magnetic fields modulate cell spreading and cytoskeletal tension, which impacts secretion of pro-angiogenic molecules and the propensity to undergo osteogenesis. The simplicity in which hydrogel mechanical properties can be modulated in situ will make this tool useful for a wide variety of applications, where temporal control over the biophysical microenvironment is desired.

5.2 Methods

General materials and methods are given in Appendix A.

Carbonyl Iron (CI) particle modification and hydrogel preparation

CI particles (grade EW) were generously provided by QED technologies. The particles were are either amino functionalized using aminopropyl trimethoxysilane or methacrylate functionalized using 3-(Trimethoxysilyl)propyl-methacrylate. The

treatment is performed by incubating the particles in the desired silane dissolved in 90% ethanol solution overnight under shaking. Modified CI particles are washed thoroughly with DI water at least 4 times before use.

For gel preparation, a pre-polymer solution mixture of acrylamide and bis-acrylamide (Fisher Scientific) is mixed according to the desired crosslinking density (here we use 3% acrylamide and 0.06% bis-acrylamide) and degassed under nitrogen gas for 10 minutes. 18 mm glass coverslips are cleaned by sonication under ethanol for 15 minutes followed by sonication in DI water for 15 minutes. Coverslips are activated for gel attachment by treatment with 0.5% solution of APTES for 3 minutes followed by thorough washing with DI water 3 times. Coverslips are then treated with 0.5% glutaraldehyde solution for 30 minutes and washed with DI water. A hydrophobic microscope slide is prepared by treatment with Rain-X (SOPUS).

The desired mixture of CI particles by volume is prepared in pre-polymer solution. Gelation is initiated by addition of 0.1% ammonium persulfate and 0.1% tetramethylethylenediamine (TEMED) and vortexing the solution. 20 µl of solution is pipetted onto the hydrophobic microscope slide and the activated coverslip is placed face down on the drop. The gel is left to solidify for ~20 minutes and is then detached from the hydrophobic slide. Gels are washed at least 3 times with DI water to remove any particles not incorporated during gelation.

For protein incorporation, fibronectin (from human plasma) at 50µg ml^{-1} is incubated on the surface of PDMS stamps for 30 minutes. Then, air is used to blow

excess solution from the surface of the PDMS stamps and fibronectin is transferred to the surface of the gel by stamping. Gels are washed several times in DI water and stored in 12 well plates until cell culture.

Scanning electron microscopy (SEM)

SEM images of dried PA hydrogels with modified CI particles were acquired using a JEOL 6060-LV scanning electron microscope under high vacuum. A thin layer of gold was sputtered onto the surfaces to ensure electrical conductivity of the samples. Images were taken at either 1,000x or 3,500x.

Fourier transform infrared spectroscopy

FTIR was performed on a Spectrum 100 (Perkin Elmer) machine in transmittance mode. Spectra were taken at each point between 450 to 4000 cm^{-1} on samples in dichloromethane on a potassium bromide salt plate. Baseline correction and normalization were performed on spectra.

Mechanical characterization

Dynamic shear measurements were performed on a rotational rheometer (combined-motor-transducer, DHR-3, TA Instruments) with a Magneto-Rheology (MR) setup for uniform and controlled application of magnetic fields from -1 T to +1 T (experimental setup shown in Figure 5.4A). Disks of samples of 1 mm thickness and 20 mm diameter were prepared, and measurements were made with a non-magnetic 20 mm diameter parallel plate fixture. An electro-magnetic coil beneath the sample imposed magnetic field lines orthogonal to the plate surface, and a hall

probe under the bottom fixed plate gave real time measurement of the external field strength during tests. An upper yoke surrounded the upper geometry to draw field lines orthogonal to the plate surfaces. Tests were run at a constant temperature of 37^{o}C, maintained by a closed-loop-control fluid circulator through the bottom MR fixture. For experiments performed in the presence of a magnetic field, oscillations were run at a frequency of 1 rad s^{-1} and shear strain amplitude of 1% (in the linear viscoelastic regime).

Cell culture

For differentiation experiments, MSCs were cultured for 10 days in mixed (1:1) bipotential adipogenic/osteogenic differentiation media (Lonza) as per the manufacturer's instructions.

Tube formation assay

Vascularization assays were performed with MSC conditioned media as described previously(25). Briefly, growth-factor-reduced basement membrane (matrigel, Trevigen) was coated on the bottom surfaces of a 48-well plate and gelled at 37°C for 30 minutes. HMVECs were seeded onto the matrigel at ~15,000 cells/well in serum and growth factor free media (EBM-2, Lonza) and conditioned media from MSCs cultured at different conditions was added. After 8 hours, tube formation was imaged using a Rebel DSLR camera (Cannon) and tube area quantified using imageJ (NIH).

Immunostaining

Surfaces were rinsed twice with phosphate buffered saline (PBS) and were then fixed with 4% paraformaldehyde for 20 minutes. Surfaces were permeabilized for 30 minutes in 0.1% Triton X-100 and then blocked in 1% bovine serum albumin (BSA) for 1 hour. Runx2 was stained with a primary rabbit-anti-Runx2 (ABCAM) overnight at 4°C and secondary 555-Alexa fluor goat anti-rabbit antibody (1:200) (Invitrogen). Actin and nuclei were stained by Alexa-Fluor 488-phalloidin (1:200) and 4,6-Diamidino-2-phenylindole (DAPI; 1:5000), respectively. Secondary staining was performed for 20 minutes at 37°C.

Fluorescence imaging and data analysis

Immunostained cells were imaged using a Zeiss Axiovert inverted fluorescence microscope (Carl Zeiss) or an IN Cell Analyzer 2000 (General Electric). Cell area was measured from phalloidin staining of the actin cytoskeleton using ImageJ and nuclear Runx2 intensity was measured using DAPI as a mask for nuclei. Runx2 intensity is reported as Nuclear intensity minus cytoplasmic intensity. Statistical significance was determined using two-tailed p-values from unpaired t-test for comparing two groups. Error bars in this chapter represent standard error.

5.3 Results

Gel concept and fabrication

We used polyacrylamide (PA) as the base polymeric hydrogel for our system, because of PA's flexibility as a cell culture platform with tunable elasticity within physiological stiffness ranges(26). Furthermore, PA has been previously used in

multiple studies with MSCs(25,27–29), which provides a wealth of preliminary data for MSC behavior on soft and stiff PA substrates. These gels are formed through radical addition polymerization (Figure 5.1A) as described previously(26).

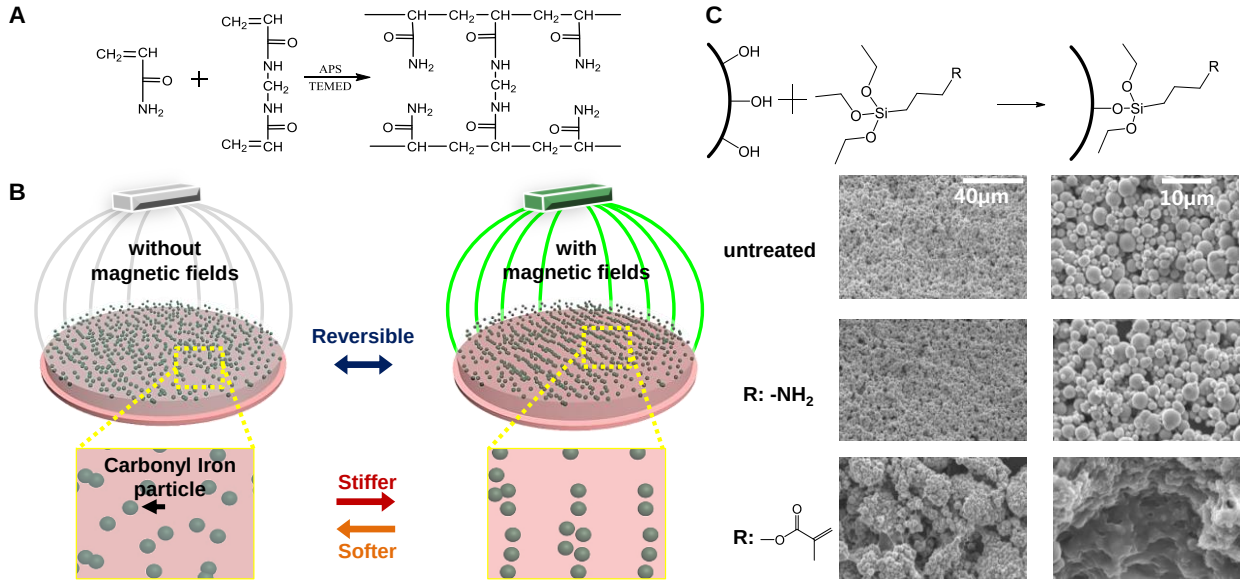

Figure 5.1 (A) Formation of polyacrylamide via radical polymerization from acrylamide and bis-acrylamide monomers. (B)Magnetoactive hydrogel system formed by incorporation of carbonyl iron particles in a polyacrylamide matrix. Subjecting these gels to magnetic fields causes alignment of the particles, stiffening the hydrogels35. (C) Silane modification of CI particles (top) Silane chemistry can be used to modularly modify the surface of CI particles. (bottom) SEM images of dried PA hydrogels with incorporated CI particles that are untreated, treated with an amine-terminated silanes or treated with a methacrylate terminated silane. The latter shows covalent incorporation into the hydrogel and aggregation behavior.

In order to add magnetic tunability to our hydrogels, we adapted the approach of Mitsumata et al. to incorporate carbonyl iron (CI) particles in carrageenan hydrogels(22) (Figure 5.1B).

In order to make the particles more stable in cell culture conditions, and allow functionalization of the particles, we used silane chemistry to modify the surface with different functional groups (Figure 5.1C, top) This has the added benefit of

allowing modular modifications to the system such as covalent incorporation of moieties to the particles or the chemical crosslinking of particles in the hydrogel network. To demonstrate the efficacy of this treatment, we used two different silanes: aminopropyl triethoxysilane (APTES) to passivate the particles to stabilize them for long term cell culture, and 3-(Trimethoxysilyl)propyl-methacrylate (TMSPM) to enable covalent incorporation into PA gels. FTIR analysis shows a change in the spectrum upon treatment with APTES and TMSPM with characteristic peaks showing chemical conjugation at ~1080 cm^{-1}, attributed to open chain siloxane groups, with the TMSPM treated particles showing characteristic peaks at ~1638 cm^{-1} (C=C) and 1720 cm^{-1} (C=O)(30) (Figure 5.2).

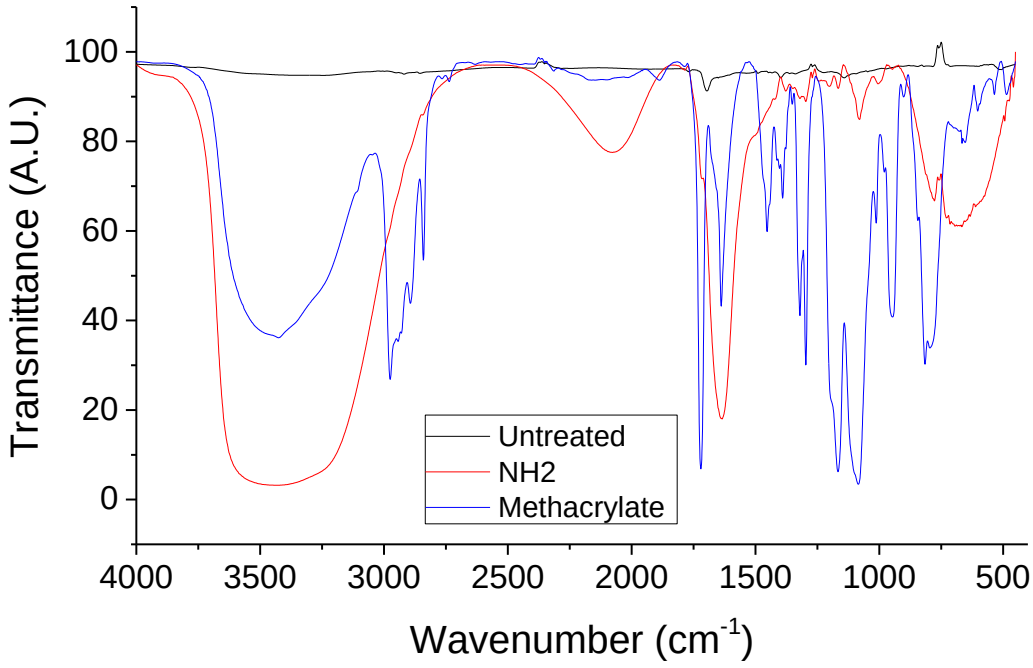

Figure 5.2 FTIR spectra of CI particles that are untreated, treated with APTES to incorporate amines (NH2) or treated with TMSPM to incorporate methacrylates.

Upon incorporation of the modified particles into the hydrogels, the gels were dried and imaged using SEM to see whether there was any visible effect on the structure (Figure 5.1C, bottom). The amine-terminated particles, while they appear similar to untreated particles in SEM, demonstrated a significant improvement in stability under prolonged cell culture conditions, where gels made with untreated particles dissolve within 10 days (Figure 5.3). The methacylate-terminated particles, on the other hand, show different characteristics to both amine terminated and untreated particles. SEM images show gel residues attached to the particles indicating covalent attachment of the hydrogel to the particles during gelation. An unforeseen consequence of the treatment, however, was aggregation of the particles into 'clumps', presumably due to heterogeneous polymerization between monomer and particles. For all particle treatments, repeated application and removal of magnetic fields does lead to some limited leaching of particles from the hydrogel, however leached particles sediment to the bottom of well plates and do not further impact cell behavior. APTES modified particles were used for the remainder of the study unless otherwise noted.

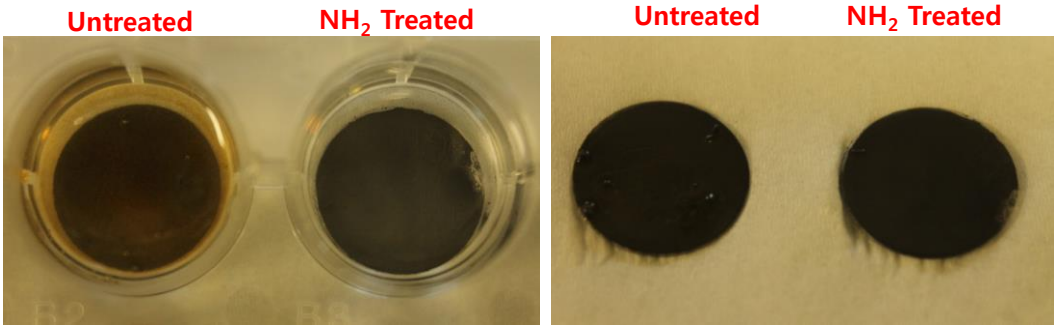

Figure 5.3 Photographs of magnetoactive hydrogels after incubation in bipotential osteogenic/adipogenic media for 10 days and then washing and transfer to PBS for 1 day.

Mechanical characterization of hydrogels

Shear rheometry was used to characterize the hydrogel's mechanical properties and their response to magnetic fields using a magnetorheological setup (Figure 5.4A). The gel composite is a viscoelastic solid as observed by creep compliance and oscillatory shear measurements (Figures 5.4B & 5.4C), with linear viscoelastic equilibrium compliance J≈0.01 Pa^{-1} (modulus G≈0.1 kPa). Figure 5.4B shows the strain amplitude dependence of the gel composite viscoelasticity at a frequency of 1 rad s^{-1}; the sweep range was chosen to avoid a nonlinear response that may irreversibly affect the sample.

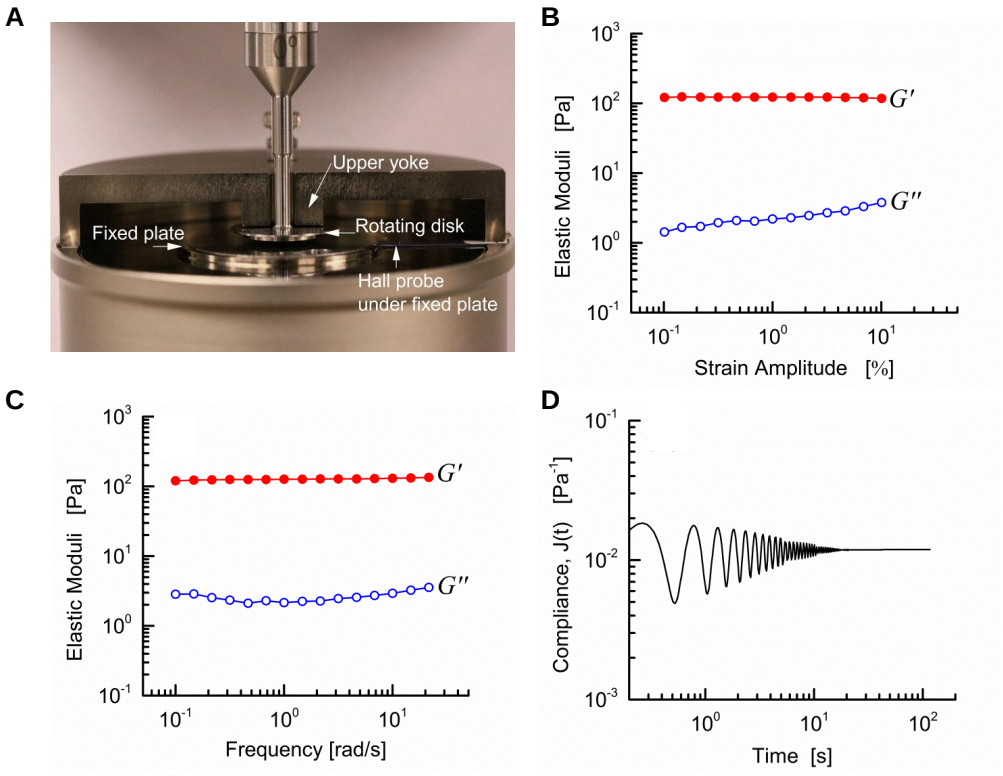

Figure 5.4 (A) A Magneto-Rheology fixture was used with a rotational rheometer for rheological measurements. (B,C,D) polyacrylamide gel with no magnetic field; (B) Strain amplitude sweep at frequency 1 rad/s indicates a nearly linear viscoelastic response up to 10% shear strain; (C) Linear viscoelastic moduli show minimal frequency dependence (constant strain amplitude 1%); (D) Creep compliance experiments (imposed shear stress 1Pa) show the response of a viscoelastic solid at times beyond 100 s. The oscillations at short times are caused by sample elasticity coupling to instrument rotational inertia (known as inertio-elastic ringing(31,32).

We observed almost constant storage modulus and a slowly rising loss modulus between 0.1% and 10% strain. This agrees with previous data for polyacrylamide(33). We use a strain amplitude of 1% for performing all further linear viscoelastic measurements on the gel. Linear viscoelastic frequency sweep measurements (Figure 5.4C) indicate minimal frequency dependence. Further information at longer timescales is obtained from a creep compliance test (Figure 5.4D). At short times, inertio-elastic oscillations are observed, due to the well-known effect of sample elasticity coupling to instrument rotational inertia. At longer times beyond 100s, the compliance J(t) is nearly constant, indicating solid-like behavior at these timescales.

The gel composite dramatically stiffens in response to magnetic field, as shown in Figure 5.5. The reproducibility of the magnetic field effect is shown in Figure 5.5A, as observed by cycling the magnetic field between 0 and 0.75T several times. Each full cycle was 1 minute (30 seconds at 0T and 30 seconds at 0.75T). The storage modulus G' at 0T ranged between 0.1-0.14 kPa and at 0.75T stiffened to 60-90 kPa. The gel recovered its elastic modulus at 0T with each cycle, indicating no irreversible disruption of the polymer network. The modulus at 0.75T increased marginally with each cycle, but this is insignificant in the context of the relative change in moduli from 0T to 0.75T. Importantly, this range of mechanical behavior corresponds to nearly the entire range of physiological stiffness observed in biology, from brain tissue to collagenous bone(27). Thus, a single hydrogel can cover the entire spectrum of physiological elasticity, dynamically, and on a single gel surface.

The sensitivity to continuously modulated magnetic field strength is shown in Figure 5.5B, with a magnetic field ramp from 0.1T to 1T. The elasticity (G') transitioned smoothly and continuously as the magnetic field was raised, starting to level off and saturate around 0.8T. Magnetic saturation is a well-known effect in magneto-responsive materials(34). Hysteresis effects are also apparent when the magnetic field is cycled through positive and negative values (Figure 5.5C), with cyclic ramps from 1T to -1 T. Between cycles, the gel appeared to attain identical values of G' at 0T, but the approach to this value depended on the direction of the field, showing signs of hysteresis in the mechanical response. When compared with cycle 1 (1T to 0T), the gel elasticity in cycle 2 is larger in the first half of the cycle (-1T to 0T), but smaller in the second half (0T to 1T). We attribute this to the magnetic hysteresis of the particles, which may consequently result in the particle network maintaining its configuration from a previous cycle (cycle 1, 0T to -1T), and rearranging to a different configuration in cycle 2 when the field was being ramped up from 0T to 1T.

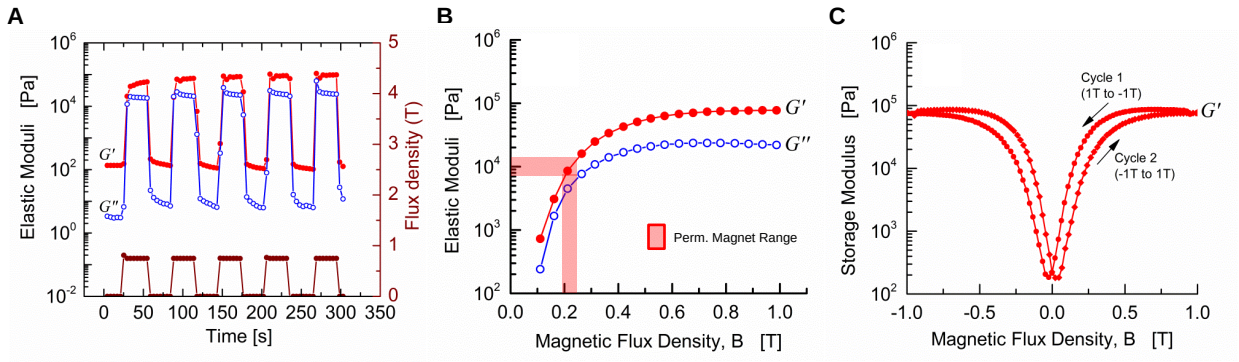

Figure 5.5 Magnetic field dependent elasticity of polyacrylamide-CI gels. (A) Pulsed magnetic field from 0T to 0.75 T showing three orders of magnitude change to elasticity. (B) A magnetic field ramp showing a continuous rise in the modulus with field strength, with the highlighted region representing magnetic flux density achieved with permanent magnets. (C) Elastic hysteresis is observed between back and forth ramps from -1T to 1T.

Next, we checked the particle fraction dependence of the composite (Figure 5.6). At B=0T, the linear elastic modulus (*G'*) shows no frequency dependence for all considered concentrations and the loss modulus (*G''*) shows weak frequency dependence before being affected by instrument rotational inertia, shown as a limit line in the figure(35). Up to a volume fraction of 30% in the composite, both moduli increase with increasing particle concentration, beyond which the composite elasticity drops with particle inclusion, and the gel degrades. The magnetic field dependent mechanical properties of each resulting composite are outlined (Figure 5.6B), and serve as a good reference for the choice of 30% particle volume fraction in the gel, which represents the maximum change in (G').

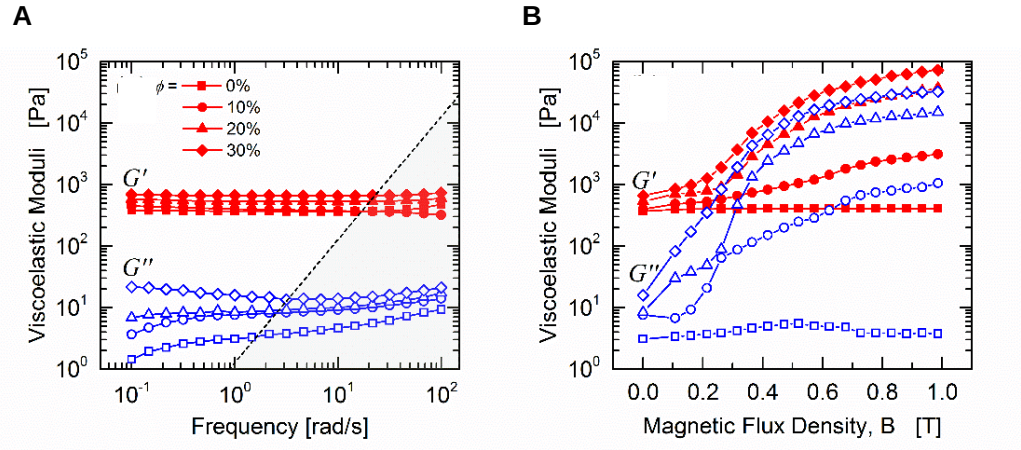

Figure 5.6 Amine treated carbonyl iron (CI) concentration dependence in polyacrylamide-CI composite elasticity. (A) Linear viscoelastic moduli of composites with varying volume fraction of CI particles, probed using oscillatory shear rheology at γ_0 = 1%, with experimental limits of instrument rotational inertia (B) Magnetic field dependent linear viscoelasticity, probed at γ_0 = 1%, ω = 1 rad/s.

To determine the effect of the surface functionality on treated/untreated CI particles in the composite, we studied the magnetic field dependent mechanical properties of untreated and amine-treated particles in the polyacrylamide gel

(Figure 5.7). The linear viscoelastic properties of the composite show no significant difference when compared to the properties of the composite with untreated particles. Both moduli show strong magnetic field dependence (Figure 5.7B) and increase ~100X as the field is ramped from 0T to 1T. The same material is then exposed to five cycles of a pulsed magnetic field from 0T to 0.75 T (Figure 5.7C). The linear viscoelastic moduli are reversible between cycles 2-5 and show ~200X increase in moduli. A larger relative change in moduli here is attributed to a faster rate of change of magnetic field, in contrast to a slow and gradual growth from 0T to 1T in the ramps shown in Figure 5.7B. A study with methacrylate treated particles in the gel was also attempted, but consistently resulted in a heterogeneous composite that showed noticeable phase separation at the volume fractions of interest, ϕ=30%.

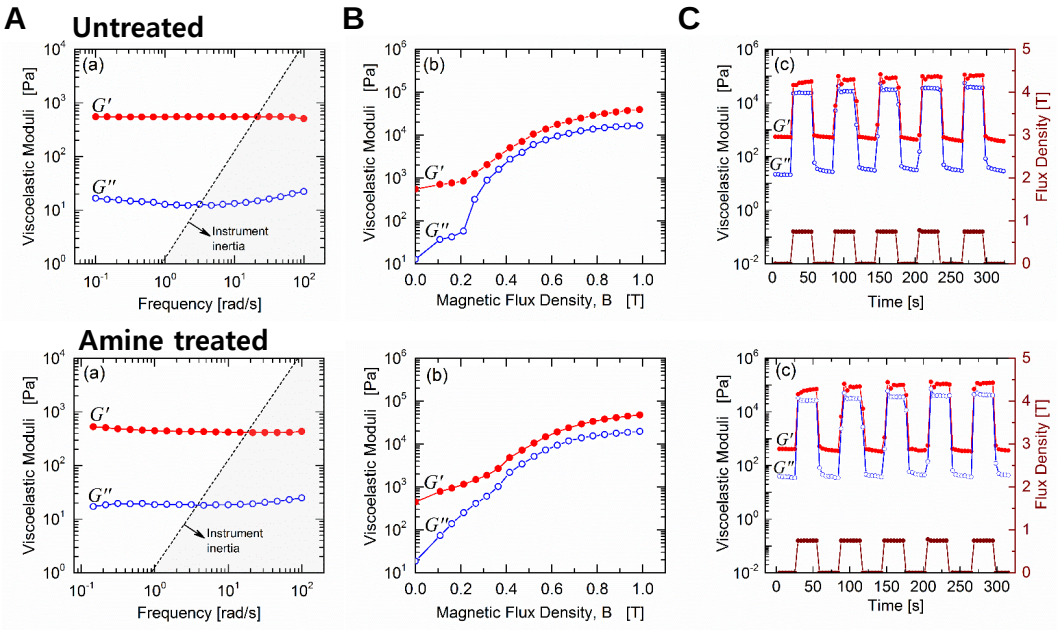

Figure 5.7 Linear viscoelasticity of composites of ϕ = 30% (top)untreated and (bottom) amine treated carbonyl iron particles in a hydrogel of polyacrylamide, probed using oscillatory shear rheology at γ_0 = 1%. Linear viscoelastic moduli show no frequency dependence in (A) before being affected by instrument rotational inertia at larger frequencies. Both moduli show strong dependence on externally applied magnetic field in (B), and show good reversibility for multiple magnetic field pulses in (C).

As a control with particles alone, we formulated a suspension of amine-treated carbonyl particles in a silicone oil-grease medium (Figure 5.8). This medium has a low yield stress of ~2 Pa which inhibits particle sedimentation for ~24 hours(36). The storage modulus and loss modulus increase with increasing particle volume fraction. We show this volume fraction dependence with a characteristic shear modulus $G_0 \equiv G'(\omega = 1 \text{ rad s}^{-1})$, both with and without magnetic field (Figure 5.8B). The suspension shows magnetic field dependent linear viscoelasticity that scales as $G_0 \sim \phi^{2.2}$, an exponent that is slightly larger than the earlier observed scaling of 1.7(37).

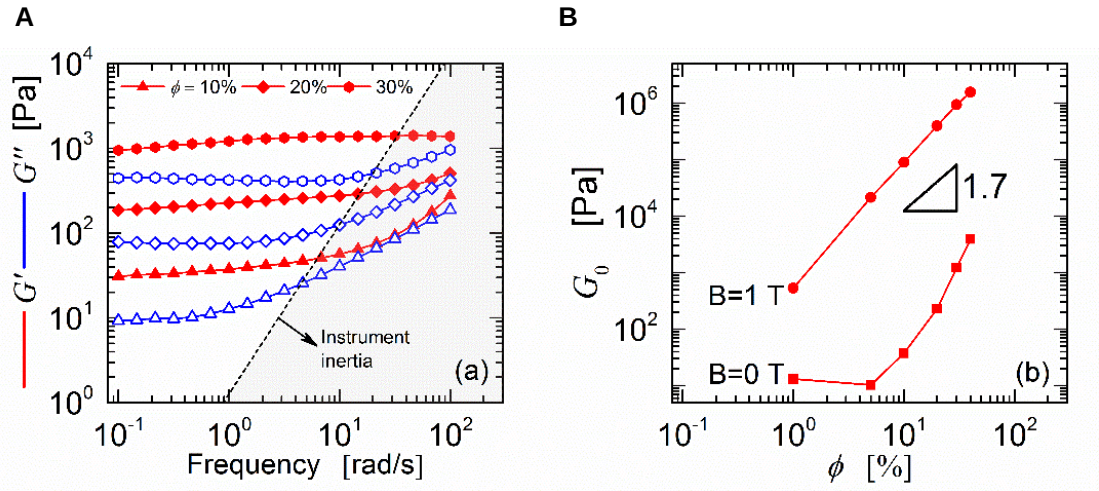

Figure 5.8 Linear viscoelasticity of amine treated carbonyl iron particles in silicone oil grease media. (A) Linear viscoelastic moduli at γ_0 = 1% shows weak frequency dependence before being affected by instrument rotational inertia at larger frequency.(B) Characteristic shear modulus $G_0 \equiv G'(\omega = 1 \text{ rad/s})$ shown for B=0 T and B=1 T. Also shown is the known modulus scaling of 1.7 with volume fraction(37).

While tunability across the entire range of elasticity is desirable, the equipment used to impose a variable magnetic field is expensive, requires electrical power, and is cumbersome in cell culture environments. An alternate solution is to use

permanent magnets which can provide a constant magnetic field, which can be changed by varying the distance between magnet and gel. We used permanent rare earth magnets attached to a well plate cover (Figure 5.9), upon which the hydrogel samples with cells in well plates can be placed. By measuring the magnetic field strength using a Hall probe, we found the field to be ~0.2-0.25T which corresponds to a storage modulus in the range ~8-15 kPa. (see Figure 5.5B) Therefore, with this setup, we can 'switch' or 'oscillate' the modulus between 0.1-0.14 Pa (no magnet) and 8-15 kPa (with magnet). Henceforth these will be given the designations 'soft' and 'stiff', respectively.

Figure 5.9 Permanent rare earth magnets taped to the underside of a well plate cover. Well plates with samples inside them can be placed on top of this well plate cover to introduce a magnetic field.

Modulation of substrate stiffness guides secretion of pro-angiogenic molecules, cell spreading and differentiation

Previously we demonstrated how increasing stiffness of fibronectin conjugated hydrogels will enhance MSC pro-angiogenic potential(25). First, to confirm protein

incorporation onto the magnetoactive gel surfaces we used fluorescently tagged fibronectin and confirmed increased fluorescence signal from the hydrogels after addition (Figure 5.10A). Next, we micropatterned fibronectin on our gel surface using a polydimethylsiloxane (PDMS) stamp presenting oval features in relief. We observed preferential adhesion to the micropatterned regions (Figure 5.10B).

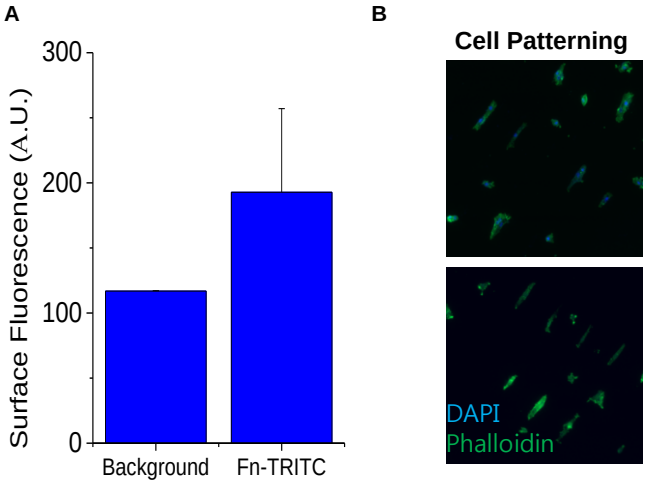

Figure 5.10 (A) Fluorescence on the surface of hydrogels with incorporated TRITC-conjugated fibronectin and washed several times compared to background. (B) MSCs patterned on magnetoactive hydrogel surfaces sing oval-patterned PDMS stamp.

We also tested the effect of magnetic fields on protein arrangement on the gel surface (Figure 5.11). Fluorescence analysis indicates negligible changes in the uniformity; however, direct gel contact with the magnet leads to the appearance of fluorescent lines suggesting some adhesion to the particles within the gel that becomes apparent after alignment in a magnetic field.

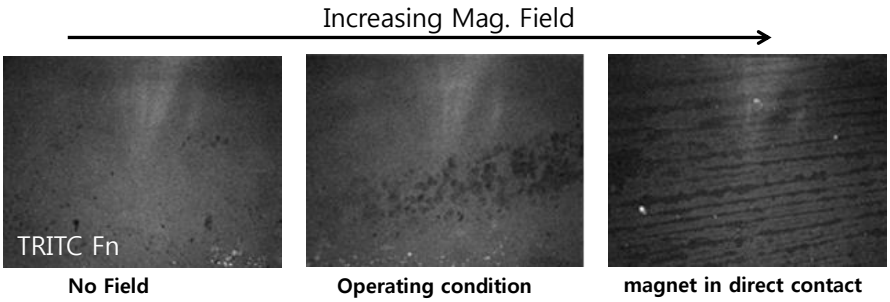

Figure 5.11 The effect of increasing magnetic field on the TRITC protein organization on the surface of magnetoactive hydrogels

We cultured MSCs on our tunable hydrogel for two days and performed a tube formation assay (hMVECs on matrigel as described previously(25)) using the conditioned medium from MSCs cultured on the surfaces with (+B) or without (-B) a magnetic field. We also used EGM-2 growth media as a positive control and unconditioned DMEM as a negative control. Quantifying the tube area from the different media (Figure 5.12) shows almost double the tube formation for MSCs cultured on stiff vs soft surfaces. This trend agrees with our expectations for MSCs on soft or stiff substrates and demonstrates the potential for using dynamic magnetoactive materials to guide angiogenesis when MSCs are a therapeutic agent.

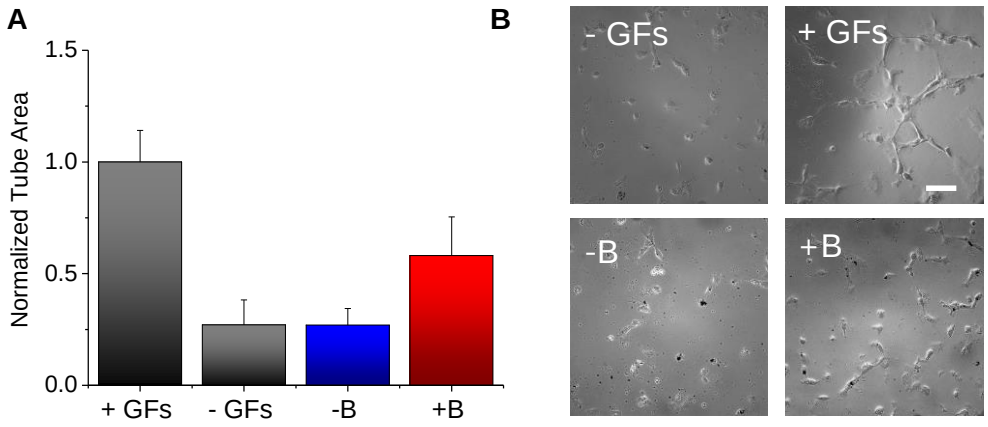

Figure 5.12 (A) hMVEC tube formation on matrigel is quantified as a function of secreted factors in the conditioned medium. Conditioned medium is obtained from MSCs cultured on magnetoactive hydrogels cultured with and without a magnetic field. EGM-2 media is used as a positive control and unconditioned DMEM is used as a negative control. (B) Representative images of tube formation on the positive, -Magnet and +Magnet conditions (scale bar:100μm)

To further investigate how changing the elasticity in-vitro will influence adherent cells, we used one of the fastest 'cellular indicators' of substrate elasticity: cell spread area. Cell spread area generally increases with substrate stiffness and the changes happen relatively quickly. We cultured MSCs on soft and stiff conditions for 4 hours and then we switched a subset of the MSCs from stiff to soft and cultured them for a further 4 hours (Figure 5.13). Overall, MSCs on soft substrates had an average area of about 750 μm^2 while those on stiff substrates had an average area of ~1,300 μm^2 (Figure 5.13B). Cells cultured on stiff-to-soft substrates reverted to an area of ~900 μm^2, just above that from soft substrates. Interestingly, some cells showed more prominent actin stress fibers when cultured on stiff vs soft substrates which persisted for 4 hours (Figure 13A, bottom). Taken together, this shows that reversible changes in substrate stiffness can lead to reversible changes in cellular spreading.

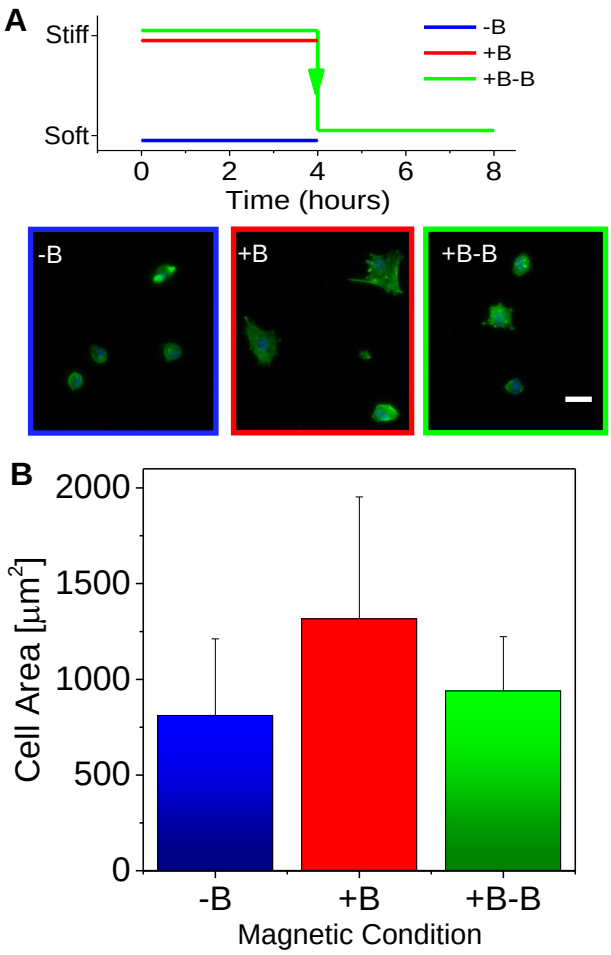

Figure 5.13 Modulating hydrogel stiffness in-vitro reversibly affects MSC spread area. (a) (top) cells were cultured with or without a magnetic field or cultured for 4 hours on a magnetic field and then then the field was switched off. (bottom) Representative images of MSCs cultured on these substrates at these different conditions (Scale bar: 50μm). (b) Quantification of average MSC area.

MSC osteogenesis is another phenomenon that has been studied extensively on hydrogels(25,27,38). Generally, going to stiffer substrates increases osteogenic marker expression. Runx2 is an important transcription factor involved in regulating lineage specification, and is the most common marker used to classify early osteogenesis. Several reports have demonstrated a 'memory effect' where the properties of a previous microenvironment influences cell state to a degree that lineage-specific activity remains apparent(8,9,17). Guvendiren et al. show a

dependence of Runx2 expression when gels are switched from soft-to-stiff at different time points, with gels switched earlier showing increased Runx2 expression(17). We performed a similar experiment with MSCs cultured on soft, stiff or switched from soft-to-stiff. First, cells were seeded and allowed to attach for 1 day at one stiffness, then the stiffness was changed at day 2, and again at day 5 (Figure 5.14A). We then imaged and quantified Runx2 expression at 10 days (Figure 5.14B & 5.14C). The experiment was performed in this way in order to see the relative effects of stiffness changes during cell attachment and spreading (up to day 2) and in the early (up to day 5) and late stages (day 5-10) of our study of early osteogenic lineage specification. We used 6 different variations labeled with H for high stiffness and L for low stiffness (e.g. HLH indicates high stiffness for 1 day, low stiffness for 4 days and high stiffness for the remaining 5 days). To highlight relative differences between samples, the data is shown as deviation of Runx2 expresssion from the average of all samples at day 10. Analysis of Runx2 expression indicates that initial stiffening plays a significant role in guiding the final differentiation state. Furthermore, stiffeness condition during the latter stages of culture (last 5 days) corresponded with the largest increase in Runx2 intensity. Surprisingly, intermediate stiffening (between days 2 and 5) did not exert a significant influence on Runx2 expression.

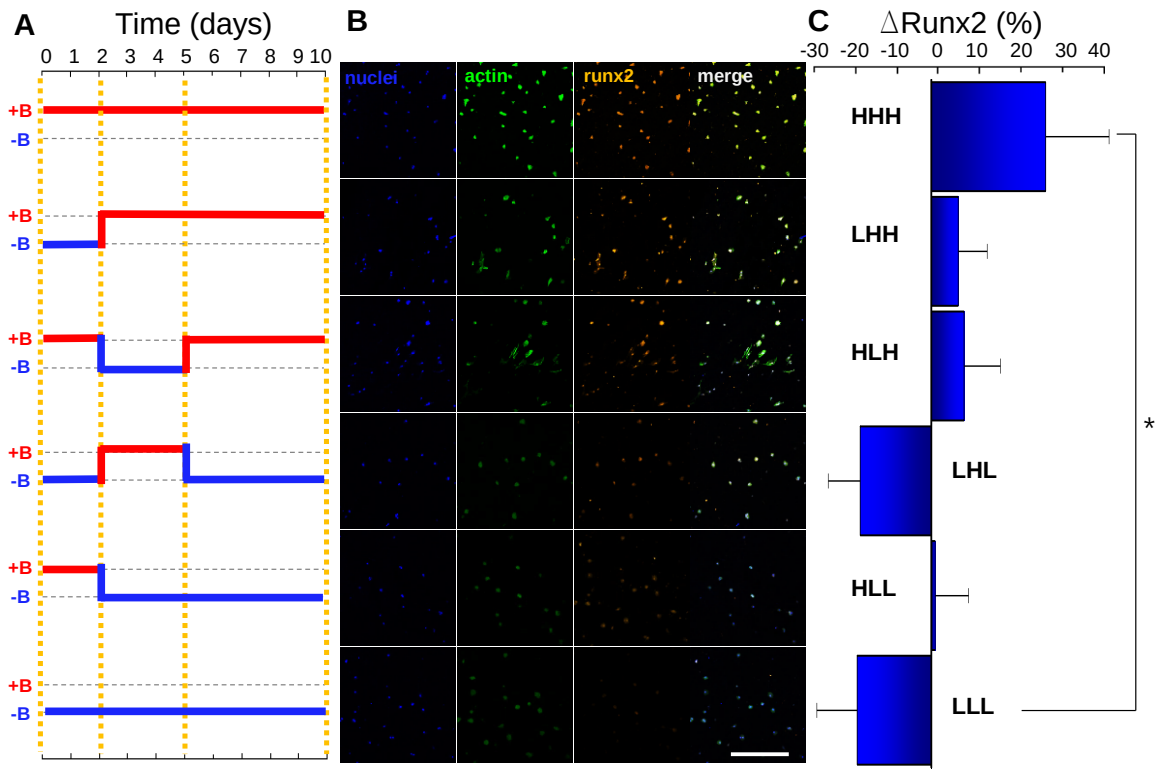

Figure 5.14 (A)Timeline of magnetic field change (B) Representative images of DAPI, Phalloidin and Runx2 of MSCs cultured for 10 days at various magnetic field profiles (scale bar: 500um). (C) Percent change of Runx2 expression in MSCs cultured for 10 days in bi-potential osteogenic/adipogenic medium at different magnetic field profiles from the overall average.

Interestingly, after 10 days the average cell area was similar between the soft and stiff conditions (Figure 5.15A). This result is somewhat surprising, and may be related to cells adapting a preferred shape after differentation, or through remodelling their microenvironment and the hydrogel properties. Nevertheless, looking at cell area vs. Runx2 expression for a random sample of 200 cells (Figure 5.15B) we observed that for virtually any particular range of areas, Runx2 expression was higher in cells on stiff matrices when compared to soft.

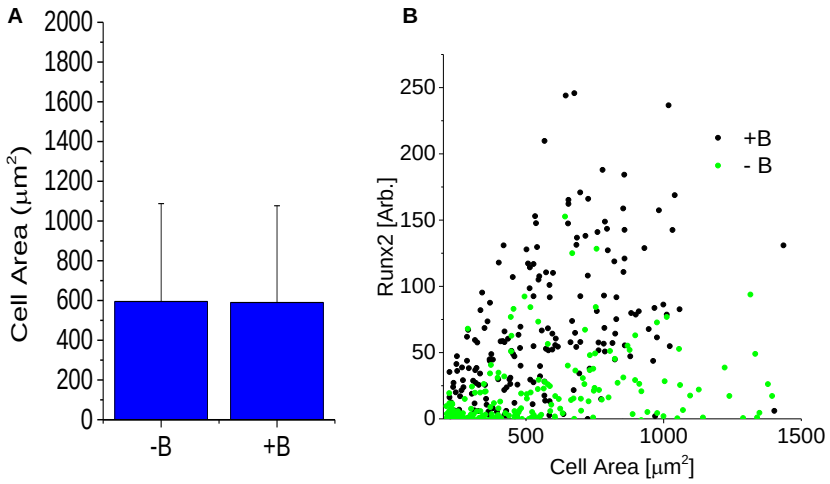

Figure 5.15 (A) Average Cell area at 10 days with and without application of a magnetic field. (B) Cell area vs Runx2 intensity for cells cultured for 10 days with and without application of a magnetic field. (-B is LLL and +B is HHH)

5.4 Discussion

We have demonstrated a magnetically tunable hydrogel system, using functionalized carbonyl iron particles in a polyacrylamide matrix, which shows a several-fold change in elasticity when subjected to magnetic fields. The CI particles reinforce the gel at higher magnetic fields, increasing elasticity reversibly. The CI particles can be modified by flexible silane chemistries for conjugation to the polymer network or other moieties. Using a magnetic field as a stimulus has the added benefit of not affecting cellular cycle and growth which has been shown for fields up to 10T(39).

Mechanical characterization shows possible modulation of storage modulus between ~0.1kPa to ~80 kPa reversibly. This accessible range of elasticities can cover most of the physiologically relevant tissue stiffness giving this platform wide applicability

as a model system for studying mechanical effects on different cellular systems in-vitro.

We show how simple and inexpensive permanent magnets can be used to dynamically stiffen hydrogels for the investigation of several cellular activities that are influenced by mechanical properties. Although this approach sacrifices the ability to continuously tune the elasticity, it allows switching between soft and stiff conditions and retains the reversibility. It is important to consider that, with particle alignment, there are some changes in protein distribution and changes in surface topography and alignment may also occur that modulate cell behavior or adhesion(23). MSCs cultured on soft substrates show nearly a 2-fold increase in spread area when a magnet is applied. The influence on cell area is reversible and the cell area is reduced after removal of the magnet; curiously however, stained actin remains brighter in cells cultured on magnetically treated gels compared to cells cultured on soft gels without an applied field. This may be related to residual "stiffening" effects caused by hysteresis we observed when magnetic fields are removed.

Using this simplified system, we show that the pro-angiogenic potential of MSCs increase when they are cultured on magnetically-stiffened substrates, which agrees with our previous observations on static polyacrylamide hydrogels. In addition to pro-angiogenic secretion, we show how the degree of MSC osteogenesis can be dynamically modulated by simply adding or removing a magnet below the culture plate. After 10 days exposure to differentiation promoting media, MSCs cultured on magnetoactive hydrogels display susceptibility to the temporal dynamics of

stiffening. MSCs initially seeded on a stiff matrix appear predisposed to osteogenesis, while initial seeding on soft matrices appears to discourage lineage commitment. Interestingly, stiffening during intermediate times in our experimet (days 2-5) did not enhance osteogenesis compared to MSCs cultured on soft gels for the entire experiment. Stiffening at later timepoints (days 5-10) exerted a larger influence on osteogenesic marker expression at 10 days. Notably, since we are evaluating Runx2 expression through immunofluorescent staining, accumulation of protein with time plays a role, giving extra weight to total time spent at each stiffness condition, perhaps explaining why the HHH condition shows higher protein expression than the LHH or HLH conditions. Overall, we speculate that mechanotransduction during early stages of culture are important for initiation of osteogenic signaling. This is consistent with previous reports of early mechanical signals promoting a susceptibility to the osteogenesis program(8).

The dynamic modulation of stem cell activity using magnetic fields demonstrates the potential of this system for studying temporal regulation of ECM mechanical properties in physiological and pathological contexts, adding tunable stiffness to other applications of magnetoactive hydrogels in tissue engineering such as on-demand drug and cell delivery(40) and modulation of surface roughness and topography(41). To our knowledge, there has only been one other study where magnetoactive hydrogels have been used in cell culture(23), and then with PDMS elastomer. Our study here facilitates bridging the gap between the need for tunable hydrogels for cell culture and magnetoactive systems to study dynamic microenvironments. Some examples of dynamic microenvironments observed in

vivo include gastrulation(42), branching morphogenesis(43), cardiovascular development and function(44), and pathophysiological processes such as fibrosis and cancer(5,45). Although the use of permanent magnets is convenient, more advanced magnetic accessories will be necessary to capture subtle changes underlying many biological processes. Nevertheless, this simple technique for studying the effect of dynamic temporal modulation of substrate mechanics on cell activity, that is flexible enough to be used in many different hydrogel platforms, may find broad applicability for cell biology studies and for 'priming' cells to an appropriate state for therapy.

5.5 References

1. Lukashev ME, Werb Z. ECM signalling: Orchestrating cell behaviour and misbehaviour. Trends Cell Biol. 1998;8(11):437–41.

2. Humphrey JD, Dufresne ER, Schwartz MA. Mechanotransduction and extracellular matrix homeostasis. Nat Publ Gr. Nature Publishing Group; 2014;15(12):802–12.

3. Watt FM, Huck WTS. Role of the extracellular matrix in regulating stem cell fate. Nat Rev Mol Cell Biol. Nature Publishing Group; 2013 Jul 10;14(8):467–73.

4. Daley WP, Peters SB, Larsen M. Extracellular matrix dynamics in development and regenerative medicine. J Cell Sci. 2008;121(Pt 3):255–64.

5. Cox TR, Erler JT. Remodeling and homeostasis of the extracellular matrix: implications for fibrotic diseases and cancer. Dis Model Mech. 2011;4(2):165–78.

6. Lu P, Weaver VM, Werb Z. The extracellular matrix: A dynamic niche in cancer progression. J Cell Biol. 2012;196(4):395–406.

7. Gilbert PM, Havenstrite KL, Magnusson KEG, Sacco A, Leonardi NA, Kraft P, et al. Substrate elasticity regulates skeletal muscle stem cell self-renewal in culture. Science. 2010 Aug 27;329(5995):1078–81.

8. Yang C, Tibbitt MW, Basta L, Anseth KS. Mechanical memory and dosing

influence stem cell fate. Nat Mater. 2014;13(6):645–52.

9. Lee J, Abdeen AA, Kilian KA. Rewiring mesenchymal stem cell lineage specification by switching the biophysical microenvironment. Sci Rep. 2014;4:5188.

10. Gaeta X, Xie Y, Lowry WE. Sequential addition of reprogramming factors improves efficiency. Nat Cell Biol. Nature Publishing Group; 2013 Jul 1;15(7):725–7.

11. Mengsteab PY, Uto K, Smith ASTT, Frankel S, Fisher E, Nawas Z, et al. Spatiotemporal Control of Cardiac Anisotropy Using Dynamic Nanotopographic Cues. Biomaterials. Elsevier Ltd; 2016;86:1–10.

12. Chaudhuri O, Gu L, Klumpers D, Darnell M, Bencherif SA, Weaver JC, et al. Hydrogels with tunable stress relaxation regulate stem cell fate and activity. Nat Mater. 2015;(November).

13. Burdick JA, Murphy WL. Moving from static to dynamic complexity in hydrogel design. Nat Commun. Nature Publishing Group; 2012 Jan;3:1269.

14. Yoshikawa HY, Rossetti FF, Kaufmann S, Kaindl T, Madsen J, Engel U, et al. Quantitative evaluation of mechanosensing of cells on dynamically tunable hydrogels. J Am Chem Soc. 2011 Feb 9;133(5):1367–74.

15. Jiang FX, Yurke B, Schloss RS, Firestein BL, Langrana NA. The relationship between fibroblast growth and the dynamic stiffnesses of a DNA crosslinked hydrogel. Biomaterials. Elsevier Ltd; 2010;31(6):1199–212.

16. Gillette BM, Jensen JA., Wang M, Tchao J, Sia SK. Dynamic hydrogels: Switching of 3D microenvironments using two-component naturally derived extracellular matrices. Adv Mater. 2010;22(6):686–91.

17. Guvendiren M, Burdick JA. Stiffening hydrogels to probe short- and long-term cellular responses to dynamic mechanics. Nat Commun. Nature Publishing Group; 2012 Jan;3:792.

18. Kloxin AM, Kasko AM, Salinas CN, Anseth KS. Photodegradable hydrogels for dynamic tuning of physical and chemical properties. Science. 2009 Apr 3;324(5923):59–63.

19. Kloxin AM, Tibbitt MW, Anseth KS. Synthesis of photodegradable hydrogels as dynamically tunable cell culture platforms. Nat Protoc. Nature Publishing Group; 2010;5(12):1867–87.

20. Rosales AM, Mabry KM, Nehls EM, Anseth KS. Photoresponsive Elastic Properties of Azobenzene-Containing Poly(ethylene-glycol)-Based Hydrogels. Biomacromolecules. 2015;150210101436008.

21. Rosales AM, Anseth KS. The design of reversible hydrogels to capture extracellular matrix dynamics. Nat Publ Gr. 2016;1(February):1–16.

22. Mitsumata T, Honda A, Kanazawa H, Kawai M. Magnetically tunable elasticity for magnetic hydrogels consisting of carrageenan and carbonyl iron particles. J Phys Chem B. 2012 Oct 11;116(40):12341–8.

23. Mayer M, Rabindranath R, Börner J, Hörner E, Bentz A, Salgado J, et al. Ultra-Soft PDMS-Based Magnetoactive Elastomers as Dynamic Cell Culture Substrata. PLoS One. 2013;8(10).

24. Mitsumata T, Ohori S, Honda A, Kawai M. Magnetism and viscoelasticity of magnetic elastomers with wide range modulation of dynamic modulus. Soft Matter. 2013;9(3):904.

25. Abdeen AA, Weiss JB, Lee J, Kilian KA. Matrix Composition and Mechanics Direct Proangiogenic Signaling from Mesenchymal Stem Cells. Tissue Eng Part A. 2014 Oct;20(19-20):2737–45.

26. Tse JR, Engler AJ. Preparation of hydrogel substrates with tunable mechanical properties. Curr Protoc Cell Biol. 2010 Jun;Chapter 10:Unit 10.16.

27. Engler AJ, Sen S, Sweeney HL, Discher DE. Matrix elasticity directs stem cell lineage specification. Cell. 2006 Aug 25;126(4):677–89.

28. Trappmann B, Gautrot JE, Connelly JT, Strange DGT, Li Y, Oyen ML, et al. Extracellular-matrix tethering regulates stem-cell fate. Nat Mater. Nature Publishing Group; 2012 Jan;11(7):642–9.

29. Lee J, Abdeen AA, Kim AS, Kilian KA. Influence of Biophysical Parameters on Maintaining the Mesenchymal Stem Cell Phenotype. ACS Biomater Sci Eng. 2015;150306103621001.

30. Lin-Vien D, Colthup NB, Fateley WG, Grasselli JG. Organosilicon Compounds. Handb Infrared Raman Charact Freq Org Mol. 1991;251–61.

31. Ewoldt RH, Mckinley GH. Creep Ringing in Rheometry or How to Deal with Oft-discarded Data in Step Stress Tests! Rheol Bull. 2007;76(1).

32. Yao NY, Larsen RJ, Weitz D a. Probing nonlinear rheology with inertio-elastic oscillations. J Rheol (N Y N Y). 2008;52(4):1013.

33. Storm C, Pastore JJ, MacKintosh FC, Lubensky TC, Janmey PA. Nonlinear elasticity in biological gels. Nature. 2005 May 12;435(7039):191–4.

34. de Vicente J, Klingenberg DJ, Hidalgo-Alvarez R. Magnetorheological fluids: a review. Soft Matter. 2011;7(8):3701.

35. Ewoldt RH, Johnston MT, Caretta LM. Experimental Challenges of Shear Rheology: How to Avoid Bad Data. In: Spagnolie SE, editor. Complex Fluids in Biological Systems. New York, NY: Springer New York; 2015. p. 207–41.

36. Park JH, Kwon MH, Park OO. Rheological properties and stability of magnetorheological fluids using viscoelastic medium and nanoadditives. Korean J Chem Eng. 2001;18(5):580–5.

37. Claracq J, Sarrazin J, Montfort JP. Viscoelastic properties of magnetorheological fluids. Rheol Acta. 2004;43(1):38–49.

38. Rowlands AS, George PA, Cooper-White JJ. Directing osteogenic and myogenic differentiation of MSCs: interplay of stiffness and adhesive ligand presentation. Am J Physiol Cell Physiol. 2008 Oct;295(4):1037–44.

39. Miyakoshi J. Effects of static magnetic fields at the cellular level. Prog Biophys Mol Biol. 2005;87(2-3):213–23.

40. Zhao X, Kim J, Cezar C a, Huebsch N, Lee K, Bouhadir K, et al. Active scaffolds for on-demand drug and cell delivery. Proc Natl Acad Sci. 2011;108(1):67–72.

41. Kiang JD, Wen JH, Del ??lamo JC, Engler AJ. Dynamic and reversible surface topography influences cell morphology. J Biomed Mater Res - Part A. 2013;101 A(8):2313–21.

42. Latimer A, Jessen JR. Extracellular matrix assembly and organization during zebrafish gastrulation. Matrix Biol. International Society of Matrix Biology; 2010;29(2):89–96.

43. Kim HY, Nelson CM. Extracellular matrix and cytoskeletal dynamics during branching morphogenesis. Organogenesis. 2012;8(2):56–64.

44. Rienks M, Papageorgiou AP, Frangogiannis NG, Heymans S. Myocardial extracellular matrix: An ever-changing and diverse entity. Circ Res. 2014;114(5):872–88.

45. Bonnans C, Chou J, Werb Z. Remodelling the extracellular matrix in development and disease. Nat Rev Mol Cell Biol. Nature Publishing Group; 2014;15(12):786–801.

CHAPTER 6

CONCLUDING REMARKS AND FUTURE PROSPECTIVES

In this work we have shown that ECM properties can have a profound impact on MSC pro-angiogenic potential. We show in Chapter 2 that elasticity, modulated by matrix composition, can affect tube formation by the MSC secretome several fold. These results may help explain the poor clinical efficacy seen with transplanted MSCs and highlight the importance of coming up with design criteria to maximize treatment efficacy and implementing them when making therapeutic biomaterials(1).

In Chapter 3, we focus more on changes in the MSCs themselves, finding changes in MSC pro-angiogenic potential based on cytoskeletal contractility. Contractility further impacts the MSC phenotype, pushing it towards a state with characteristics of activated pericytes(2). This time the results not only point us towards criteria for maximizing MSC therapeutic potential but also to possible molecular markers that can be used to easily identify this pro-angiogenic phenotype in vitro and study the effects of matrix properties on achieving this phenotype without having to perform functional angiogenesis assays.

In order for these insights to actually influence developing therapies, however, steps should be taken towards translation(3). Hydrogels patches for enhancing angiogenesis are a very active area for research with, for example,

thermoresponsive hydrogels(4), patterned hydrogel patches(5) or hypoxia inducible hydrogels(6) have all been developed and tested for the enhancement of angiogenesis in vitro or in vivo. Hence, working towards translation would broaden the impact of this work and open it up towards practical application.

We take the preliminary steps towards translation of our work in Chapter 4 by developing a PEG-based hydrogel system based on elastic and composition design criteria formulated in Chapter 2. We further show that this system can be used to spatially guide angiogenesis in vitro. Future work towards testing the insights gleaned from chapters 2, 3 & 4 on more relevant in vivo models would be very valuable in fully realizing the potential of this work. For example, the in ovo vascularized chick chorioallantoic membrane models (CAMs)(7) can offer a facile system to test the effects of MSCs cultured on various substrates/patterns on in ovo angiogenesis, as shown in Chapter 3 where some of the effects we see in vitro persist in vivo. MSCs can be detached after culturing in the desired conditions and added to CAMs to discern their more direct effects on the vascularized membrane. Furthermore, PEG-based plugs can be used to encapsulate MSCs in shaped island to investigate their effects on both the extent of angiogenesis and the spatial patterning aspects. More work using advanced mouse models to study stimulated angiogenesis in model systems such as myocardial infarctions or hind-limb ischemia(8) would further enhance the applicability of this work towards theraputics.

Finally, the work in Chapter 5 demonstrating a tool by which matrix properties can be modulated in vitro where temporal changes in matrix properties can be studied.

This may be useful for studying changes in native cell behaviors (myofibroblasts, myocytes, pericytes, etc.) during myocardial infarction, for example, where the ECM elasticity decreases and increases in the post infarction myocardium. This can also help identify optimum windows for therapeutic efficiency.

Overall this works provides several insights into how MSC therapeutic behavior is and can be modulated via extracellular matrix properties. However, in order to realize the benefits of this work for actual therapies, further work towards showing the in-vivo applicability is needed as well as further work to understand the precise molecular pathways and physical changes that mediate the final functional changes. This would enable more precise control over the intended behavior of eventual therapies.

References

1. Ranganath SH, Levy O, Inamdar MS, Karp JM. Harnessing the mesenchymal stem cell secretome for the treatment of cardiovascular disease. Cell Stem Cell. Elsevier Inc.; 2012 Mar 2;10(3):244–58.

2. Caplan AI, Correa D. The MSC: An injury drugstore. Cell Stem Cell. Elsevier Inc.; 2011;9(1):11–5.

3. Ankrum J, Karp JM. Mesenchymal stem cell therapy: Two steps forward, one step back. Trends Mol Med. Elsevier Ltd; 2010 May;16(5):203–9.

4. Bak S, Ahmad T, Lee Y Bin, Lee J, Kim EM, Shin H. Delivery of a Cell Patch of Cocultured Endothelial Cells and Smooth Muscle Cells Using Thermoresponsive Hydrogels for Enhanced Angiogenesis. Tissue Eng Part A. 2016;22(1-2):182–93.

5. Jeong JH, Chan V, Cha C, Zorlutuna P, Dyck C, Hsia KJ, et al. "Living" microvascular stamp for patterning of functional neovessels; Orchestrated control of matrix property and geometry. Adv Mater. 2012;24(1):58–63.

6. Park KM, Gerecht S. Hypoxia-inducible hydrogels. Nat Commun. 2014;5(May):1–12.

7. Ponce ML, Kleinmann HK. The chick chorioallantoic membrane as an in vivo angiogenesis model. Curr Protoc Cell Biol. 2003;Chapter 19:Unit 19.5.

8. Greenberg JI, Suliman A, Barillas S, Angle N. Chapter 7 Mouse Models of Ischemic Angiogenesis and Ischemia-Reperfusion Injury. Methods Enzymol. 2008;444(08):159–74.

APPENDIX A

GENERAL METHODS

Materials

Lab Chemicals were purchased from Sigma-Aldrich unless otherwise stated. Hydrazine hydrate was purchased from Fisher Scientific. Human extracellular matrix Proteins (fibronectin, collagen I and laminin α1) were purchased from Sigma. Tissue culture plastic was purchased from Fisher Scientific. Cell culture media and reagents were purchased from Gibco. Human MSCs were purchased and tested for purity from Lonza and were positive for CD105, CD166, CD29, and CD44, negative for CD14, CD34, and CD45 by flow cytometry. Growth factor reduced basement membrane extract was purchased from Trevigen. hMVECs were purchased from cell-systems. EGM-2 growth factor supplemented media was purchased from Lonza. The use of human cell lines in this work was reviewed and approved by the University of Illinois at Urbana-Champaign Biological Safety Institutional Review Board.

Polyacrylamide gel fabrication

18mm coverslips were activated by treatment with 5% 3-aminopropyltrimethoxysilane solution followed by treatment with 5% glutaraldehyde solution. Hydrophobic slides were prepared by treatment with RainX (SOPUS). 1ml of a mixture of acrylamide and bis-acrylamide monomers were mixed

with 10uL ammonium persulfate (APS) initiator and 1 µL tetraethylmethylenediamine (TEMED) to make a working solution (Varying acrylamide and bis-acrylamide concentrations to obtain different stiffness). 20 µL of this mixture was pipetted between the activated and hydrophobic coverslips and left to polymerize. The gels were then submerged in 1 ml of 55% aqueous hydrazine hydrate for 2 hours followed by washing with glacial acetic acid and DI water for 1 hour each. Fibronectin, type I collagen and laminin (alpha I) were made up to 50 µg/ml solutions and 3.6mg/mL sodium periodate was added for 30 minutes to oxidize the protein. 50 µL of oxidized protein was pooled onto the activated gel surfaces for 1 hour. The gels were washed extensively with PBS before cell culture. Since polyacrylamide is generally non-fouling, there was no need to block the substrates for non-specific adhesion.

Soft Lithography

For patterning substrates, polydimethylsiloxane (PDMS, Polysciences Inc.) stamps were fabricated by polymerization upon a patterned master of photoresist (SU-8, MicroChem) created using UV photolithography through a laser printed mask. Stamps featuring circular patterns of 3000 μm^2 were used. Oxidized protein was pooled onto the stamp for approximately 1 hour and then dried with air. The stamp was then placed face down on the activated gel surface for 30 seconds before removal. The gels were washed extensively with PBS before cell culture.

Cell culture

MSCs were passaged in DMEM low glucose media supplemented with 10% fetal bovine serum (FBS) and 1% penicillin/streptomycin (p/s). The media was changed every 4 days and the cells were passaged at around 80% confluence. hMVECs were cultured on tissue culture plastic coated with attachment factor (Life Technologies) in EGM-2 growth factor supplemented media. The media was changed every 4 days and the cells were passaged at around 80% confluence.

Immunofluorescence

For Immunofluorescence studies, the surfaces were rinsed twice with PBS then fixed with 4% paraformaldehyde (PFA) in PBS for 20 minutes followed by permeabilization using 0.1% TRITON X-100 for 30 minutes. The surfaces were blocked in 1% bovine serum albumin (BSA). The desired staining agents are then added.

Vascularization assays

Conditioned media was collected from the cultured MSCs (p2-p8) and the cells were fixed and stained at a desired time. 25 µL of matrigel was pipetted into each well of a 48 well plate. The plate was then placed in the incubator for 30 minutes to form the gel structure. hMVECs of low passage (p2-p6) were seeded at ~15,000 cells/well. 500 µL of conditioned media obtained from the gels at the desired time were added at each condition. The assay was incubated and Images of the wells were taken at different time-points using a Cannon Rebel DSLR camera on an inverted microscope at 40x zoom.